Numerical Modelling of Coastal Erosion using MIKE21

Rohit Rajesh Kulkarni

ERASMUS MUNDUS MSc PROGRAMME

COASTAL AND MARINE ENGINEERING AND MANAGEMENT
CoMEM

NUMERICAL MODELLING OF COASTAL EROSION USING MIKE21

Norwegian University of Science and Technology, Trondheim, Norway
25th June 2013

Rohit Kulkarni
4192486

The Erasmus Mundus MSc Coastal and Marine Engineering and Management is an integrated programme organized by five European partner institutions, coordinated by Delft University of Technology (TU Delft).
The joint study programme of 120 ECTS credits (two years full-time) has been obtained at three of the five CoMEM partner institutions:

- Norges Teknisk- Naturvitenskapelige Universitet (NTNU) Trondheim, Norway
- Technische Universiteit (TU) Delft, The Netherlands
- City University London, Great Britain
- Universitat Politècnica de Catalunya (UPC), Barcelona, Spain
- University of Southampton, Southampton, Great Britain

The first year consists of the first and second semesters of 30 ECTS each, spent at NTNU, Trondheim and Delft University of Technology respectively.
The second year allows for specialization in three subjects and during the third semester courses are taken with a focus on advanced topics in the selected area of specialization:
- Engineering
- Management
- Environment
In the fourth and final semester an MSc project and thesis have to be completed.
The two year CoMEM programme leads to three officially recognized MSc diploma certificates. These will be issued by the three universities which have been attended by the student. The transcripts issued with the MSc Diploma Certificate of each university include grades/marks for each subject. A complete overview of subjects and ECTS credits is included in the Diploma Supplement, as received from the CoMEM coordinating university, Delft University of Technology (TU Delft).

Information regarding the CoMEM programme can be obtained from the programme coordinator and director

Prof. Dr. Ir. Marcel J.F. Stive
Delft University of Technology
Faculty of Civil Engineering and geosciences
P.O. Box 5048
2600 GA Delft
The Netherlands

NORWEGIAN UNIVERSITY OF SCIENCE AND TECHNOLOGY

DEPARTMENT OF CIVIL AND TRANSPORT ENGINEERING

Report Title: **Numerical Modelling of Coastal Erosion using MIKE21**		Date: 25/06/2013 Number of pages (incl. appendices): 80		
		Master Thesis	x	Project Work
Name: **Rohit Kulkarni**				
Professor in charge/supervisor: **Prof. Raed Lubbad**				
Other external professional contacts/supervisors: -				

Abstract:

The purpose of this research is to model coastal erosion at a site on the Ural coast of the Baydara Bay, Russia. The research carried out in this thesis, aims to create a model to represent the hydrodynamics and sediment transport patterns prevalent at the site, using MIKE21 developed by DHI. The model is calibrated using the available data. The model results were found to be in good agreement with the collected data. The results show a high bed resistance value which is due to the vegetation and possible ice content in the sediment layer.

In the second part of the research, the hydrodynamic conditions for a more recent time frame are presented for which the sediment transport pattern is also predicted. A sensitivity analysis of the sediment transport is presented for the following parameters: grain size diameter, importance of waves and importance of model formulations. The sensitivity analysis shows that the waves are of primary importance compared to tidal currents. The sensitivity of results to variation in sediment grain size are also discussed. In conclusion, limitations of the model and scope of future research are outlined.

MASTER THESIS

(TBA4920 marine Civil Engineering, master thesis)

Spring 2013

for

Rohit Kulkarni

Numerical Modelling of Coastal Erosion Using MIKE21

BACKGROUND

Coastal zones are one of the most important areas for human activities and infrastructure growth. However, the systems are dynamic and need to be studied extensively before any infrastructure is planned in order to avoid damages due to natural processes such as erosion. An important tool to assess these systems is numerical modelling of the coast to predict the environmental characteristics of the area. Many modelling suites exist today to try and analyse the coastal features so that an informed decision can be made regarding any developments. MIKE21 is such an integrated modelling suite, commercially marketed by DHI (formerly known as Danish Hydraulic Institute). It includes modules that represent various processes in coastal dynamics.

The coastal problems in the Arctic region have yet to be given sufficient importance. Although, there is an increasing trend to analyse the systems as more and more infrastructure is being planned in the Arctic coastal zone (Rachold, V. et al., 2005). SAMCoT (Sustainable Arctic Marine and Coastal Technology) is centre for excellence at NTNU, focusing on development of technology necessary for sustainable development of Arctic region. Climate change is a major concern in relation to coastal erosion in the Arctic, due to the lack of sea ice and melting of permafrost. This would lead to increased coastal erosion affecting the population in the area as well as damage to the existing infrastructure. SAMCoT has been

involved in a number of expeditions in the last couple of years to collect data from locations in the Arctic to assess this problem.

Baydara Bay has been selected as a location for the purpose of this research study. The selection of the site is done based on the data made available from expeditions arranged by SAMCoT to the Ural coast on Baydara Bay. The area is of particular interest as important infrastructure projects have been planned in the region which will require detailed information regarding the coastal geomorphology and evolution of the coastline. It is situated in the southern part of Kara Sea. The Ural coast has dominant abrasive and accumulative characteristics due to thermal as well as hydrodynamic processes. These hydrodynamic processes and sediment transport have been found to be active only in the summer season, during which the Bay is ice-free (Sergey Mironyuk, 2006).

TASK DESCRIPTION

The previously discussed model, MIKE21, will be used to analyse the hydrodynamic condition and sediment transport patterns at the location. The task will be carried out in two parts:

- The initial part of study will focus on calibration of the model with data available from the site. Using the calibrated parameters, the hydrodynamic condition for the most recent data will be simulated for a specific period.
- A sensitivity analysis for the sediment transport rates near the site of interest will be carried out. Influence of the parameters governing sediment transport and physical processes will also be analysed as a part of this research.

The dominant processes in the Bay will be discussed reflecting the results obtained from the simulation. Shortcomings of the research will be outlined with scope of further improvement in future studies.

Initial References

Rachold, V., Are, F. E., Atkinson, D. E., Cherkashov, G., & Solomon, S. M., 2005. Arctic coastal dynamics (ACD): An introduction. *Geo-Marine Letters*,*25*(2), 63-68.

Sergey G. Mironyuk., 2006, November. Geological consequences of the construction and operation of pipeline water crossing the Baydaratskaya Bay (Kara Sea). Article published online (in Russian) at www.Safeprom.ru (Accessed: 13th February 2013)

General about content, work and presentation

The text for the master thesis is meant as a framework for the work of the candidate. Adjustments might be done as the work progresses. Tentative changes must be done in cooperation and agreement with the professor in charge at the Department.

The reporting of the work should be academic anchored and well described with respect to the theoretical and scientific basis so that the work could be implemented in the field of international research.

In the evaluation thoroughness in the work will be emphasized, as will be documentation of independence in assessments and conclusions. Furthermore the presentation (report) should be well organized and edited; providing clear, precise and orderly descriptions without being unnecessary voluminous.

The report shall include:

- Standard report front page (from DAIM, http://daim.idi.ntnu.no/)
- Title page with abstract and keywords.(template on: http://www.ntnu.no/bat/skjemabank)
- Preface
- Summary and acknowledgement. The summary shall include the objectives of the work, explain how the work has been conducted, present the main results achieved and give the main conclusions of the work.
- Table of content including list of figures, tables, enclosures and appendices.
- If useful and applicable a list explaining important terms and abbreviations should be included.
- The main text.
- Clear and complete references to material used, both in text and figures/tables. This also applies for personal and/or oral communication and information.
- Text of the Thesis (these pages) signed by professor in charge as Attachment 1..
- The report musts have a complete page numbering.

Advice and guidelines for writing of the report is given in: "Writing Reports" by Øivind Arntsen. Additional information on report writing is found in "Råd og retningslinjer for rapportskriving ved prosjekt og masteroppgave ved Institutt for bygg, anlegg og transport" (In Norwegian). Both are posted on http://www.ntnu.no/bat/skjemabank

Submission procedure

Procedures relating to the submission of the thesis are described in DAIM (http://daim.idi.ntnu.no/).

Printing of the thesis is ordered through DAIM directly to Skipnes Printing delivering the printed paper to the department office 2-4 days later. The department will pay for 3 copies, of which the institute retains two copies. Additional copies must be paid for by the candidate.
On submission of the thesis the candidate shall submit a CD with the paper in digital form in pdf and Word version, the underlying material (such as data collection) in digital form. Students must submit the submission form (from DAIM) where both the Ark-Bibl in SBI and Public Services (Building Safety) of SB II has signed the form. The submission form including the appropriate signatures must be signed by the department office before the form is delivered Faculty Office.

Documentation collected during the work, with support from the Department, shall be handed in to the Department together with the report.

According to the current laws and regulations at NTNU, the report is the property of NTNU. The report and associated results can only be used following approval from NTNU (and external cooperation partner if applicable). The Department has the right to make use of the results from the work as if conducted by a Department employee, as long as other arrangements are not agreed upon beforehand.

Tentative agreement on external supervision, work outside NTNU, economic support etc.

Separate description to be developed, if and when applicable. See http://www.ntnu.no/bat/skjemabank for agreement forms.

Health, environment and safety (HSE) http://www.ntnu.edu/hse

NTNU emphasizes the safety for the individual employee and student. The individual safety shall be in the forefront and no one shall take unnecessary chances in carrying out the work. In particular, if the student is to participate in field work, visits, field courses, excursions etc. during the Master Thesis work, he/she shall make himself/herself familiar with " Fieldwork HSE Guidelines". The document is found on the NTNU HMS-pages at http://www.ntnu.no/hms/retningslinjer/HMSR07E.pdf

The students do not have a full insurance coverage as a student at NTNU. If you as a student want the same insurance coverage as the employees at the university, you must take out individual travel and personal injury insurance.

Start and submission deadlines

The work on the Master Thesis starts on 7th February 2013

The thesis report as described above shall be submitted digitally in DAIM at the latest 4th July 2013 at 3pm.

Professor in charge: Raed Lubbad

Other supervisors: -

Trondheim, 15th February 2013. (Revised: 20th June 2013)

_____

Professor in charge (sign)

I dedicate this thesis to my parents for their endless love and support.

Trondheim, 25-06-2013

Acknowledgements

Abstract

Coastal erosion is a problem that is increasingly being faced world over. This erosion is important not only in tropical areas but also in the Arctic region. Many numerical models exist today to predict coastal erosion at a given site. There has not been much progress in modelling erosion due to waves in combination with thermo-mechanical erosion occurring in the Arctic coasts. SAMCoT (Sustainable Arctic and Marine Coastal Technology) at NTNU (Norwegian University of Science and Technology, Trondheim) has initiated research in Baydara Bay, Russia to analyse and study the erosion occurring at the site and to arrive at an understanding of the processes involved. A site on the Ural coast of the bay has been selected for the surveys and is the location studied for this research.

The research carried out in this thesis aims to create a model to represent the hydrodynamics and sediment transport patterns prevalent at the site using MIKE21 developed by DHI. MIKE21 is a comprehensive coastal modelling suite which simulates hydrodynamics, wave field, sand transport, mud transport and advection-diffusion of environmental pollutants. As the research is in its initial stages, the data from the site for calibration is not available at this point of time. Calibration has been attempted based on the current data provided by Dr. S. Ogorodov (Senior researcher, Moscow State University) collected in August 2006. The model results were found to be in good agreement with this collected data. The results show a high bed resistance value which is attributed to the vegetation and presence of permafrost in the sediment layer.

Using the results, the hydrodynamic conditions for a more recent time frame are presented for which the sediment transport pattern is also predicted. Absence of sufficient field data has guided the research to provide a sensitivity analysis of sediment transport at the site of interest. The idea behind this is to provide a starting point for further research that can be continued based on the results obtained in this study. A sensitivity analysis of the sediment transport is presented for the following parameters:

- Grain size diameter
- Importance of waves
- Importance of model formulations

The sensitivity analysis shows that the waves are of primary importance compared to tidal currents. The sensitivity of results to variation in sediment grain size are also discussed. In conclusion, limitations of the model and scope of future research are outlined.

Contents

List of Figures

List of Tables

1   Introduction

1.1   Background

Coastal erosion is a problem that needs to be addressed, more so in areas where any infrastructure development is planned. For example, for the design of submerged pipelines, it is important to know the change of the beach profile and the bathymetry due to the hydrodynamic conditions and the sediment transport patterns prevalent there. Coastal erosion problems related to infrastructure development are present not only near the site of actual erosion but in several cases, also at locations down-drift of the erosion site.

To study the coastal erosion effects, it is important to understand the processes which are active in the area. A very helpful tool available for engineers is numerical modelling, which can predict the coastal erosion for a given set of environmental conditions. For any numerical model, it is difficult to predict the exact hydrodynamic and sediment transport patterns correctly at a location, as these processes involve many complex interactions which are difficult to model in their entirety. Numerical models make some assumptions for calculating these interactions. The errors arising from such assumptions are reduced by calibrating and validating the results with data collected from the site.

The Norwegian University of Science and Technology (NTNU) hosts a centre for research-based innovation called "Sustainable Arctic Marine and Coastal Technology (SAMCoT)". It focusses on analysing the Arctic coastal & offshore areas and gathering knowledge about the environment by selecting locations and arranging expeditions with the help of industry and academic partners to collect valuable data that can be used for further research. Baydara Bay in Russia is being monitored for the purpose of understanding the hydrodynamic and sediment transport patterns prevalent in that bay.

The motivation of this research was to arrive at an understanding of the hydrodynamic and sediment transport pattern in the area and combine it with the geotechnical understanding of the cliff erosion surveyed by SAMCoT. This will lead to a comprehensive understanding of the processes active in the area, arriving at results that can be validated by data collected on site.

The aim of the current research is to prepare a model representing the hydrodynamic and meteorological conditions at the site in Baydara Bay using MIKE21 and evaluating the sediment transport patterns at that location. MIKE21 by DHI, Denmark is a comprehensive and robust modelling suite capable of applying a flexible mesh over the area of interest. This greatly increases the accuracy of the model. It has modules capable of extracting bathymetry and tidal

data, analysing spectral waves, calculating hydrodynamic conditions at required time steps and determining the details of sediment transport at desired location.

The research will aim at identifying the critical factors in hydrodynamic modelling for this site and providing a sensitivity analysis for the parameters governing sediment transport. Validation of the model may not be possible as the data from the site is not available at this point of time. The approach followed in this study results from a lack of data and hence is more focused on the hydrodynamic and sediment transport processes involved in general than on the validation of the model.

1.2   Outline of report

The report first outlines the important coastal processes with focus on the formulations and their numerical modelling in Chapter 2. The model used in the research, **MIKE21**, is discussed briefly along with its modules in Chapter 3. Chapter 4 describes the area selected for the research, Baydara Bay in Russia, with focus on the problems faced on the Ural coast of the bay with regards to coastal erosion. The data available at the site is also outlined in this chapter.

Chapter 5 discusses the model setups and results for the simulations conducted for the research. This chapter is divided into two parts – **Calibration runs** – where the model was run for one month in August 2006 to tune the model to the data available and – **Main run** – where the most recent data available for the site is used to arrive at an understanding of the hydrodynamic conditions present on the Ural coast of the Baydara bay. In the last part of this chapter a sensitivity analysis is presented for the sediment transport rates at the site of interest. Chapter 6 concludes the report with brief interpretation of the results and Chapter 7 recommendations for future scope of work.

2   Coastal Morphodynamics

Coastal morphodynamics of any site is dependent on many factors such as the environmental conditions, sediment properties, human intervention and their complex interaction. These natural changes lead to problems, for e.g. coastal erosion, when the area that is affected is important for human activities. To avoid excessive or unwanted morphodynamic changes at a desired location, proper understanding of the area is necessary before planning any kind of infrastructure.

Many theories and formulations have been developed till date trying to understand the complex processes active in the coastal zone. A brief introduction to these theories of hydrodynamics and sediment transport are presented in the subsequent sections. The focus of the description is on the application of these theories in numerical models.

It is important to note that these formulations are ultimately based on certain empirical parameters which were arrived upon by using experimental or laboratory results. The effect of these parameters is evident mostly in the variation of results, for example of sediment transport, as they are sensitive to the calibration and need to be validated for each location and situation.

2.1   Coastal hydrodynamics

Coastal hydrodynamics refers to the part of the coastal process which deals with wave propagation, transformation and dissipation, wave induced water level changes and long-shore and cross-shore currents due to wave, wind and tidal actions.

For modelling the waves arriving onshore, various transformations that the wave goes through have to be considered, such as, refraction, shoaling and wave breaking. These transformations are modelled by various software packages (SWAN, WAMTECH, HISWA, MIKE) available today using different techniques. These analyses require a database of meteorological parameters (such as wave height, wave period, wind speed and direction) to be given as an input, defining the environmental conditions at the desired location. A brief overview of the method for analysing this database is presented in the next section.

2.1.1 Spectral analysis

Spectral analysis is a statistical representation of the sea state using sine waves to represent the irregularity of the surface with different frequencies of which, the amplitudes and phases can be determined using Fourier analysis. For a time record with finite duration, the Fourier analysis can be written in terms of sine (or cosine) functions that fit an integer number of times, for the duration of the record.

A spectrum can then be plotted with the frequencies and the energy of the system on x and y axes respectively.

The wave spectrum is proportional to the wave energy distribution as a function of the wave number as shown in Equation 1,

$$E = \rho g Var(\eta) = \rho g \int\limits_k \Psi(k) d^2 k \qquad (1)$$

Where, E is wave energy, ρ is the density of fluid, η is the surface elevation, k is the wave number ($2\pi/L$) and function Ψ (k) signifies the density of waves around the wave number.

An energy spectrum of a wave field represents the distribution of waves in frequency domain. This makes it easier to understand the characteristics of the sea state. A narrower spectrum represents a more regular wave field. For larger and longer waves, the spectrum shifts towards the lower frequencies and contains more energy. A spectrum with two significant peaks signifies the presence of two distinct wave fields: swell and sea waves (Figure 2.1).
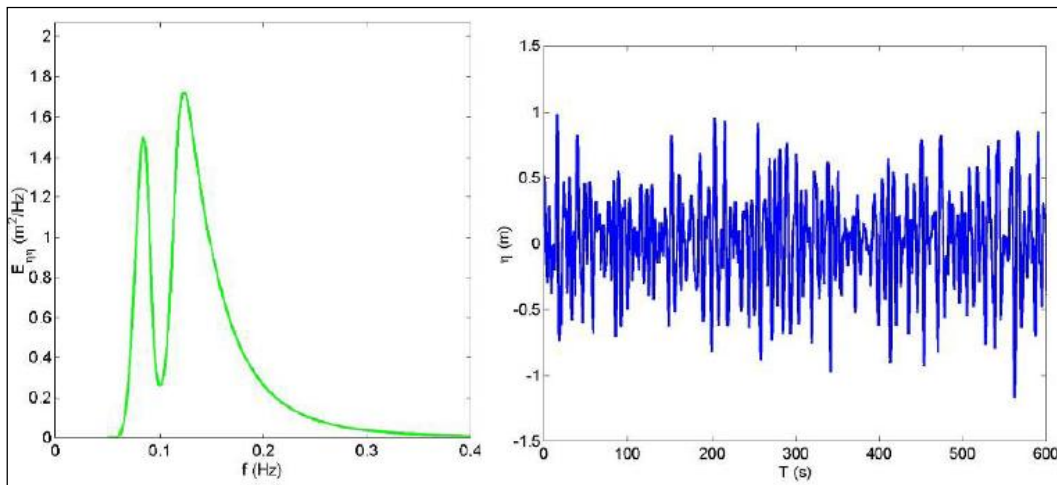
FIGURE 2.1 BI-MODAL SPECTRUM OF SEA AND SWELL (SOURCE: BOSBOOM J & STIVE M, 2012)

A directional wave spectrum shows the distribution of phases over the frequency range. The wind-generated waves develop and propagate in the direction of the wind, although there is an angular spread of energy over the mean direction. Directional spectrum can be plotted using various formulations, most common of which is the *cosine squared* and *cos-2s* distribution. The spectrum analysis reveals the dominant frequencies in the wave record. The spectral peak is the frequency at which most of the energy is concentrated.

Many important characteristics of the sea state can be represented and calculated from a spectrum with the assumption that the random surface is supposed to be

Gaussian. For example, the standard deviation of the surface elevation of the signal can be calculated from the area under the spectrum. More information regarding the equations and calculations can be found in Holthuijsen (2007).

2.1.2 Energy balance

A method of determining the changes of wave transformations is to apply the law of conservation of energy to the system. The total energy of a wave propagating across a wave field can be represented by,

$$E = \frac{1}{8} \rho g H_{rms}^2 \tag{2}$$

Where E is the wave energy, ρ is the density of the fluid and H_{rms} is the significant wave height. The simpler software packages are based on a spectrally integrated energy balance. Solving the energy balance numerically returns information regarding wave transformation such as the change in wave height (H), wave length (L), celerity (c), and wave direction (θ) in a wave field approaching the shore. The general equation representing the energy conservation can be written as below (Holthuijsen, 2007):

$$\frac{\partial E}{\partial t} + \frac{\partial}{\partial x}\left(Ec_g \cos\theta\right) + \frac{\partial}{\partial y}\left(Ec_g \sin\theta\right) = S - D \tag{3}$$

In the equation, θ represents the wave direction with respect to x-axis which is aligned normal to the shoreline, and S and D are the energy generation and dissipation terms respectively. S represents the processes that impart energy to the system such as wind and D is the term representing dissipative processes such as wave breaking. Energy conservation requires certain assumptions to be made to the wave action balance to arrive at, for example, a spatially constant peak period and the assumption that the total wave energy in the field propagates at the wave group celerity (c_g).

In presence of a current, the conservation of energy equation does not hold as there is transfer of energy between the waves and currents. This is important as generally there are currents present in the oceans that need to be modelled. In this case, instead of energy balance, wave action density (N) is used, defined as,

$$N = E/\sigma_r \tag{4}$$

Where, E is the energy density and σ_r is relative angular frequency ($\sigma_r = 2\pi f_r$). The wave action density spectrum varies in time and space and can be defined by two wave phase parameters: wave number magnitude and direction (or wave

direction) and angular frequency. Wave action balance equation (in Cartesian co-ordinates) is given as (Komen et al. 1994):

$$\frac{\partial N}{\partial t} + \nabla.(\vec{\nu}N) = \frac{S}{\sigma} \tag{5}$$

Where, $N(\vec{x}, \sigma, \theta, t)$ is the action density, t is time, $\vec{x} = (x, y)$ are the Cartesian co-ordinates, $\vec{\nu} = (c_x, c_y, c_\sigma, c_\theta)$ is propagation velocity of a wave group in four dimensional phase space. ∇ is the four dimensional differential operator. More details regarding the wave action balance may be obtained from Komen et al. (1994) and Young (1999).

2.1.3 Wave transformation

The term S, in Equation 3 signifies different source terms that describe various phenomenon such as wind input, wave energy transfer due to wave-wave interaction, white capping, bottom friction, and depth induced breaking. Airy's linear wave theory is among the most famous research that describes the wave transformations for simplified gravity waves. Many theories have been proposed regarding inclusion of these processes in wave modelling and any combination can yield satisfactory results based on the scenario and calibration of parameters. A brief description of the major processes affecting near-shore wave transformations is presented in this section.

Wind input can be considered as a primary driving force in offshore wave climate. The effect of wind on wave growth increases with wind velocity as well as the fetch length. Wave growth due to wind is usually modelled in linear or non-linear mode. For the linear model, the most commonly used model is the one proposed by Ris et al. (1994) and for non-linear growth, Janssen (1991) is preferred which uses a logarithmic profile for calculation of the wind growth parameter.

In deep waters, non-linear quadruplet wave-wave interactions play an important role in the development of wind generated waves (Philips, 1981; Young and Van Vledder, 1993). Hasselmann (1962) developed the framework and formulated an integral expression for these interactions, known as Boltzmann integral, where he found out that a set of four waves (quadruplet) could exchange energy when the following resonance conditions are met (Hasselmann, 1962):

$$\begin{aligned} \vec{k_1} + \vec{k_2} &= \vec{k_3} + \vec{k_4} \\ \omega_1 + \omega_2 &= \omega_3 + \omega_4 \end{aligned} \tag{6}$$

In which ω_j is the radian frequency and k_j is the wave number (j=1, 2, 3, 4) which are related to each other through the dispersion relation ($\omega^2 = gk$).

Although, solution of Boltzmann integral is very complicated as it requires solving a 6-dimensional integral. To model these interactions a simplified method known as Discrete Interaction Approximation (*DIA*) was introduced by Hasselmann et al. (1985) which preserves a few but important characteristics of the full solution.

Similarly as the waves reach shallow waters (*d/L < 0.05*), there are non-linear effects due to various factors such as shoaling, refraction, diffraction and bottom friction, that influence the wave characteristics, namely – asymmetry and skewness. Many non-linear theories have been proposed (Stokes, Cnoidal, Boussinesq, etc.) to take into account these processes. Non-linear effects become very important as they are crucial in determining the wave induced sediment transport and are usually modelled using the simplified theory of Eldeberky and Battjes (1994). In deep waters, the wave breaking is caused due to the limiting wave steepness. Miche (1994) expressed this limiting steepness based on Stokes' wave theory:

$$\left[\frac{H}{L} \right]_{\mathrm{max}} = 0.142 \tanh(kd) = 0.142 \text{ (for deep waters)} \approx \frac{1}{7} \qquad (7)$$

Where, H_{max} and L_{max} are the limiting wave height and wave length respectively, k is the wave number and d is the water depth.

For modelling of white capping, the model proposed by Komen et al. (1996) is generally preferred as it includes the adjustment for the dissipation source function (Janssen et al. 1989) to obtain a balance between wind input and dissipation at higher frequencies.

In near shore zone, bathymetry plays an important role in wave transformations such as shoaling, refraction, bottom friction and depth induced breaking. Shoaling refers to the increase in wave height due to energy conservation as the wave travels from deep waters to shallow waters. Refraction is the change in direction of the wave front due to the bathymetric contours present near shore. This occurs due to the fact that wave front travels faster in the deeper parts than it does in the shallower parts.

Depth induced breaking is the most crucial process for energy dissipation in the surf zone. It occurs when the waves enter a very shallow zone and the wave height can no longer be supported by the water depth (Equation 7). The formulation proposed by Battjes and Janssen (1978) is widely used to model wave breaking. All the formulations propose a breaking parameter (index) which varies as per the calibration with the experimental data. According to the linear wave theory it is

approximately equal to $0.78 (= \dfrac{H_b}{h_b})$, where H_b is the breaking wave height and h_b

is the breaking water depth. Other theories, for example Ruessink et al. (2003), suggest a breaker index dependent on wave number and depth.

Bottom friction is a critical parameter in modelling of the wave transformations. Many different theories have tried to predict the formulation for modelling bottom friction, although the results are spread over a wide spectrum (Komen et al., 1994; Weber, 1991; Tolman, 1994; Nielsen, 1979; Swart, 1976; etc.). It has been defined using various empirical coefficients and parameters dependent on grain size diameter.

Bottom friction is the cause of some of the aforementioned processes – shoaling, depth-refraction and dissipation of energy. Most models used today have an option of specifying the formulation to be used for calibrating the model using the bottom friction parameter as it varies for different locations. Bottom friction modelling is also dependent on whether currents are included in the model, as different formulations exist for these cases.

The development of numerical models over the years can be classified into three generations (Komen et al., 1996). The first generation models were not capable of including the aforementioned non-linear effects. The second generation (in 1980's) parameterised the non-linear interactions but the solution was obtained using a coupled discrete scheme. The latest generation (third) is capable of explicitly reproducing the physical processes defining the two-dimensional sea state, although it relies on calibration of the model for every location.

2.1.4 Wave induced setup and currents

As waves travel across the ocean surface they also transfer momentum in the direction of travel. The momentum can be considered as a net flux of mass between wave trough and crest associated with wave propagation. In the non-breaking zone of ocean, this net flux is related to the wave amplitude in a non-linear function. In the surf zone, this flux is substantially larger than outside consisting of two parts: non-breaking and roller (refer Roelvink and Stive, 1989; Nairn et al. 1990 for details).

Considering a closed boundary (coastline), there must be a return current under the wave trough level to compensate for the propagating flux. This is the undertow current responsible for seaward movement of sediment. It is considered as the primary process responsible for beach erosion during heavy storms.

Radiation stresses are the depth integrated and wave averaged excess momentum fluxes due to waves as defined by Longuet-Higgins and Stewart (1964). A change

in the momentum flux (radiation stress) causes wave forces to act on the fluid affecting the mean water motion and levels. Radiation stresses are responsible for set-up, set-down and longshore current in the near shore zone.

Time and wave averaged equations for the radiation stresses derived from the linear wave theory are as mentioned below (Longuet-Higgins and Stewart, 1964):

$$Sxx = \overline{\int_{-h_0}^{\eta} (\rho u_x)u_x dz} + \overline{\int_{-h_0}^{\eta} p_{wave} dz} \tag{8}$$

$$Syy = \overline{\int_{-h_0}^{\eta} (\rho u_y)u_y dz} + \overline{\int_{-h_0}^{\eta} p_{wave} dz} \tag{9}$$

$$Sxy = \overline{\int_{-h_0}^{\eta} (\rho u_x)u_y + \tau_{xy} dz} = \overline{\int_{-h_0}^{\eta} (\rho u_x)u_y dz} \tag{10}$$

$$Syx = \overline{\int_{-h_0}^{\eta} (\rho u_y)u_x dz} \tag{11}$$

Where, u_x and u_y are the water particle velocities in x and y direction respectively, p_{wave} is the hydrostatic pressure component of the wave and S_{xx} and S_{yy} are the normal stresses that include the hydrostatic pressure in the water column. S_{xy} & S_{yx} are the shear stress components of the wave. The shear stress due to waves (τ_{xy}) is considered as zero (Equation 10) due to the assumption of irrotational fluid in linear wave theory. The forces that are setup in the water column due to these stresses result in set-up and set-down. Cross-shore currents are a result of these changes in water level due to the normal radiation stresses (S_{xx} & S_{yy}). Longshore currents are a result of the forces due to the shear radiation stresses (S_{xy} & S_{yx}) in the water column.

2.1.5 Shallow water equations

Using all the processes defined in the sections before, a model usually determines the solution of the three (or two) dimensional incompressible Reynolds averaged Navier-Stokes equations subject to the assumptions of Boussinesq and hydrostatic pressure. The local continuity equation integrated over depth (2D) can be written as:

$$\frac{\partial h}{\partial t} + \frac{\partial \overline{hu}}{\partial x} + \frac{\partial \overline{hv}}{\partial y} = hS \tag{12}$$

Where, h is the water depth and u and v are water particle velocities in x and y direction respectively, S is the energy source-dissipation term.

The two depth averaged, horizontal momentum equations for x- and y-components are, respectively (Holthuijsen, 2007):

$$\frac{\partial \overline{hu}}{\partial t} + \frac{\partial \overline{hu^2}}{\partial x} + \frac{\partial \overline{hvu}}{\partial y} = f\overline{hv} - gh\frac{\partial \eta}{\partial x} - \frac{h}{\rho_0}\frac{\partial p_a}{\partial x} - \frac{gh^2}{2\rho_0}\frac{\partial \rho}{\partial x} + \frac{\tau_{sx}}{\rho_0} - \frac{\tau_{bx}}{\rho_0} -$$
$$\frac{1}{\rho_0}\left(\frac{\partial Sxx}{\partial x} + \frac{\partial Sxy}{\partial y}\right) + \frac{\partial}{\partial x}\ hT_{xx}\ + \frac{\partial}{\partial y}\ hT_{xy}\ + hu_sS \tag{13}$$

$$\frac{\partial \overline{hv}}{\partial t} + \frac{\partial \overline{hvu}}{\partial x} + \frac{\partial \overline{hv^2}}{\partial y} = f\overline{hu} - gh\frac{\partial \eta}{\partial y} - \frac{h}{\rho_0}\frac{\partial p_a}{\partial y} - \frac{gh^2}{2\rho_0}\frac{\partial \rho}{\partial y} + \frac{\tau_{sy}}{\rho_0} - \frac{\tau_{by}}{\rho_0} -$$
$$\frac{1}{\rho_0}\left(\frac{\partial Syx}{\partial x} + \frac{\partial Syy}{\partial y}\right) + \frac{\partial}{\partial y}\ hT_{xy}\ + \frac{\partial}{\partial y}\ hT_{yy}\ + hv_sS \tag{14}$$

Where t is the time; x and y are the Cartesian co-ordinates; η is the surface elevation; d is the still water depth; $h = \eta + d$ is the total water depth; u and v are velocity components in x and y direction; f is the Coriolis parameter; g is gravitational acceleration; ρ is the density of water; τ_{sx}, τ_{sy} are the x and y components of surface wind and τ_{bx} and τ_{by} are the components of bottom stress; T_{ij} includes viscous friction, turbulent friction and differential advection estimated using eddy viscosity formulation based on depth averaged velocity gradients.

The right-hand side of Equation 13 and 14 constitute the input and boundary conditions provided to any model to calculate the current components and water particle velocities. The solution of these equations is dependent on the scheme applied by the model and different assumptions may result in different outcome. The resulting values of current and water particle velocities are responsible for sediment transport occurring in the near-shore coastal zone.

Turbulence modelling is usually included in the momentum equations in the terms containing laminar stresses and Reynolds stresses. It can be either used as a constant in the horizontal stress terms or by using the Smagorinsky's formulation (1963) to express sub-grid scale transports by using an effective eddy viscosity related to characteristic length scale (Lily, 1989).

2.2   Sediment transport

Considering the hydrodynamics outlined in the sections before, the end result is the change in coastal morphology that affects the coastal infrastructure and usage. This change in morphology is due to sediment transport occurring due to wave and current action (primarily). It is defined as the movement of sediment particles through a well-defined plane over a certain period of time. Apart from the hydrodynamic conditions, the movement of sediment particles depends on the characteristics of the transported material (grain size, fall velocity, etc.) which are outlined in Section 2.2.1.

The interaction between hydrodynamics and sediment is very complex and even more difficult to model. To this day, the modelling of sediment transport is based on empiricism. A formulation is tested against experimental or real life scenarios and parameters in the formulation are calibrated accordingly to obtain desired results. Generally, to reduce complexity, the sediment transport is divided into two modes – bed load and suspended load which are outlined briefly in Section 2.2.2.

Different formulations have different parameters to define the different processes and the choice between the parameters is difficult and needs to be made, based on prior experience or by trial and error. The formulations themselves are often based on specific situations and need to be analysed properly before being applied to any location. Although the basic processes defined in all the formulations are same, the parameterization is different which may result in different solutions.

2.2.1 Sediment properties

The sediments commonly found in the coastal zone are silt, clay, sand, gravel and cobbles in increasing order of their diameter. As stated before, the properties of sediments influence the sediment transport occurring at any location. Many characteristic properties of sediments that are used to classify them are grain size diameter, porosity, relative density, bulk density, fall velocity etc.

Grain size diameter and grading of the sediment are defined in terms of a cumulative distribution of grain sizes. A median particle diameter D_{50} is considered as representative of the sediment and the grading is defined as D_{90}/D_{10}. Sediment is considered as well sorted if D_{90}/D_{10} is small (<1.5) and well graded or

poorly sorted for bigger values of D_{90}/D_{10} (>3). The numbers 50, 90 and 10 in D_{50}, D_{90} and D_{10} represent the portion or percentage of sediment by weight passing through the given standard sieve size.

The grain density (ρ_s) depends on the mineral content of the sediment and for sands it is usually considered as 2650 kg/m³. Relative density is the ratio between density of the sediment and the density of the fluid (usually considered as 1030 kg/m³ for saline water bodies). The porosity is an important property of sediments defining the amount of pore spaces in the volume.

Fall velocity is defined as the vertical free fall velocity of a sediment particle in still and clear water. It is the balance between the downward directed gravity force and upward directed drag force acting on the sediment particle. The fall velocity (ω_s) of a particle depends on its size, density and magnitude of drag coefficient C_D (which in turn is dependent on shape of particle, roughness and Reynolds number) as shown in the equation below:

$$w_s = \sqrt{\frac{4(s-1)gD}{3C_D}} \tag{15}$$

Where, s is the relative density of the sediment and D is the sediment grain size. Sediment can be transported if the water movement applies a large enough shear stress τ_b on the grains. The critical shear stress describes the point of initiation of motion. The equilibrium of forces, whether vertical, horizontal or moment equilibrium is considered, gives an expression of the form:

$$(\rho_s - \rho)\,gD^3 \propto \tau_{b,cr}D^2 \tag{16}$$

Where, ρ_s is the density of sediments and ρ is the density of fluid. From the previous proportionality, the critical Shields parameter θ_{cr} can be deduced:

$$\theta_{cr} = \frac{\tau_{b,cr}}{\rho_s - \rho\ \ gD} = C \tag{17}$$

The constant C is determined experimentally. For sand positioned smoothly on a flat bed, C is found to be around 0.05. Figure 2.2 shows measured values of C as a function of the Reynolds number (R_e). The darker band separates two zones: the area above the bands indicates movement of sediment particles according to the experiments. The band shows therefore initiation of motion, and this can be seen to be approximately 0.05.
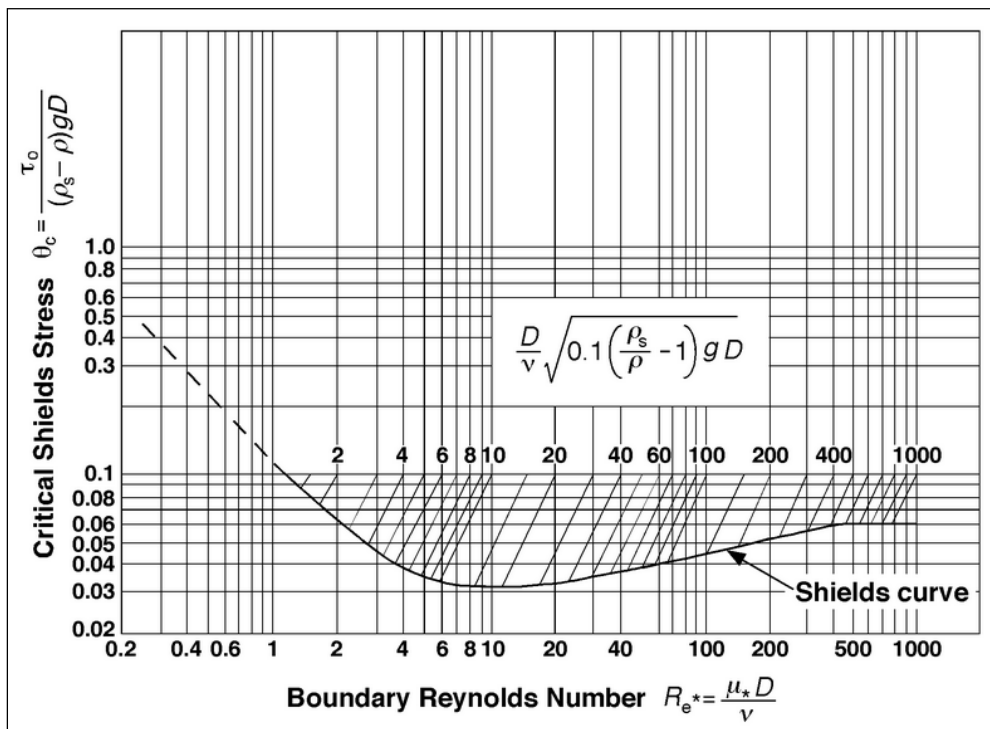
FIGURE 2.2 SHIELDS' DIAGRAM (SOURCE: SHIELDS A., 1936)

A number of explicit sediment transport formulas for modelling bed load, suspended load and total load have been developed over the years. In all the models the main parameter responsible for controlling motion of sediment transport is Shield's parameter defined in Equation 17.

2.2.2 Bed load and suspended load transport

The mechanisms behind bed load and suspended load are fairly different. It is common to use separate transport formulations for the two different modes of transport.

Bed load transport is almost entirely determined by the bed shear stress acting on the sediment particles that roll along the bed. Therefore, the bed load formulations are usually expressed in terms of bed-shear stress due to currents and waves. As soon as the bed shear stress exceeds a critical value, sediment particles start rolling or sliding over the bed. If the bead shear stress increases further, the sediment particles move across the bed by jumping over each other. As long as the jump lengths are limited to about a few times the particle diameter, this motion is termed as bed load transport.

In the bed load layer, turbulent mixing is often assumed to be negligible, so that it only slightly influences the motion of sediment particles. Gravity restricts the vertical particle motion. Bed load transport can be assumed to respond

13

instantaneously to the bed shear stress although there are formulations that use time averaged shear stress in the calculations (Bijker, 1967). Even so, most of the approaches for bed load transport formulation are based on this assumption and sediment transport is considered directly proportional to shear stress on the grains.

There are many formulations that have made attempts to explain the bed load transport processes, such as, Kalinske (1947), Meyer-Peter and Muller (1948), Einstein (1962), Frijlink (1952), Rottner (1959), Ackers-White (1973), etc. A comparison between them in Figure 2.3 shows that they all represent the dimensionless transport as a function of a Shields parameter. It can be seen that the predicted transport rates for a certain value of Shields parameter have a large order of variation and hence, the calibration of sediment transport for a given location and condition are crucial.

Further complexities are introduced in calculating the bed load transport when the combined effects of waves and currents are introduced, which need to be taken care of in nearshore applications. Both instantaneous and time averaged approaches have been developed to calculate the shear stress. The instantaneous bed load transport vector S_b for waves and currents combined can be expressed in a dimensionless form as below (van Rijn L.C., 1993):

$$\Phi_b(t) = \frac{S_b(t)}{\sqrt{(s-1)gD_{50}^3}} \tag{18}$$

Where, Φ_b is a dimensionless parameter, s is the relative density of sediments, D_{50} is the sediment mean grain size and the denominator represents the square root of specific underwater weight of sediment grains.

In a generalized equation the instantaneous bed shear stress can be represented as:

$$\Phi_b(t) = f(\theta'(t), \theta_{cr}) \tag{19}$$

Where f is the algebraic operator and θ_{cr} defined in Equation 17. Similarly time averaging Equation 19 results in the time-averaged bed load sediment transport:

$$\langle \Phi_b(t) \rangle = \langle f(\theta'(t), \theta_{cr}) \rangle \tag{20}$$

Where $\langle \ \rangle$ denotes time averaging. In Figure 2.3, the y-axis is the dimensionless transport, Φ_b, defined in Equation 18 and on the x-axis is the Shields parameter, θ_{cr}, defined in Equation 17.
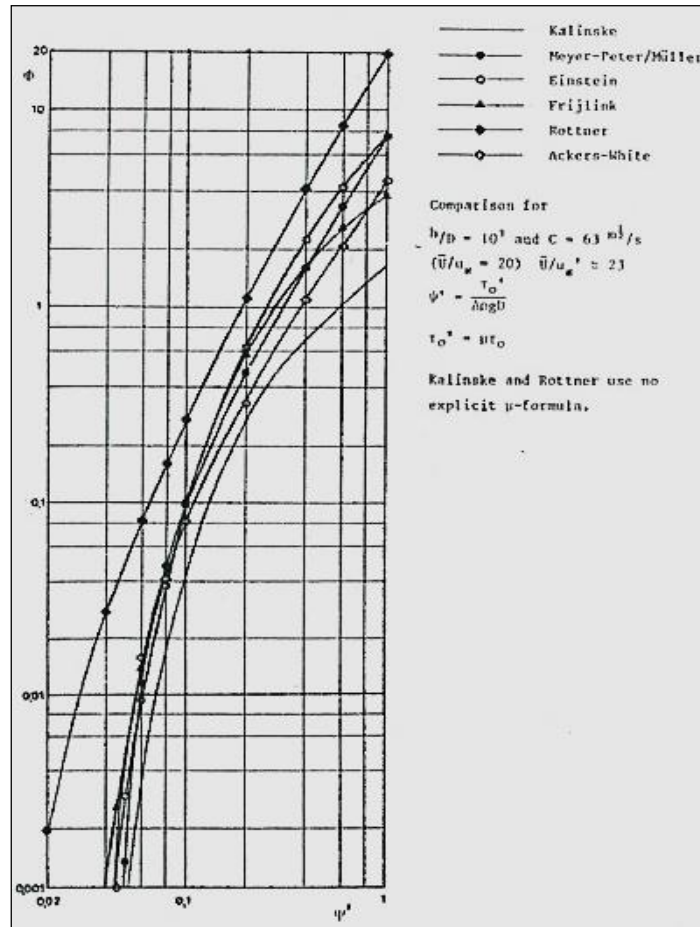
FIGURE 2.3 COMPARISON OF VARIOUS BED LOAD TRANSPORT FORMULATIONS
(SOURCE: BOSBOOM J & STIVE M, 2012)

Without detailed modelling of the vertical velocity structure and turbulence, the computation of $\theta'(t)$ can be attempted by using the quadratic friction law suggested by Grant and Madsen (1979):

$$\tau_b(t) = \frac{1}{2} \rho f'_{cw} \left| u_0(t) \right| u_0(t) \tag{21}$$

Where u_0 is the time dependent near bottom horizontal velocity vector and f'_{cw} is skin friction factor for combined wave current motion. For time averaged shear stress calculations, a different friction factor is used in different formulations.

Suspended load transport occurs above the bed load layer. When the actual bed shear stress is much larger than the critical bed shear stress, the particles are lifted from the bed and come into suspension. This is due to the turbulent upward forces that have to be larger than the submerged weight of the sediments.

The suspended sediment transport can be calculated by integrating the suspended sediment flux *uc* (where u is the velocity and c the concentration) from the top of the bed load layer to the water level (Figure 2.4).
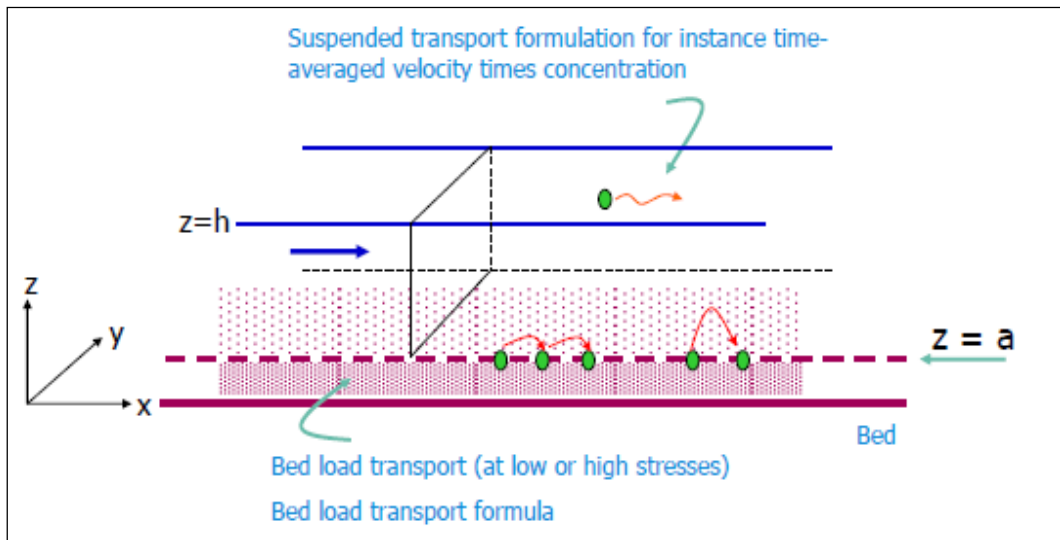
FIGURE 2.4 SEDIMENT TRANSPORT MODES (SOURCE: BOSBOOM J & STIVE M, 2012)

The instantaneous velocity (*u*) and concentration (*c*) at any given height can be considered to be part of a mean and oscillatory component, fluctuating on wave scale but having a zero time mean.

$$
\begin{aligned}
u &= U + \tilde{u} \\
c &= C + \tilde{c}
\end{aligned}
\tag{22}
$$

In which U & C are time averaged velocity and current, and $\tilde{u}$ and $\tilde{c}$ are oscillating components. Time averaging the suspended sediment transport gives:

$$
\underbrace{\left\langle S_s \right\rangle}_{\substack{\text{time-averaged sediment} \\ \text{transport rate}}} = \underbrace{\int_a^h UC dz}_{\text{current-related part}} + \underbrace{\int_a^h \overline{\tilde{u}\tilde{c}} dz}_{\text{wave-related part}}
\tag{23}
$$

Where *h* and *a* are as shown in Figure 2.4.

In order to obtain the sediment concentration, a mass balance equation for the sediment needs to be solved (Bagnold, 1966):

$$\underbrace{\frac{\partial c}{\partial t}}_{\substack{\text{change in sediment} \\ \text{concentration}}} + \underbrace{\frac{\partial uc}{\partial x}}_{\substack{\text{net import of sediment} \\ \text{by the horizontal fluid} \\ \text{velocity}}} + \underbrace{\frac{\partial vc}{\partial y} + \frac{\partial wc}{\partial z}}_{\substack{\text{net upward transport} \\ \text{of sediment by vertical} \\ \text{fluid velocity}}} - \underbrace{\frac{\partial w_s c}{\partial z}}_{\substack{\text{net downward transport} \\ \text{with fall velocity}}} = 0$$

$$(24)$$

Where, u, v and w are water particle velocities along x, y and z axes respectively (z being vertical), c is the sediment concentration and ω_s is the sediment fall velocity.

The horizontal advective terms are usually neglected and the Equation 24 is reduced to:

$$\frac{\partial c}{\partial t} + \frac{\partial wc}{\partial z} - \frac{\partial w_s c}{\partial z} = 0 \tag{25}$$

In most formulations the upward vertical fluid velocity is neglected and time averaged turbulent velocity of the fluid is introduced to account for diffusion of the sediment in the vertical profile. The turbulent diffusivity ($\nu_{t,s}$) can be considered as equal to turbulent viscosity of water or a mixture of water and sediments. In both cases the influence of sediment particles on turbulence structure of field is taken into account. Many empirical formulations have been proposed that introduce eddy viscosity dependent on sediment concentration. The non-steady advection-diffusion equation used to model sediment transport can be generalised as:

$$\frac{\partial c}{\partial t} - w_s \frac{\partial c}{\partial z} - \frac{\partial}{\partial z} \nu_{t,s} \frac{\delta c}{\delta z} = 0 \tag{26}$$

These calculations are applicable to plane beds and the introduction of rippled beds introduces another upward transport by eddies generated by the ripples. To account for these combined diffusive and convective processes different models are proposed, for example k-ω model (Wilcox, 1994) or k-ε model (Launder and Spalding, 1974; van Rijn, 1987), etc.

2.2.3 Principles of transport modelling

Theoretically the processes have been outlined in the previous sections, although it is not so straightforward and many complications need to be dealt with before modelling of sediment transport:

- The Shields diagram is only valid for uniform flow on a flat bed. Some effects such as bed ripples or the effect of the combination of unidirectional and oscillatory flow on initiation of motion are largely unknown.
- Gradation of the bed material could play a role, especially for poorly sorted sediment (bed armoring).
- Critical flow velocity will be smaller for downward sloping beds and higher for upward sloping beds.
- Presence of cohesive sediment may increase severely the resistance against erosion.

Many formulations have been used in numerical modelling of sediment transport, such as Engelund and Hansen (1967), Van Rijn (1984), Engelund and Fredsøe (1976), etc. which use different empirical expressions to try to understand the sediment transport rates occurring for any given area. All the models use calibration parameters that can vary for different locations and conditions, and need to be adjusted against collected field data.

3   Numerical model - MIKE21

This section describes the numerical modelling suite (MIKE21 by DHI) used for running the simulations. A brief description of the modules of the software package in MIKE21 is also presented.

MIKE21 by DHI is a complete coastal modelling suite capable of features such as:

- Design data assessment for coastal and offshore structures

- Optimisation of port layout and coastal protection measures

- Environmental impact assessment of marine infrastructures

- Optimisation of renewable energy systems

- Water forecast for safe marine operations and navigation

- Coastal flooding and storm surge warnings

- Inland flooding and overland flow modelling, and many more

It includes modules such as Spectral Wave, Boussinesq Wave, Hydrodynamics, Sediment Transport, Mud Transport, Oil Spill, River Channel Design, etc. In this project, the modules Spectral Waves (SW), Hydrodynamics (HD) and Sediment Transport (ST) were used, along with the pre-processing modules of MIKE21.

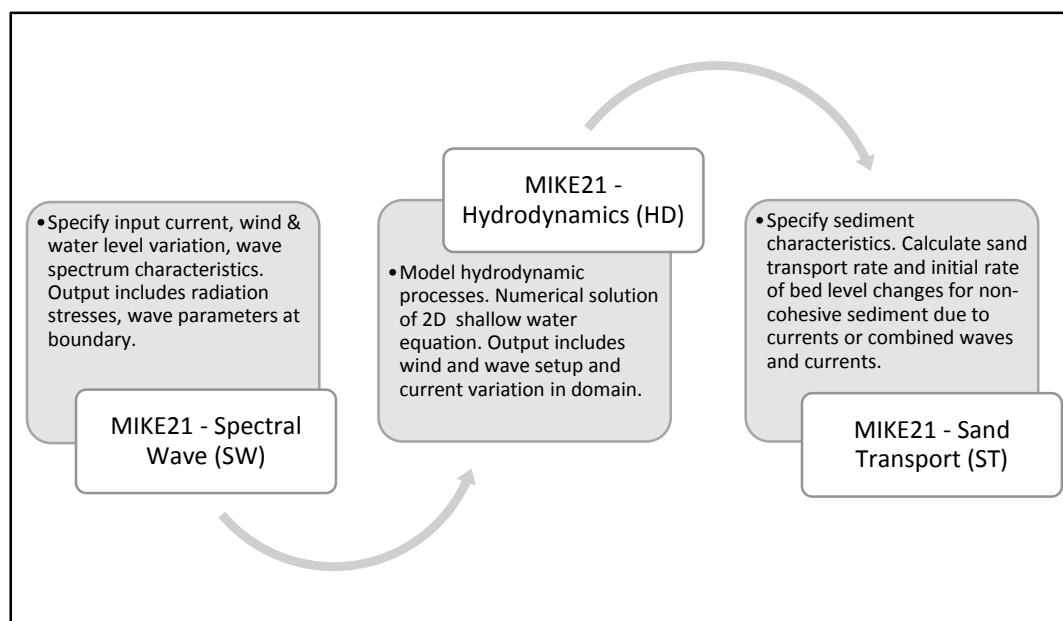A brief overview of the interaction between these modules is shown in Figure 3.1.

FIGURE 3.1 MIKE21 MODULE FLOWCHART

3.1 MIKE21 Spectral Waves (SW)

MIKE 21 SW is a 3rd generation spectral wind-wave model that simulates the growth, decay and transformation of wind-generated waves and swells in offshore and coastal areas. It solves the spectral wave action balance equation formulated in either Cartesian or spherical co-ordinates. At each element, the wave field is represented by a discrete two-dimensional wave action density spectrum. The model includes wave growth by action of wind, non-linear wave-wave interaction, dissipation by white-capping, dissipation by wave breaking, dissipation due to bottom friction, refraction due to depth variations, and wave-current interaction. Transformation of the offshore wave conditions to near shore could be conveniently carried out using this model. As the model works on a triangular mesh grid, the grids could be varied as per requirement and the accuracy of output desired. Accordingly, a coarser mesh is used for offshore area and very fine mesh in the areas of interest.

The formulations used in calculating the wave transformations have been outlined in Section 2.1.1, 2.1.2 and 2.1.3. MIKE21 SW includes two different formulations:

- Directional decoupled parametric formulation
- Fully spectral formulation

The directional decoupled parametric formulation is based on a parameterization of the wave action conservation equation. The parameterization is made in the frequency domain by introducing the zeroth and the first moment of the wave action spectrum as dependent variables (Holthuijsen et al., 1989). The fully spectral formulation is based on the wave action conservation equation (Equation 5) where the directional-frequency wave action spectrum is the dependent variable. The discretization of the governing equation in geographical and spectral space is performed using cell-centred finite volume method.

The time discretization can be applied as quasi-stationary or instationary formulations. In the quasi stationary mode, time is removed as an independent variable and a steady state solution is calculated at each time step using modified Newton-Raphson iterative procedure or iteration in the time domain. In the instationary formulation, time integration is based on a fractional step approach where each time step involves calculation of solution for the source function as well as propagation function. An unstructured mesh technique is used in the geographical domain. (MIKE21 SW Manuals, 2012)

The model, in general, requires the following inputs:

Digitised bathymetry: Basic model parameters describing the extent of the model area, the grid spacing of the computational grid, the time step and the duration of the simulation.

Boundary conditions: A spectral formulation has to be specified as an initial condition and the wave parameters (Significant wave height (H_s), Peak period (T_p), Wave direction and Directional spreading) have to be specified at all open boundaries.

Details of the boundary and initial conditions setup for the model are outlined in Chapter 5.

3.2 MIKE21 Flow Model Flexible Mesh (FM)

3.2.1 Hydrodynamics (HD)

MIKE 21 Flow Model – HD is a modelling system for 2D free surface flows based on flexible mesh approach. MIKE 21 Flow Model is applicable to the simulation of hydraulic and environmental phenomena in lakes, estuaries, bays, coastal areas and seas. It may be applied wherever stratification can be neglected. The hydrodynamic module simulates water level variations and flows in response to a variety of forcing functions in lakes, estuaries and coastal regions. The effects and facilities include:

- Bottom shear stress
- Wind shear stress
- Barometric pressure gradients
- Coriolis force
- Momentum dispersion
- Evaporation
- Flooding and drying
- Wave radiation stresses

MIKE 21 HD is a non-linear model and as such one of the most advanced and comprehensive hydrodynamic models available. It simulates in the time domain, the propagation of flows and takes the effects of the tidal variations and wave driven currents into account. The wave tide interaction is also taken in to account. The HD module is based on the numerical solution of the two dimensional shallow water, depth averaged Reynolds averaged Navier-Stokes equations (Equation 13 & 14) explained briefly in Section 2.1.5.

The spatial discretization of the equation is performed using a cell-centred finite volume method. The spatial domain is discretized by subdivision of the

continuum into non-overlapping elements. In the horizontal plane, an unstructured grid is used comprising of triangles or quadrilateral elements. An approximate Riemann solver is used for computation of the convective fluxes, which makes it possible to handle discontinuous solutions. An explicit scheme is used for time integration. (MIKE21 HD Manuals, 2012)

The model, in general, requires the following inputs:

Digitised bathymetry.

Boundary conditions: In MIKE21, hydrodynamic model requires either the surface elevation or flux at all open boundary points specified on the boundary. The choice of variation at an open boundary can either be surface level or flux passing through open boundary.

Details of the boundary and initial conditions setup for the model are outlined in Chapter 5.

3.2.2 Sediment Transport (ST)

MIKE21 Flow Model – ST describes erosion, transport and deposition of sand under the action of currents and waves or pure current. It is specifically suited for application to coastal engineering problems for studying sediment transport studies of non-cohesive sediments. The hydrodynamic basis of ST module is calculated using the HD module of MIKE21 Flow Model FM. The sand transport calculations are carried out using a mean horizontal velocity component.

The ST module can calculate sediment transport rates using two different model types:

- Pure current
- Combined wave and current

The sediment transport is calculated in two modes: bed load and suspended load (Section 2.2.2). For pure current model, the bed load and suspended load are calculated separately whereas for combined wave and current actions, the total load is calculated. For the pure current model, the formulations available in the model are:

- Engelund and Hansen (total load)
- Van Rijn (bed load + suspended load)
- Engelund and Fredsøe (bed load + suspended load)
- Meyer-Peter and Muller (bed load)

In the model with combined waves and currents, sediment transport tables need to be generated for the general spectrum of wave field. These are then used in the calculations to find transport rates using linear interpolation. Currently only one fraction of sediment input is allowed in both cases. There is also a provision for including the effects of morphological changes on the hydrodynamics of the area which in turn affect the sediment transport pattern. (MIKE21 ST Manuals, 2012)

The model, in general, requires the following inputs:

Selection of model (and formulation, if pure current) to be used.

Sediment properties such as D_{50}, porosity, gradation, relative density.

Boundary conditions: Specification of fraction concentration and layer thickness is required as initial condition and equilibrium or non-equilibrium conditions need to be specified at all boundaries in the model.

Details of the boundary and initial conditions setup for the model are outlined in Chapter 5.

4   Case study: Baydara Bay, Russia

4.1   Introduction

Gas fields discovered in Yamal peninsula (east of Baydara Bay) are important for the economic development of the region and need to be utilised. Development of these gas fields requires infrastructure growth in the form of pipelines across Baydara Bay (Figure 4.1). Construction of four submerged pipelines and two cable crossings across the bay has been planned, of which construction and commissioning of two pipelines is already complete. The pipelines transport the extracted gas to north-western Russia for further processing. Considering the significance of such projects, it is very important to design the pipelines with as much confidence as possible.
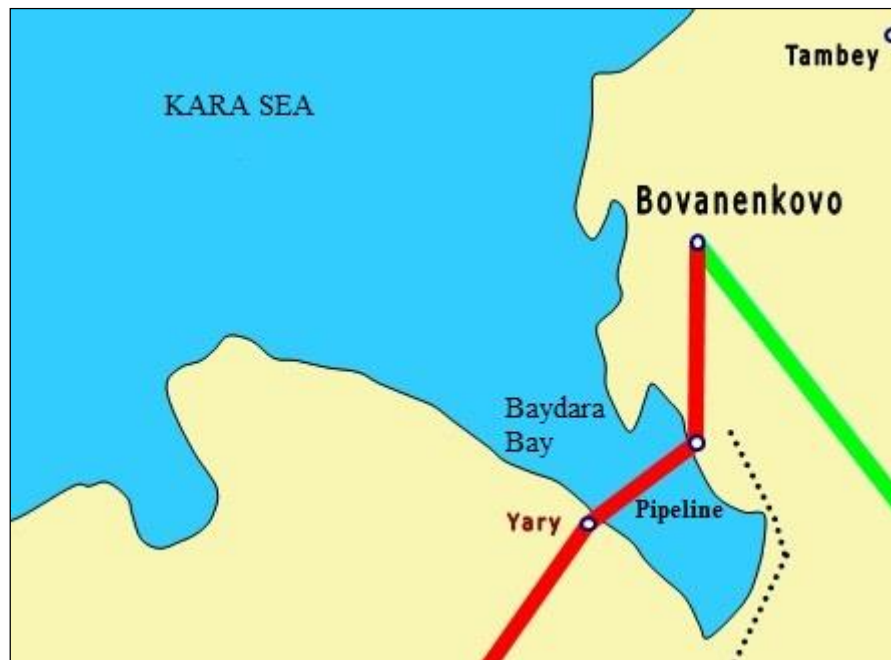

FIGURE 4.1 BAYDARA BAY - LOCATION OF GAS PIPELINE (SOURCE: WWW.EEGAS.COM)

4.2   Area description

The location selected for the purpose of the research is Baydara bay situated in the southern part of Kara Sea, Russia (Figure 4.2). The area has also been surveyed as a part of the work carried out by SAMCoT, Work Package 6, Task 6.1 as a joint study with MSU (Moscow State University) and SINTEF. The bay is situated between the two peninsulas of Yugra and Yamal. It is approximately 350 km long and 250 km wide at the mouth. The study area lies in the northern geo-cryological zone and has practically continuous permafrost.

FIGURE 4.2 LOCATION - BAYDARA BAY (SOURCE: GOOGLE EARTH API)

According to the SAMCoT Report (2013), the climatic conditions are uneven during a year and are dependent on the solar radiation, the atmospheric circulation and the proximity to a cold sea. The local climate is severe with a long-snow winter, two short transition seasons (spring/autumn) and a short cold summer. The average annual ambient temperature lies in between -7 to -10°C.
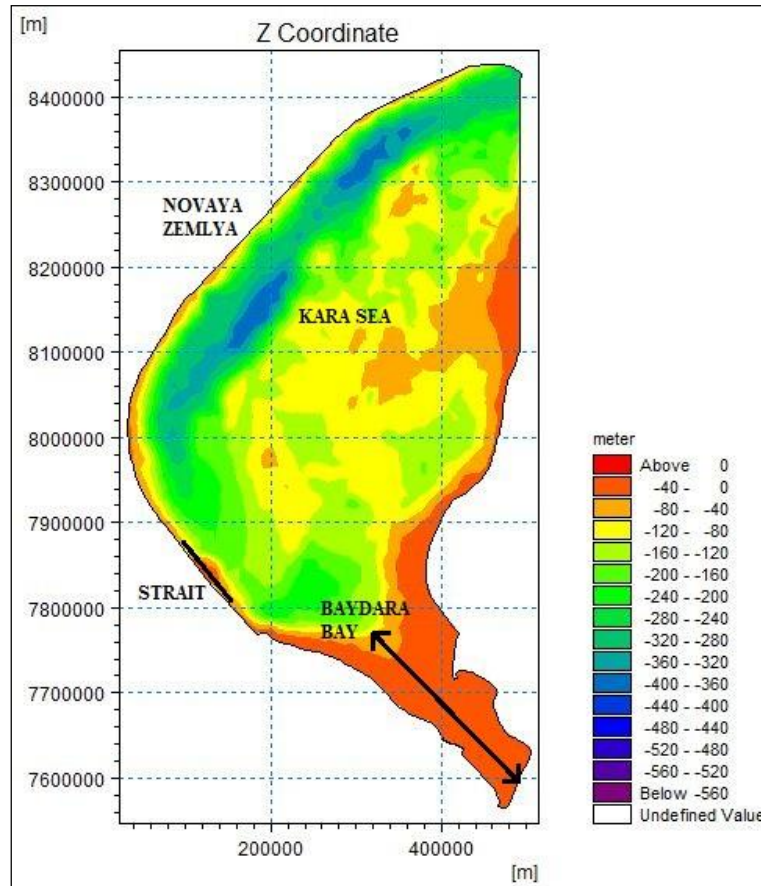
FIGURE 4.3 BATHYMETRY - KARA SEA AND BAYDARA BAY (SOURCE: MIKE21 & C MAP, JEPPESEN CHARTS, 2012)

The bay is characterized by presence of permafrost for most part of the year. The thermo-mechanical processes active during the spring season, lead to soilfluction (slumping) of the cliffs. This cliff material slides down to the beach face. The waves, which are strong only during the summer season, cause the erosion of the cliff by removing this material from the beach face.

The bathymetry of the area (Figure 4.3) shows that the bay is shallow with an average depth of around 25-30 m. A fetch length of around 750 km is available for wave growth. Presence of a strait on the western side of the sea results in an increased influence of tidal currents near the mouth of the bay.

According to Odisharia, G. E. et al., (1998), the currents near the area of interest lie in the range of 0.18 – 0.25 m/s with marginally higher velocities during flooding. However, as per the knowledge of the author, no studies have concentrated on developing a model to understand the effect, if any, of these currents on the Ural and Yamal coasts.

The site studied by SAMCoT on the Ural coast of Baydara bay is shown in Figure 4.4. Aerial photographic analysis shows that the area has been experiencing coastal erosion with an average rate of 1.5 m/year and the maximum rate recorded is 7.5 m/year (SAMCoT Report, 2013).

The tidal data available through MIKE C-Map is presented in later chapters. The wind data is available from Norwegian Meteorological Institute (NMI) and also, a detailed wind and pressure map is extracted from the database maintained by the European Centre for Medium-Range Weather Forecasts (ECMWF).
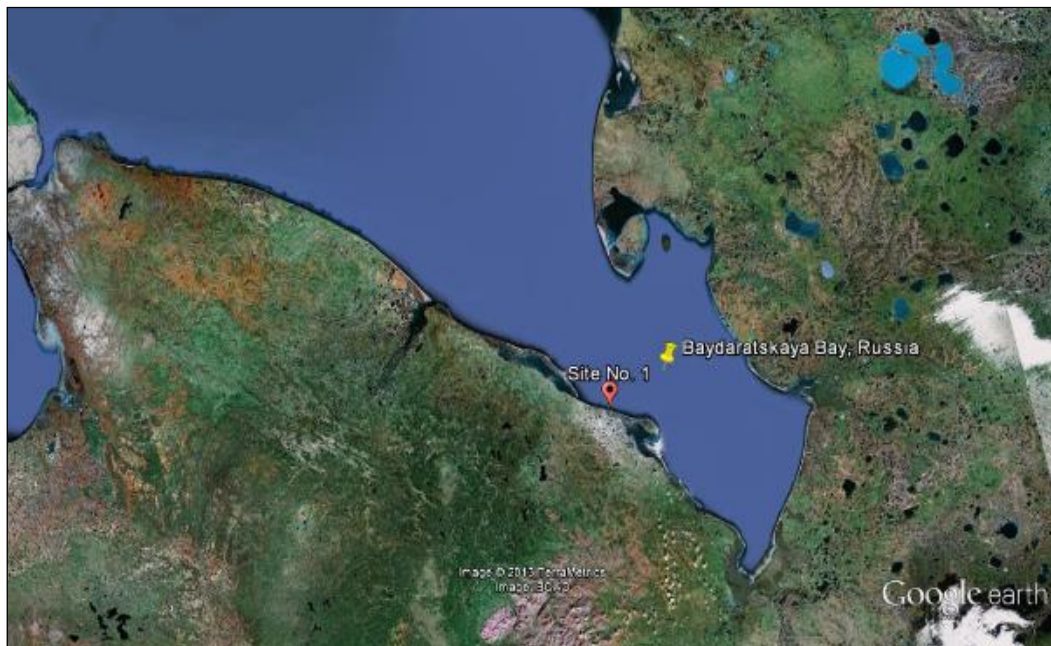

FIGURE 4.4 SAMCoT - STUDY SITE (SOURCE: GOOGLE EARTH API)

4.3   Problem description

Historically, Ural coast was considered to be in equilibrium and the only sediment transport processes active were found to be aeolian or due to ice formation (I.O. Leont'yev, 2003). Although recent aerial photographic imagery (SAMCoT, 2013) shows that the cliff and coastal erosion on Ural coast had been under estimated and the current rate of erosion is found to be around 1.5 m/year (Figure 4.5).

FIGURE 4.5 API AND GIS MAPPING - POSITION OF COASTLINE AND CLIFF LINE OVER 7 YEARS
(SOURCE: SAMCOT REPORT, 2013)

For now, the expeditions by SAMCoT have focused on collecting data at onshore sites along the bay. There has been extensive data collection regarding bore samples, soil temperature, ice and water content of soil. This data is being analysed to study the onshore thermo-mechanical erosion of the cliffs along the bay.

This thermo-mechanical erosion when coupled with removal of eroded material from beach face by waves, results in the coastal erosion occurring at the site. Hence, it is important to model these dependent processes correctly to arrive at an understanding of the area. The study presented here is based on the data collected during these expeditions and is a beginning step to combine the geotechnical as well as hydrodynamic processes to ultimately arrive at a comprehensive model to predict coastal erosion in the Arctic region.

At the moment there is no computational model that accurately predicts hydrodynamic and sediment transport characteristics in the Baydara bay. This is mainly due to lack of data for calibration from this area. Some of the datasets that are available will be used in this model to compare with the results obtained.

Critical parameters affecting the hydrodynamic and sediment transport in the region also need to be identified which can be investigated in further studies. Some representative data was made available by Dr. S. Ogorodov (Senior Researcher, Lomonosov Moscow State University, Moscow, Russia) recently, which was used to calibrate the model.

4.4   Selection of numerical model – MIKE21

There are a number of numerical models available today ranging from open source (Delft3D by Deltares) to commercial (MIKE21 by DHI). The choice of selection of MIKE21 was based on different factors. The advantage of using the MIKE21 modelling suite is the provision of flexible mesh which enables much more accurate representation of the actual area. 2D application was considered to be sufficient to arrive at a reasonably accurate model of the area. The flexible mesh approach allows a reduction of grid size locally at areas of special interest. The possibility of extracting bathymetry data from MIKE C-Map was also an advantage, as data obtained through Jeppesen chart database is of higher resolution than that obtained via open source.

NTNU also has an advantage in building competence in a model that is used worldwide, so that further research may be carried out using MIKE at the university. A detailed description of the modules within the modelling suite is presented before in Section 3.1 and 3.2 of the report.

4.5   Approach

This section details the methodology followed in determining the direction of research. The separate modules of the software package are discussed in the further sections. Data availability and computational expense define the approach of any project. For this thesis, the available data was acquired via NMI, Jeppesen charts and ECMWF website.

The main aim of the project is to arrive at a general idea of the hydrodynamic conditions present in the Baydara Bay. It is understood that it is the first step in the direction of realising the conditions in the area, and later, attempt a unified model which will include provision of thermo-mechanical erosion also. Considering all the constraints, a somewhat coarse model of the entire Kara Sea was run to obtain a set of boundary conditions that could be used further to evaluate the conditions at the site of interest. A smaller and much refined mesh for the Ural coast, was then used to arrive at an understanding of the hydrodynamics and sediment transport near the site of interest. Some general representation of the data collected at the Ural coast by Dr. S. Ogorodov was made available recently and an attempt was made to calibrate the model accordingly.

The model is first run for a period of one month (01 Aug 2006 to 31 Aug 2006) and calibrated according to the current data obtained. The model is then run for one summer season (01 July 2011 to 20 November 2011) to determine the hydrodynamic conditions present in the area. The period was chosen based on the presence of most recent data available for the area.

Sensitivity analysis for sediment transport was also carried out over a small coastline for which the boundary conditions were extracted using the larger and coarser mesh. The sensitivity of the model is tested for the following conditions:

- Importance of waves
- Effect of formulations
- Sediment grain size diameter

Finally, the conclusion and recommendations from the project are presented.

4.6 Data

The following section outlines the data that was used in setting up the model, such as bathymetry, wind and wave data, sediment data, etc. The content, origin and reliability of the data have also been discussed briefly.

4.6.1 Bathymetry

The data for bathymetry is obtained from Jeppesen charts extracted using MIKE C-Map. MIKE C-Map uses Jepessen charts to extract data for different locations. Jepessen charts are available for the entire world with a better resolution of the area than available through open source (NOAA website). Due to unavailability of wind or wave data near the site of interest, the proposed plan of action includes downscaling of the boundary conditions from a larger domain to the area of interest.

Figure 4.6 shows the interpolated bathymetry of Kara Sea based on the data extracted from MIKE C-Map. It can be seen that the bay itself is shallow with an average depth of 20 m (Figure 4.7).
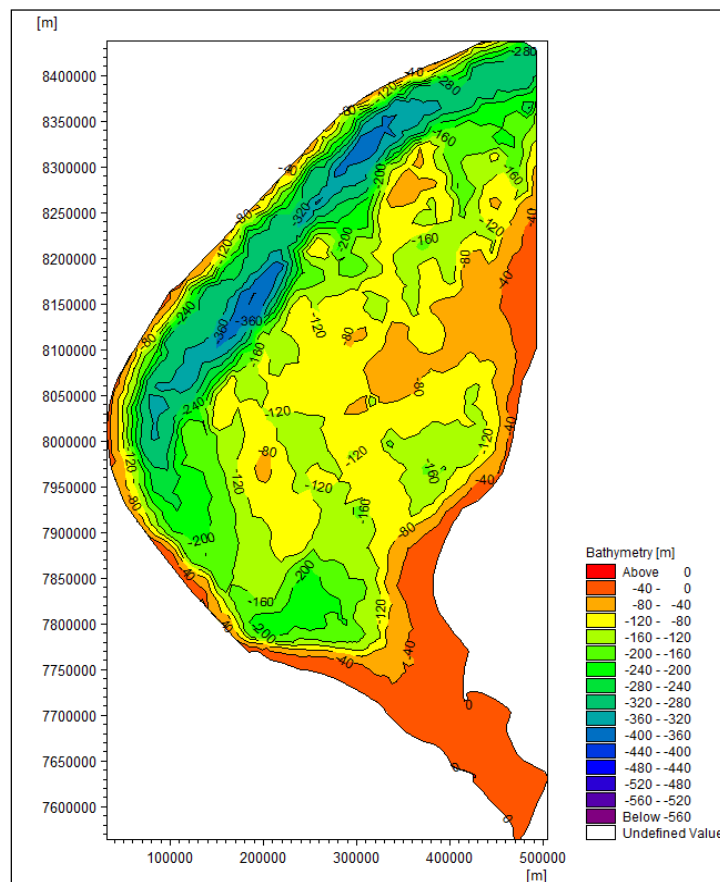

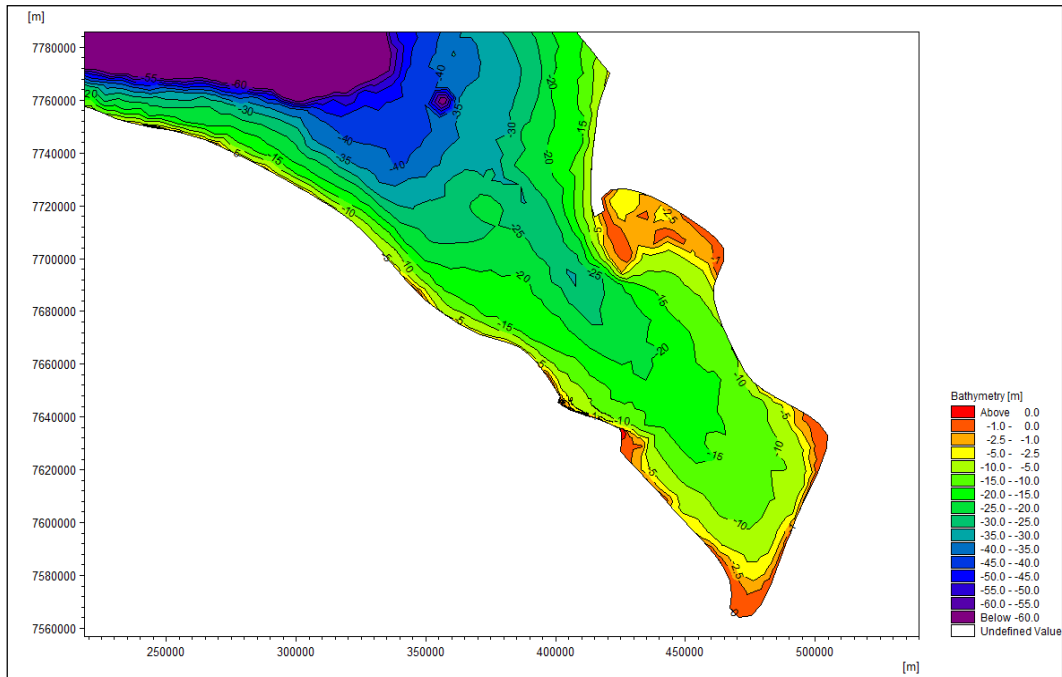FIGURE 4.6 BATHYMETRY - KARA SEA (SOURCE: C-MAP)

FIGURE 4.7 BATHYMETRY – BAYDARA BAY (SOURCE: MIKE C-MAP)

The bathymetry of the site of interest on the Ural coast is as shown in Figure 4.8.
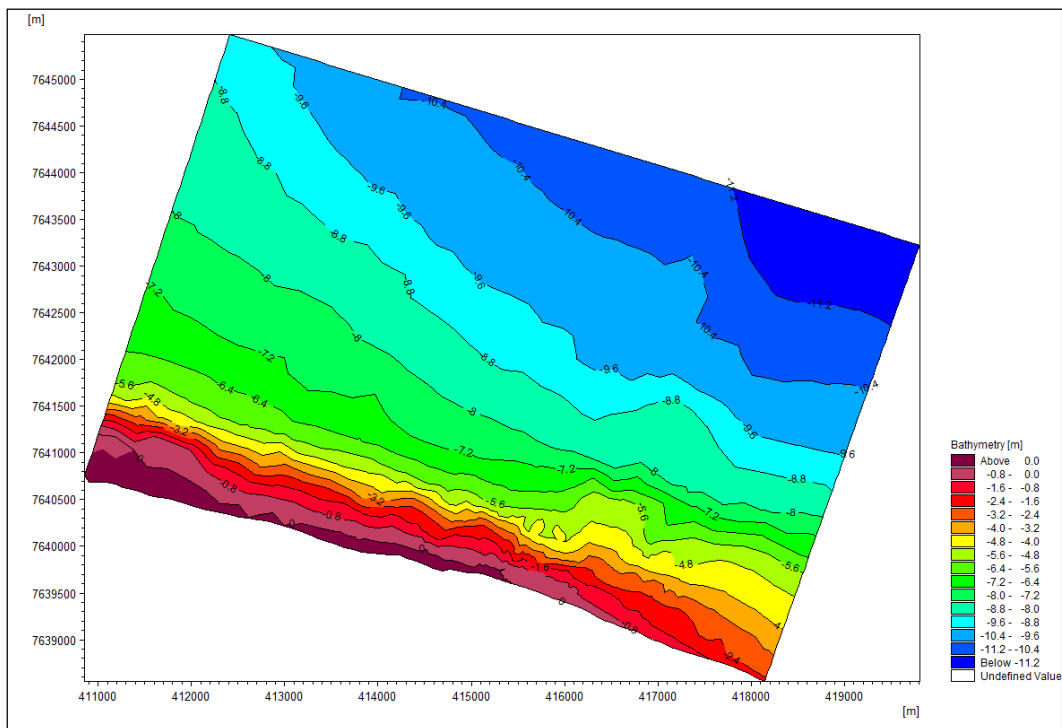

FIGURE 4.8 BATHYMETRY - URAL COAST (SOURCE: MIKE C-MAP)

4.6.2 Water level and tides

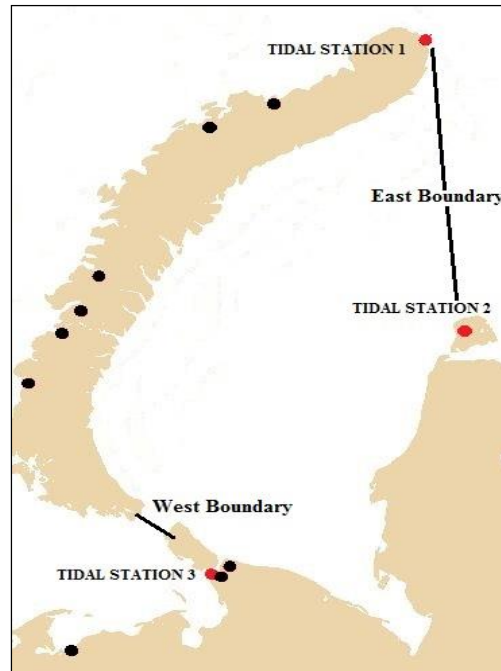The tidal data was extracted from MIKE C-Map's tidal database at the locations shown in Figure 3.11.

FIGURE 4.9 TIDAL STATIONS AT MODEL BOUNDARIES

The tidal levels at edges of the eastern boundary (Tidal Station 1 - Zhelaniya & Tidal Station 2 - Ragozina) were averaged across the length to arrive at an assumed linear water level variation at the boundary. The closest tidal station available near the strait on the western boundary was Bukhta Varneka whose water level variation was transferred across the line.

Figure 4.10 and Figure 4.11 show the tidal level variation at the boundaries. The tidal characteristic at the western boundary is mixed with predominantly semi diurnal type. The tide at the station Zhelaniya has a diurnal characteristic whereas the tide at the station Ragozina has a semi-diurnal characteristic. The tidal level at these two stations is interpolated across the boundary on 10 points across an approximate distance of 400 km between them

These assumptions in the water level variation across the boundaries are made since the actual area of interest is far away from the boundaries and its influence on the results is assumed to be negligible.
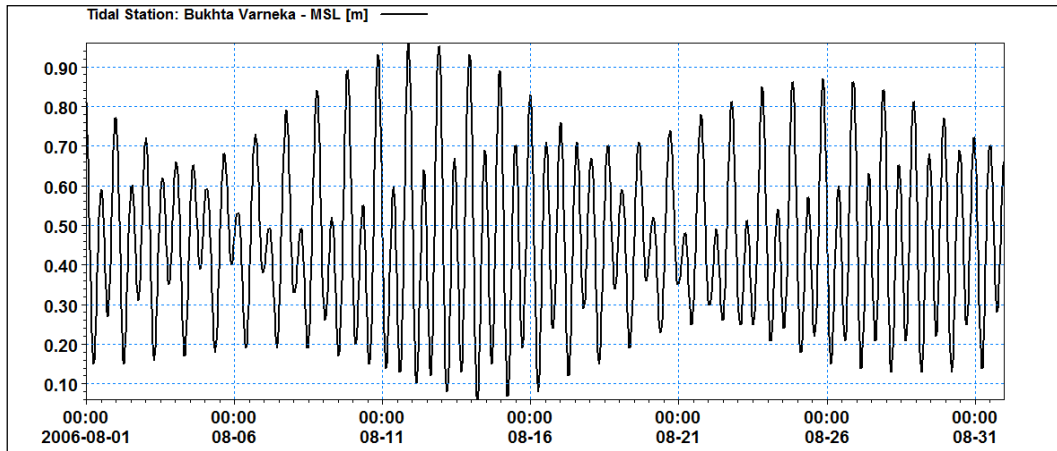
FIGURE 4.10 TIDAL ELEVATION AT WEST BOUNDARY (SOURCE: MIKE C-MAP)
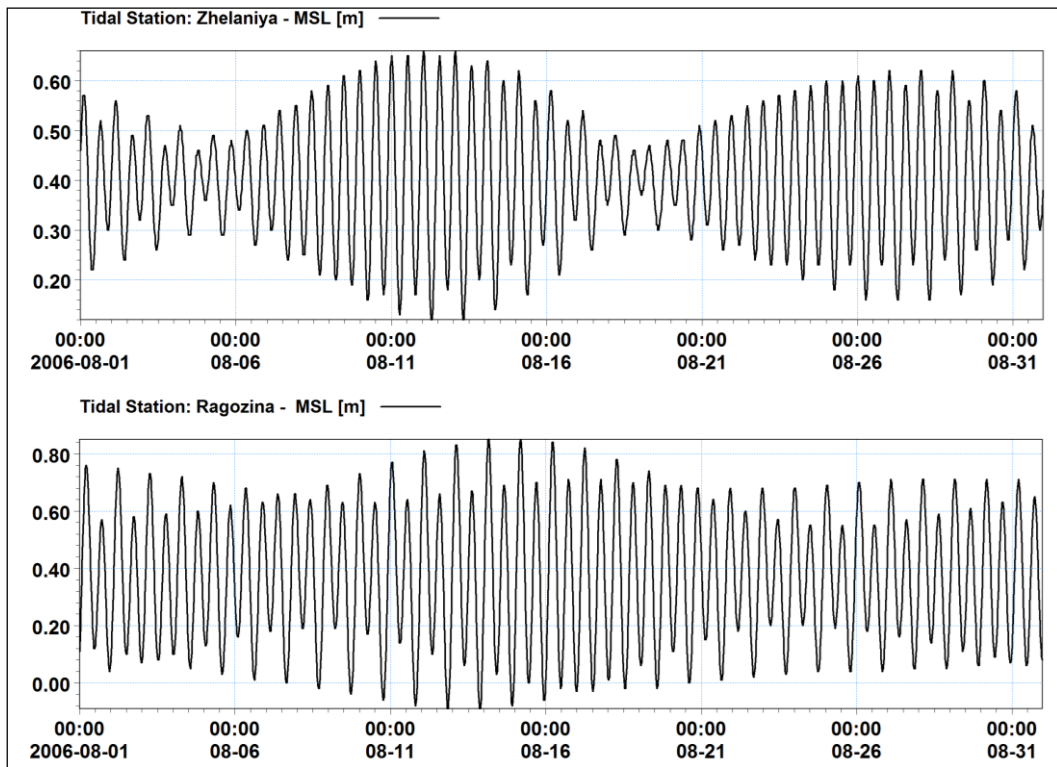

FIGURE 4.11 TIDAL ELEVATION AT EAST BOUNDARY (SOURCE: MIKE C-MAP)

3.6.3 Wind

Wind and wave data is available from the Norwegian Meteorological Institute (NMI) at the locations shown in Figure 4.12.

FIGURE 4.12 LOCATIONS OF DATA AVAILABILITY THROUGH NMI

A wind rose diagram over a period of the 5 months in 2011 that are analysed is shown in Figure 4.13 for location 3, near the mouth of the bay. Wind distribution shows that the prominent sector is North and North West with an average wind speed of 7.2 m/s.
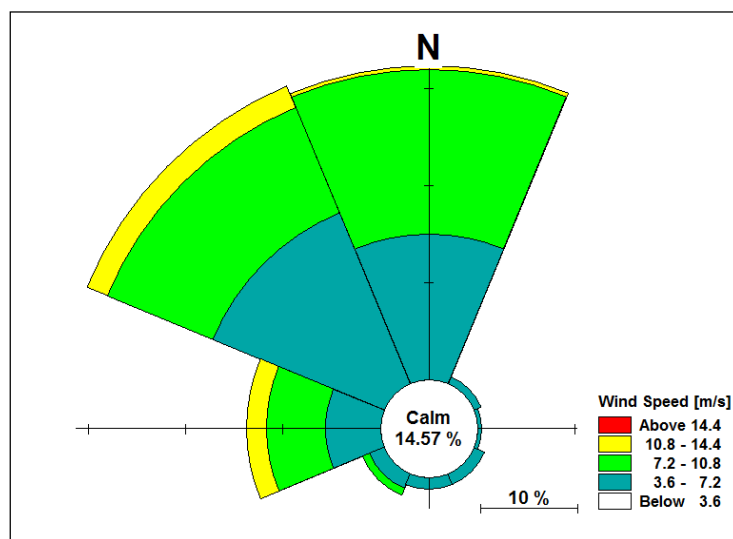

FIGURE 4.13 WIND ROSE PLOT AT MOUTH OF BAY (LOCATION 3, SOURCE: NMI DATA)

Wind data used as input in the simulation is extracted from ECMWF database. It is available in the form of resolved wind velocity components in the x and y direction. Details of the extracted wind data are discussed in Section 5.1.1.1. Figure 4.14 shows the comparison between the wind data from NMI and ECMWF at the mouth of the bay. It is seen that the both the datasets are consistent with each other.
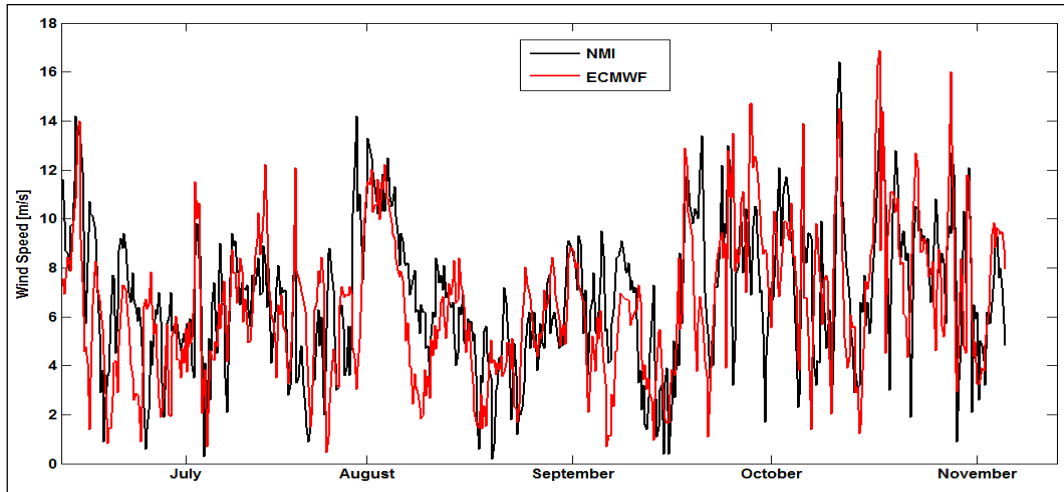

FIGURE 4.14 COMPARISON OF NMI AND ECMWF WIND DATA FOR SUMMER 2011

Analysis of the wind data for the period of summer in 2011 is also presented. Different fits were attempted such as, Weibull with Method of Moments (MoM), lognormal distribution, Gumbel and normal (Gaussian) distribution fit. It can be seen that the wind data is well represented by a normal distribution fit (Figure 4.15).
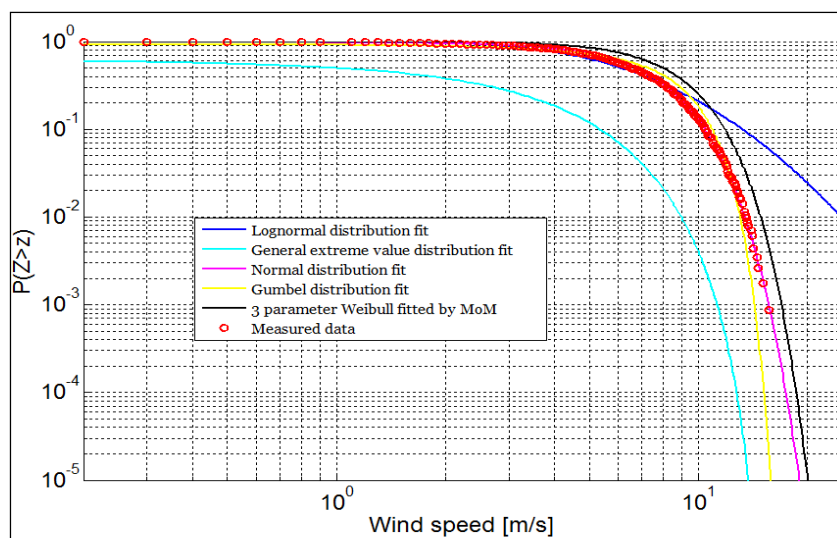

FIGURE 4.15 WIND DATA PROBABILITY ANALYSIS - BASIC CURVE FITTING

3.6.4 Waves

Waves have a seasonal characteristic in Baydara Bay. They are found to be influenced by the fetch length available over the Kara Sea. The shallow bay area results in depth induced breaking and the waves that reach the shore have significantly smaller wave heights. The annual significant wave height averages between 0.5-1 m with an average peak period of 6 seconds. Analysis of the wave data of over 6 years in the bay shows that the waves are present only during July-December (Figure 4.16). The average significant wave height at the entrance of the bay is around 0.5 m with a peak period of 4.8 seconds.

Wave data is provided by Norwegian Meteorological Institute at the locations shown in Figure 4.12. The wave data on locations 0, 1 and 2 is interpolated across the eastern boundary to be used as an input in the model simulation.
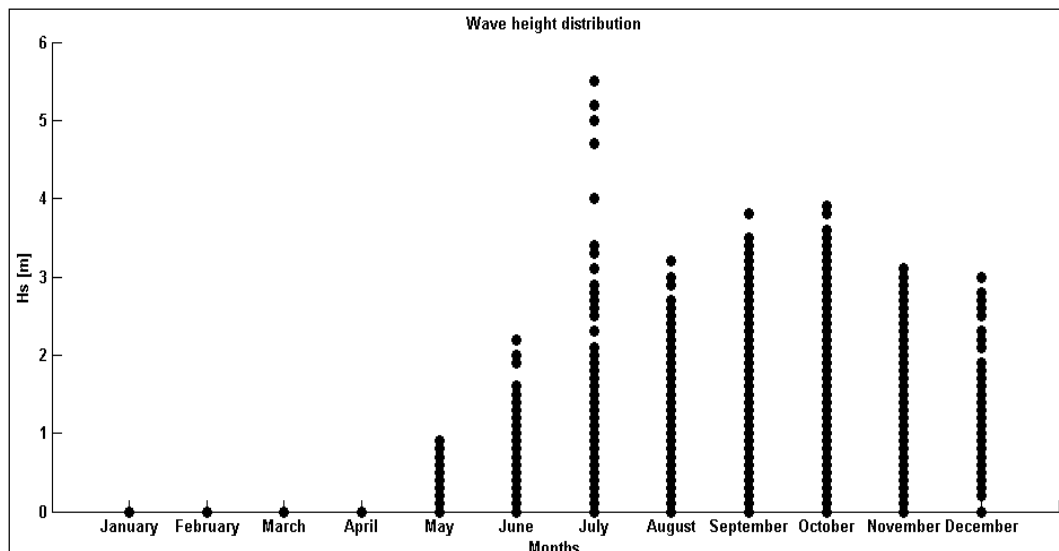

FIGURE 4.16 MONTHLY WAVE HEIGHT DISTRIBUTION OVER 6 YEARS (SOURCE: NMI DATA)

Wave data for the period of August 2006 at location 3 indicates that for around 20 days in the beginning of the month, there are no waves inside the bay. This is due to the presence of ice across the bay during the period during which no values were recorded.

For the analysed summer season of 2011, the wave rose plot in Figure 4.17 shows that the North and North West direction is the predominant sector with an average significant wave height of 0.8 m. For the locations offshore (1, 2 & 3), the average significant wave height lies in the range of 1-1.2 m with an average peak period of 5.7 seconds. No information is available regarding directional spreading of the waves in the offshore locations and hence, a value of 30° is chosen considering uniform spreading (Donelan, M. A., et al., 1985).
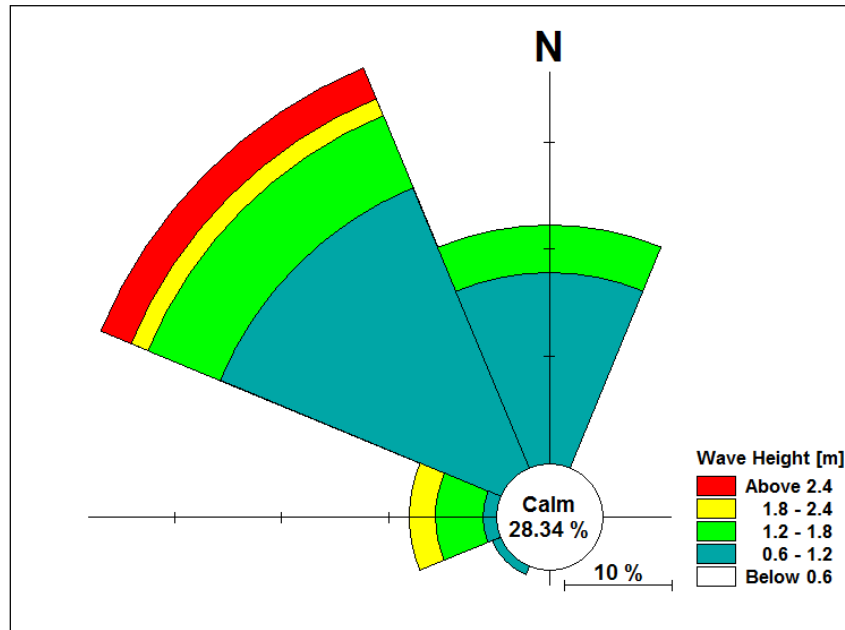
FIGURE 4.17 WAVE ROSE PLOT AT MOUTH OF BAY (LOCATION 3, SOURCE: NMI DATA)

The scatter plots of waves for the wind-sea, swell and the resultant total waves for the period of summer (July-November) 2011 at the mouth of the bay are presented in Figure 4.18, Figure 4.19 and Figure 4.20. The scatter plot for the waves show that the shorter period sea waves cover a wider band, however the swell waves are mostly restricted to NW and NNW direction. The resulting waves also conform to this band.

FIGURE 4.18 WIND SEA SCATTER PLOT (LOCATION 3, SOURCE: NMI DATA)

FIGURE 4.19 SWELL SEA SCATTER PLOT (LOCATION 3, SOURCE: NMI DATA)
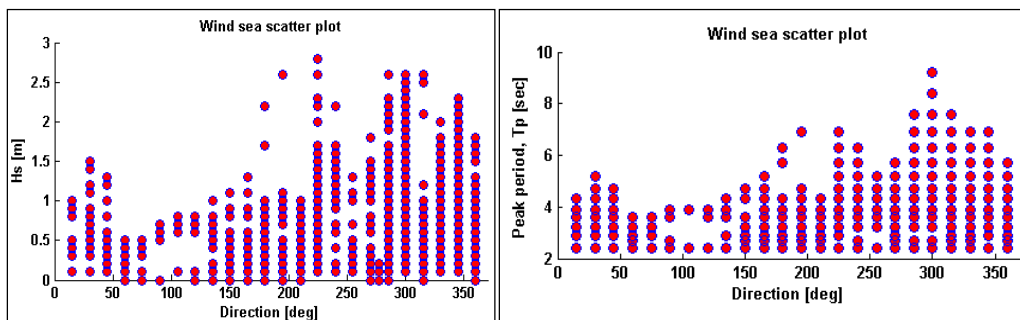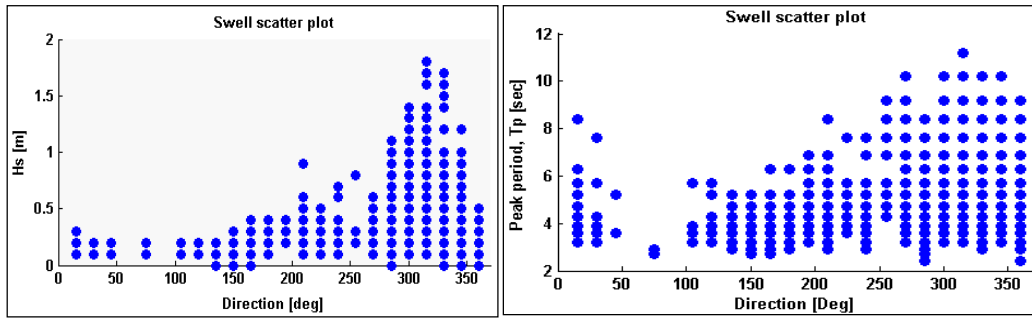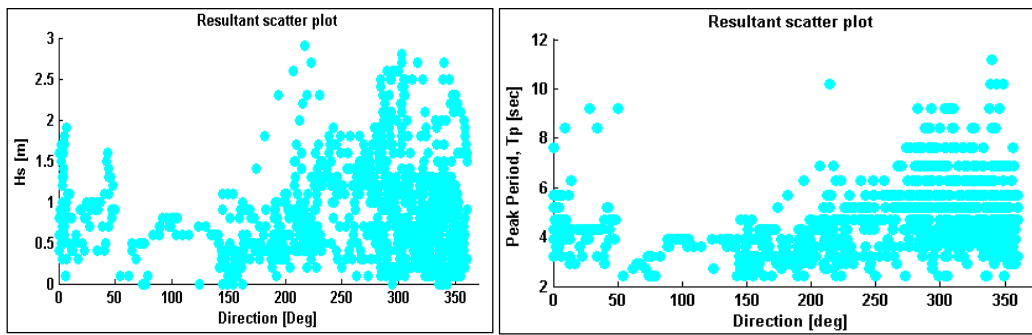

FIGURE 4.20 RESULTANT SEA SCATTER PLOT (LOCATION 3, SOURCE: NMI DATA)

3.6.5 Sediments

The bay is characterised by mixture of fine sand and clay. The average grain size diameter at the site of interest is recorded as between 0.35-0.4 mm (Source: Personal communication with Dr. S. Ogorodov, Senior researcher, Moscow State University). From the site investigations undertaken by SAMCoT, it was found that the sediment in the cliff has a specific density of around 2.64 g/m^3 (SAMCoT Report, 2013). Although the bores were taken on the cliffs on the shoreline, it is assumed that the material being transported by the waves is represented by them.

It can be seen in Figure 4.21 that the area of interest has a sediment transport pattern moving towards the inside of the bay for the given period as shown by the blue arrow. The graphs shown in the figure near the coast line are representative grain size distributions diagrams showing the percentage content of each grain size. It can be seen that the sediment distribution most of the sites along the Ural coast, shows a grain size diameter range of 0.2-0.5 mm. The red dotted lines near the area of interest (marked in figure) shows the location of the proposed pipeline across the Baydara Bay.
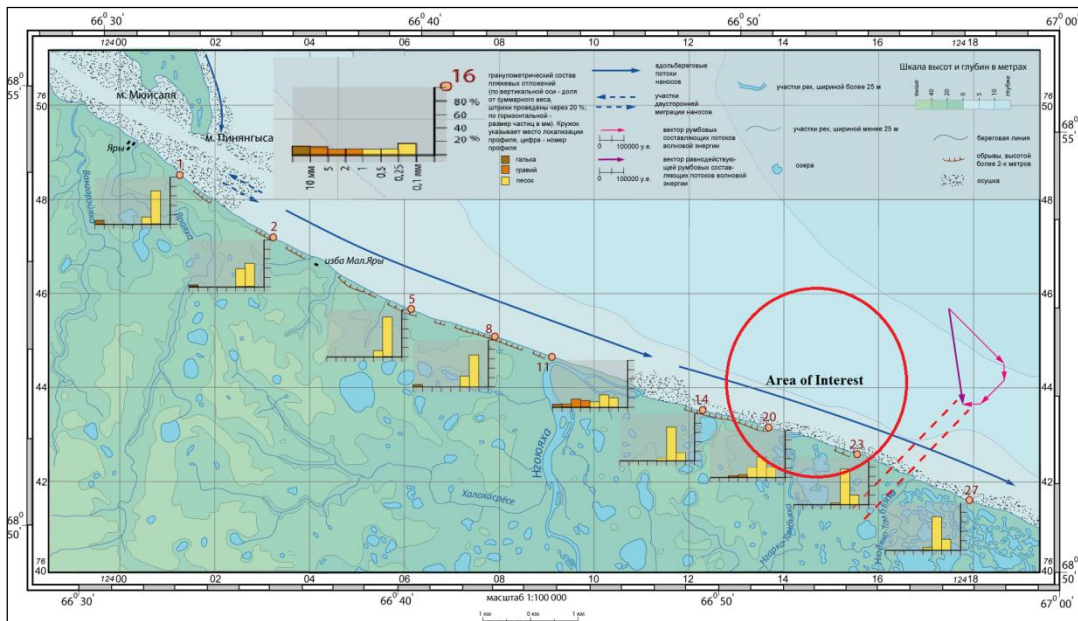
FIGURE 4.21 LITHODYNAMICS OF URAL COAST
(SOURCE: DR. S. OGORODOV, MOSCOW STATE UNIVERSITY)

5   Results

As discussed in Section 4.5, the model simulations were divided into two parts:

- Large area (Coarse mesh - Kara Sea) – arrive at boundary conditions nearshore using offshore boundary conditions
- Small area (Fine mesh – Ural coast) – calibrate using available data, calculate hydrodynamic conditions for most recent data and carry out sensitivity analysis for sediment transport for the same

The time for which the model simulated the conditions was:

- 01 August 2006 to 31 August 2006 – to obtain results for calibration
- 01 July 2011 to 20 November 2011 – to model conditions for most recent data available

A summary of the model simulation runs is presented in Figure 5.1.

FIGURE 5.1 SUMMARY OF SIMULATION RUNS

5.1 Calibration runs

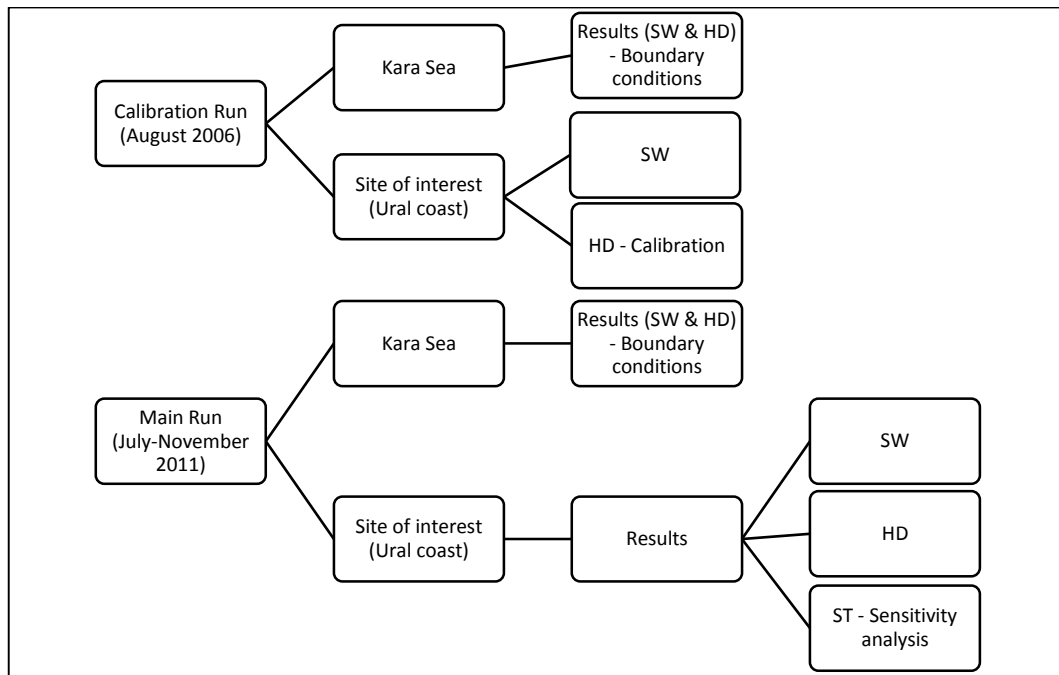The aim of these runs was to calibrate the parameters for the hydrodynamic conditions based on the current data set provided by Dr. S. Ogorodov (Senior researcher, Moscow State University) for the Ural coast in 2006. Accordingly, the model was run for the time period of 1 month from 01 August 2006 to 31 August 2006. The runs were divided in two parts as mentioned before

- Kara Sea
- Site of interest (Ural coast)

The Kara sea simulations were required to transfer the offshore boundary conditions to the Ural coast where the hydrodynamic conditions have to be studied. The results from the Kara sea runs were extracted as boundary conditions to be used in the simulation for smaller area with finer mesh.

5.1.1 Kara Sea

The model is run for the entire domain of Kara Sea to arrive at boundary conditions to be used for the simulation for the site of interest on Ural coast for the period of August 2006. The results are also compared against the data obtained from the Norwegian meteorological institute.

5.1.1.1 Model setup

The aim of this model run was to obtain boundary conditions near the site of interest. Both SW and HD modules were run with the data described in Section 4.6. The simulation periods and time step applied in the study are given in Table 5-1.

TABLE 5-1 SIMULATION PERIOD AND TIME STEP – KARA SEA – CALIBRATION RUNS

Sl. No.	Period	Duration	Time step (seconds)		Remarks
			SW	HD	
1	1st August 2006 to 31st August 2006	30 days	1800	1800	For obtaining boundary conditions for site of interest (Ural coast)

A nested approach was used in creating the mesh to minimise the errors in calculating the results. Figure 5.2, Figure 5.3 and Figure 5.4 show the details of the larger mesh created. For the larger domain in the mesh, a resolution of 13 km was used (Figure 5.2) progressively reducing to 5 km for Baydara Bay (Figure 5.3) and for the coastline of interest a resolution of 500 m was applied (Figure 5.4). The total number of elements used in the mesh is 8232 with 4399 nodes. The Courant–Friedrichs–Lewy (CFL) number was chosen as 0.8 for stability as recommended by the authors of the software in the user manual.
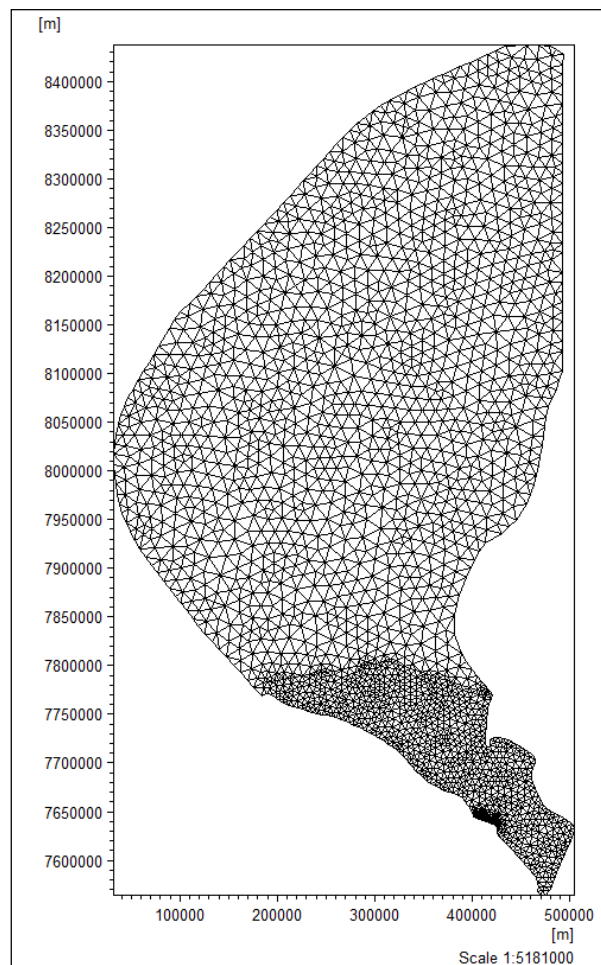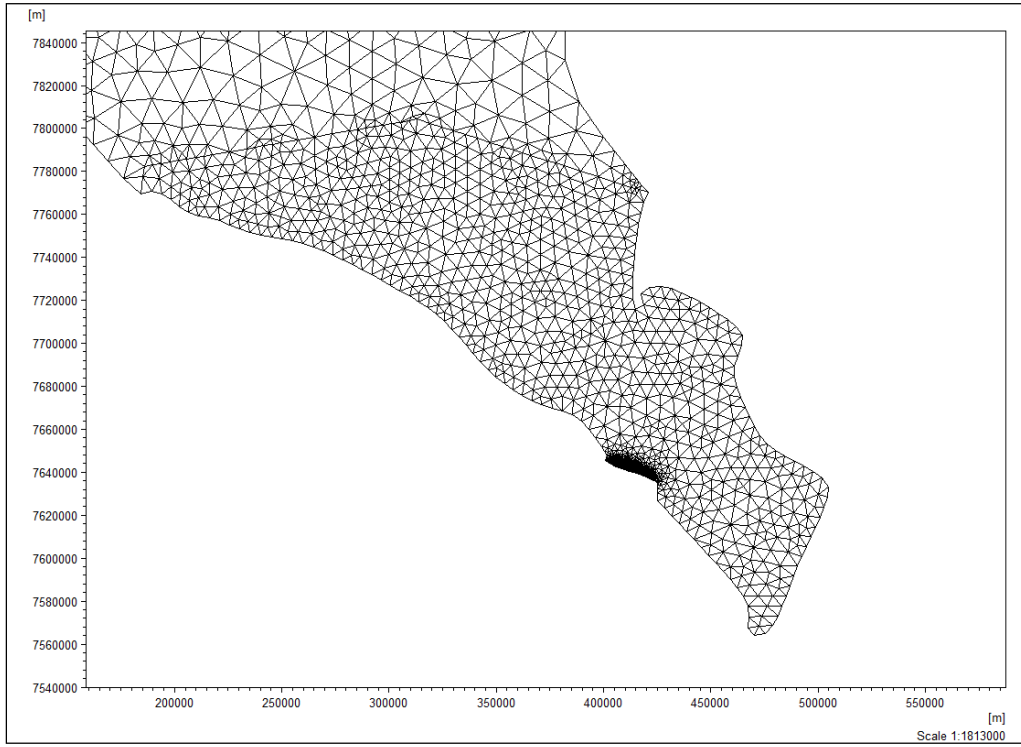

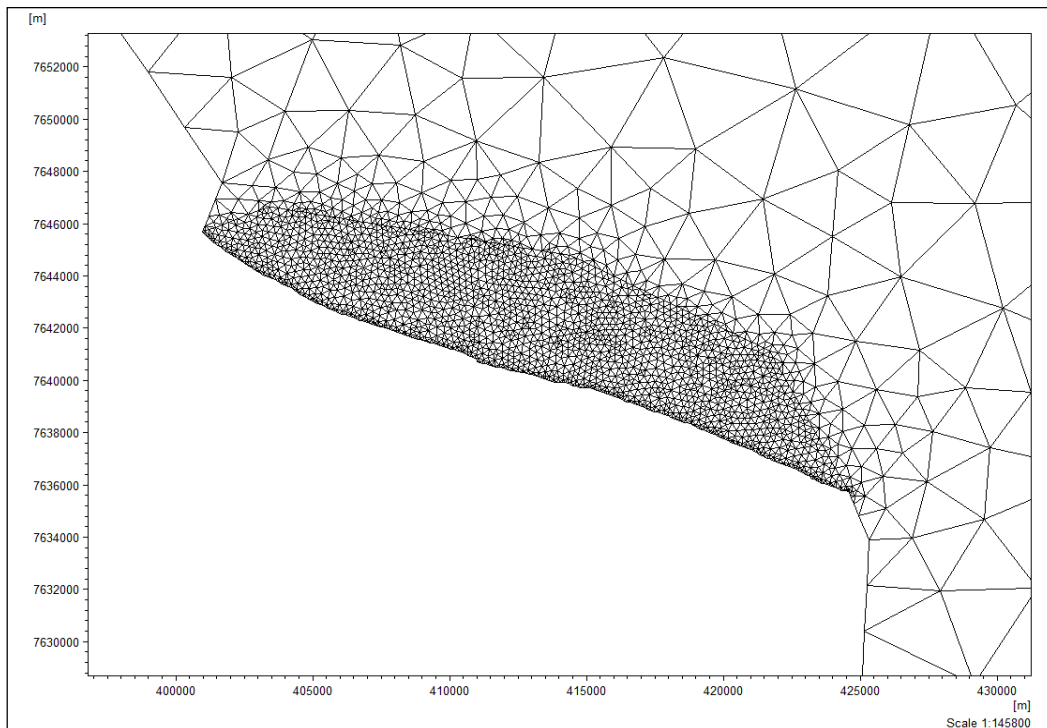FIGURE 5.2 KARA SEA MESH

FIGURE 5.3 BAYDARA BAY MESH

FIGURE 5.4 MESH AT SITE OF INTEREST

The interpolated bathymetry using C-Map data is shown in Figure 5.5.
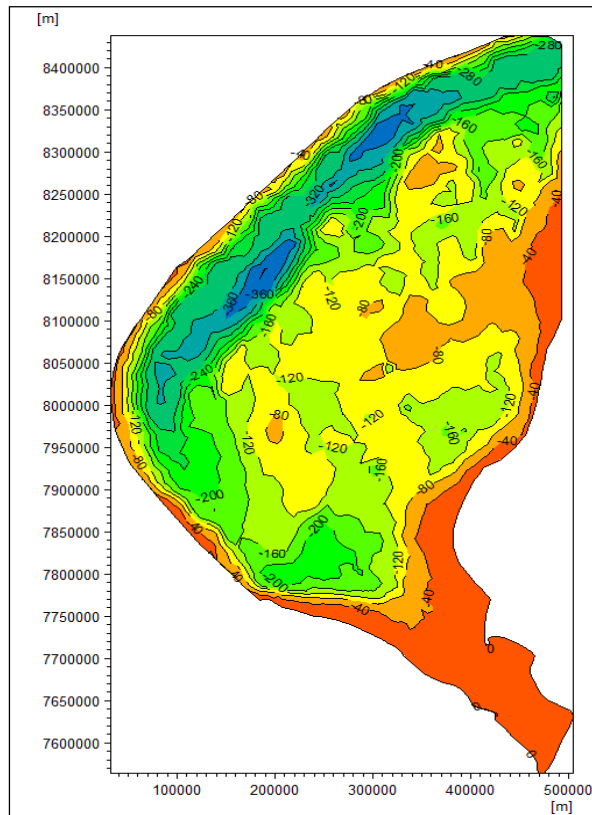
FIGURE 5.5 BATHYMETRY - KARA SEA

The boundaries defined for the area are shown in Figure 5.6. The choice of the boundaries was defined by the data available (See also: Figure 4.12).
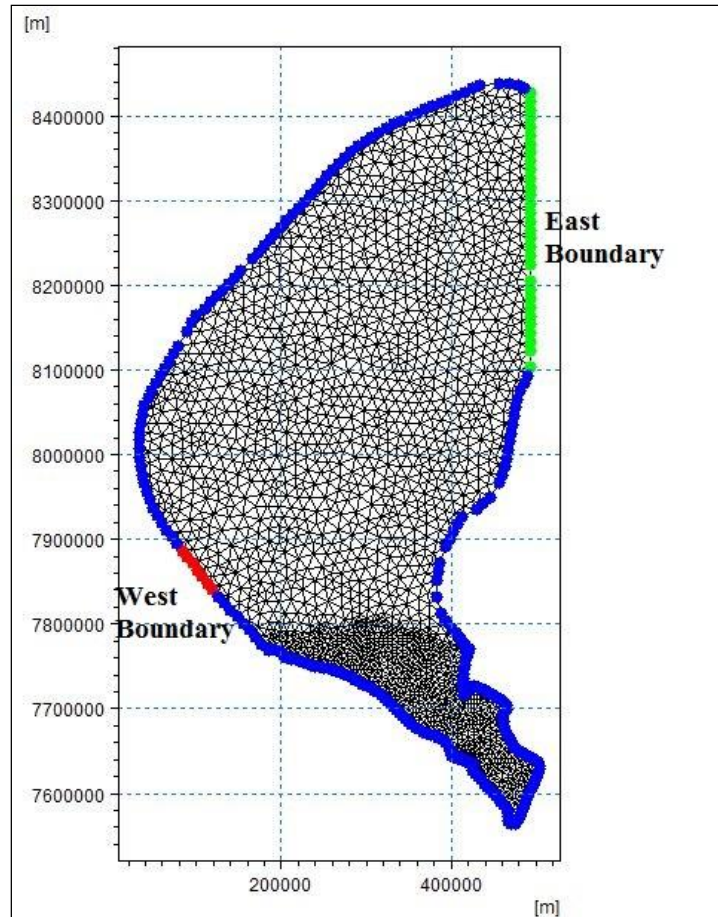
FIGURE 5.6 DOMAIN BOUNDARIES

For the Spectral Wave module, fully spectral and instationary formulation were used with logarithmic time discretization and a separation of wind-sea and swell at a threshold period of 8 seconds. The time step of 1800 seconds was chosen considering the large extent of the area (more than 240 km^2) as a smaller time step increases the simulation time by a large amount. Also considering the large area of the domain, Coriolis forcing and tidal potential were also included in the runs to improve accuracy.

The major parameters that are used for calibration – Manning's number, n or its reciprocal, M and eddy viscosity coefficient (Smagorinsky formula) were kept at default values for these runs considering the effect of these variables will be negligible over such a large domain. The parameters used are as shown in Table 5-2.

TABLE 5-2 SIMULATION PARAMETERS

Sl. No.	Parameters	Values
1	Bed resistance – Manning's number [$m^{1/3}$/s]	1/n = m = 32
2	Eddy viscosity coefficient (Smagorinsky formulation)	0.28

The distribution of wind across the profile was extracted from the database at ECMWF's interim reanalysis (Dee D.P, et al., 2011). ERA-Interim products are publicly available on the ECMWF Data Server, at a 0.75° resolution, including several parameters such as wind components, wind gusts, cloud cover, mean sea level pressure, precipitation, etc. The data for wind was obtained as U & V components of wind velocity at 10 m height for the entire Kara Sea at an interval of 6 hours. U and V components of the wind velocity are calculated from decomposing the wind magnitude and direction along the two horizontal axes: x and y. Figure 5.7 shows an example view of U component of velocity for the area.

A detailed wind map was prepared for the period of simulations covering the entire area describing the wind velocity component variations as well as mean sea level pressure distribution.
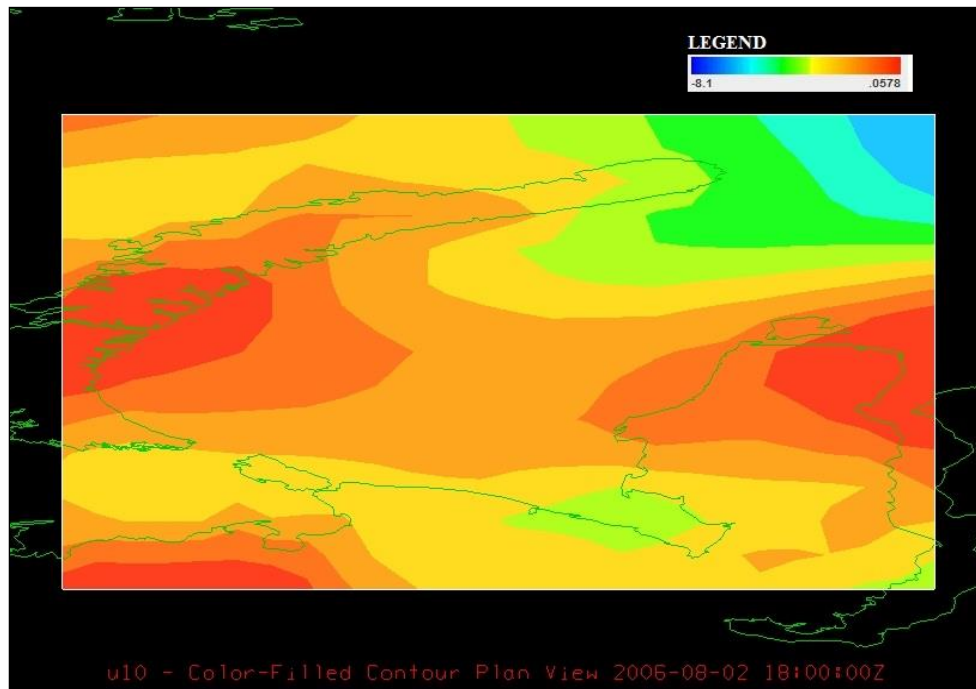

FIGURE 5.7 HORIZONTAL WIND VELOCITY COMPONENT (M/S) CONTOUR PLAN OVER KARA SEA (SOURCE: ECMWF)

An initial water level variation of 0.41 m was applied as an average value based on the tidal data at the boundaries. Diffraction and ice coverage were not considered in the simulation. Energy transfer between waves was considered to be due to quadruplet wave interactions. A default wave breaking parameter of 0.8 was applied and the bottom roughness was kept at default value of 0.04 m (Nikuradse's roughness). The wave characteristics have been discussed in Section 3.6.4. At eastern boundary the wave parameters were applied as varying in time and along the line to obtain a more realistic offshore conditions. The western boundary was assumed as a lateral boundary, where the wave parameters are interpolated linearly across the boundary based on the first time step. A soft start of 7200 seconds was used to linearly arrive at the first time step to avoid sudden changes. A JONSWAP spectrum with default parameters was used to generate initial conditions across the domain.

The results obtained from the SW run were then applied across the domain in HD run for August 2006 as wave radiation varying in time and domain. Higher order space and time discretization were used for solving with a default CFL number of 0.8. A barotropic model was used for density calculations. For the eddy viscosity calculation, Smagorinsky formulation was applied with the default coefficient of 0.28. Coriolis and default tidal components were also included in the simulation considering the large area of domain.

An initial level of 0.41 m was applied across the domain interpolated from the tidal variation at both the boundaries. At the eastern boundary the mean sea level was applied as varying in time and along the line (as mentioned in Section 4.6.2). Similarly, the mean sea level variation from the tidal data was applied as boundary condition on the western boundary. Wind was applied as components in x & y axes along with mean sea level pressure data extracted from ECMWF. A similar soft start as SW, of 7200 seconds was applied to avoid sudden changes in the water level.

The results of these two configurations of SW & HD were then used in the finer mesh as boundary conditions (Section 5.1.2) to arrive at results to check against the data available.

5.1.1.1 Results

The offshore conditions were transferred to the nearshore coastal area using the results of these simulations. The wave field was found to be dependent largely on the wind condition applied over the domain. The wave heights in the Kara Sea were found to reach a maximum of 4.67 m with a peak period of 5.29 second. The wave height and directional distribution for one time step is shown in Figure 5.8.
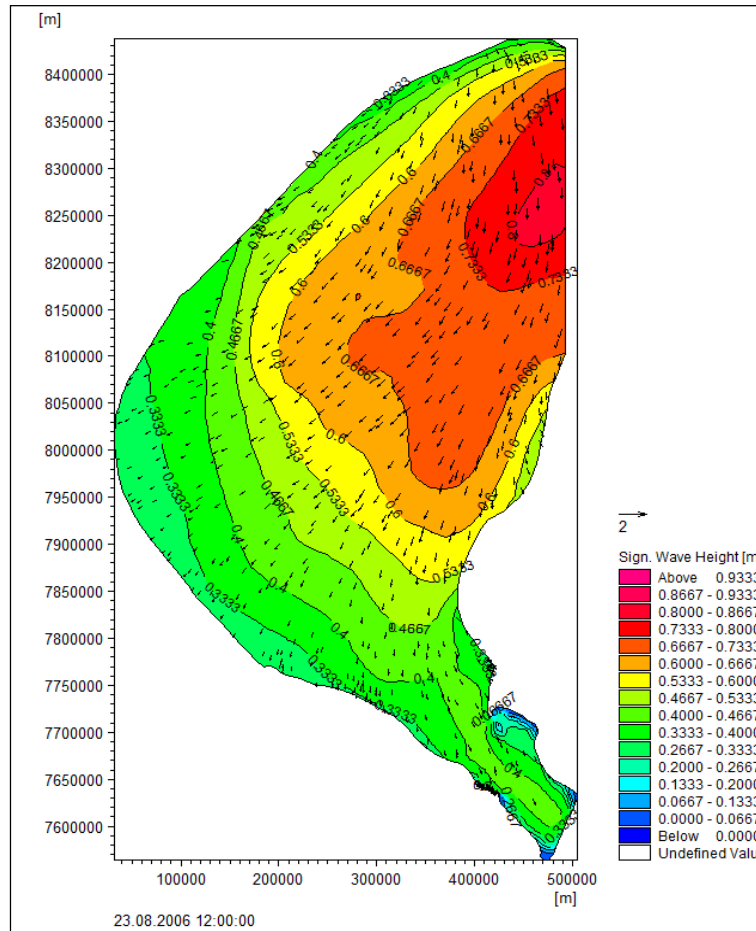
FIGURE 5.8 MODEL EXTRACTED WAVE CONTOURS AND DIRECTION - KARA SEA

The model results were found to be in good comparison with the data available from NMI at the mouth of the bay (Figure 5.9). It should be noted that the wave data for the period of August 2006 in the bay was only for 10 days as the bay was frozen for the first 20 days of August. The discrepancies between the two can be accounted for considering the frequency of time record and inclusion of ice coverage over the bay.
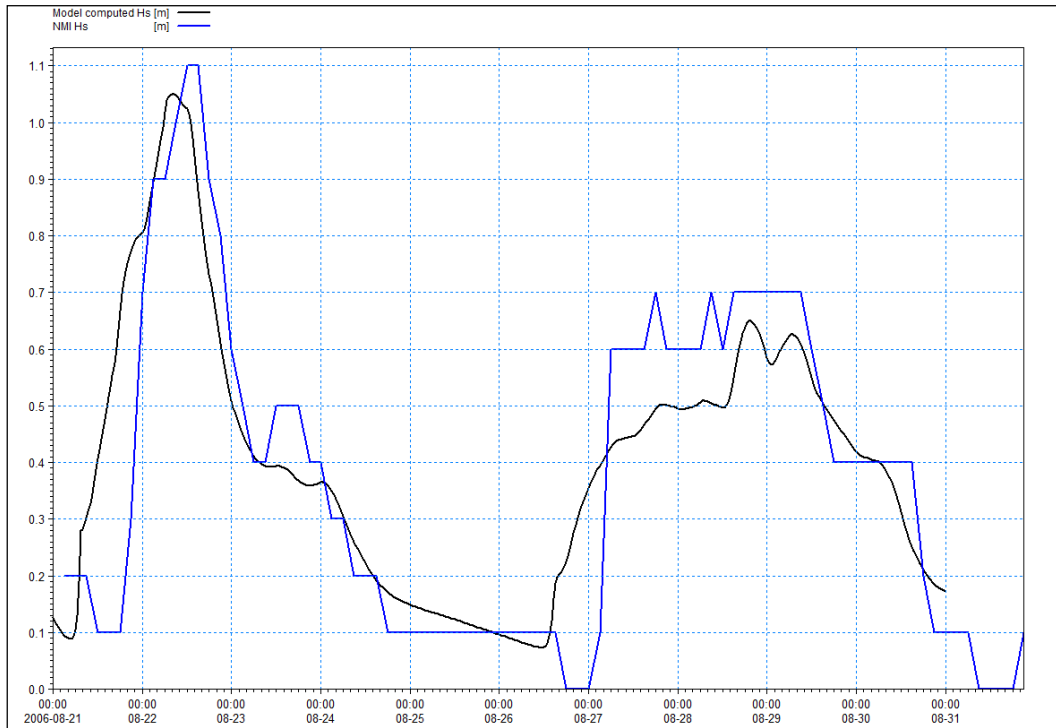
FIGURE 5.9 TIME SERIES OF MODELLED VERSUS OBSERVED WAVE HEIGHT

Figure 5.10 shows the wave rose plot at the mouth of the bay for the period in August 2006 when waves are active (21st August to 31st August). Considering the short duration, the wave directions, in general, are in agreement with the observed data from NMI.
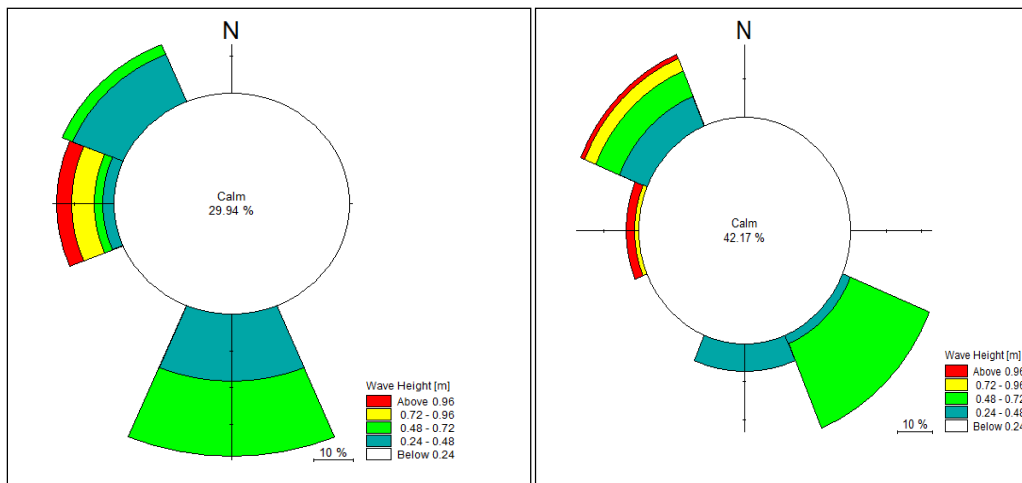
FIGURE 5.10 WAVE ROSE PLOT AT MOUTH OF BAY. **LEFT**: MODELLED DATA, **RIGHT**: NMI DATA

The hydrodynamic simulations show the current and surface level variation for Kara Sea (Figure 5.11 and Figure 5.12) for the period of August 2006. The current

variation in the bay area is in the range of 0.1 to 0.5 m/s. Larger currents in the range of 1 to 4 m/s were found at the strait at the western boundary. These values were also in the range as discussed in correspondence with researchers at SINTEF Marine Resource Technology (Personal communication with - Ingrid Ellingsen and Thomas McClimans).
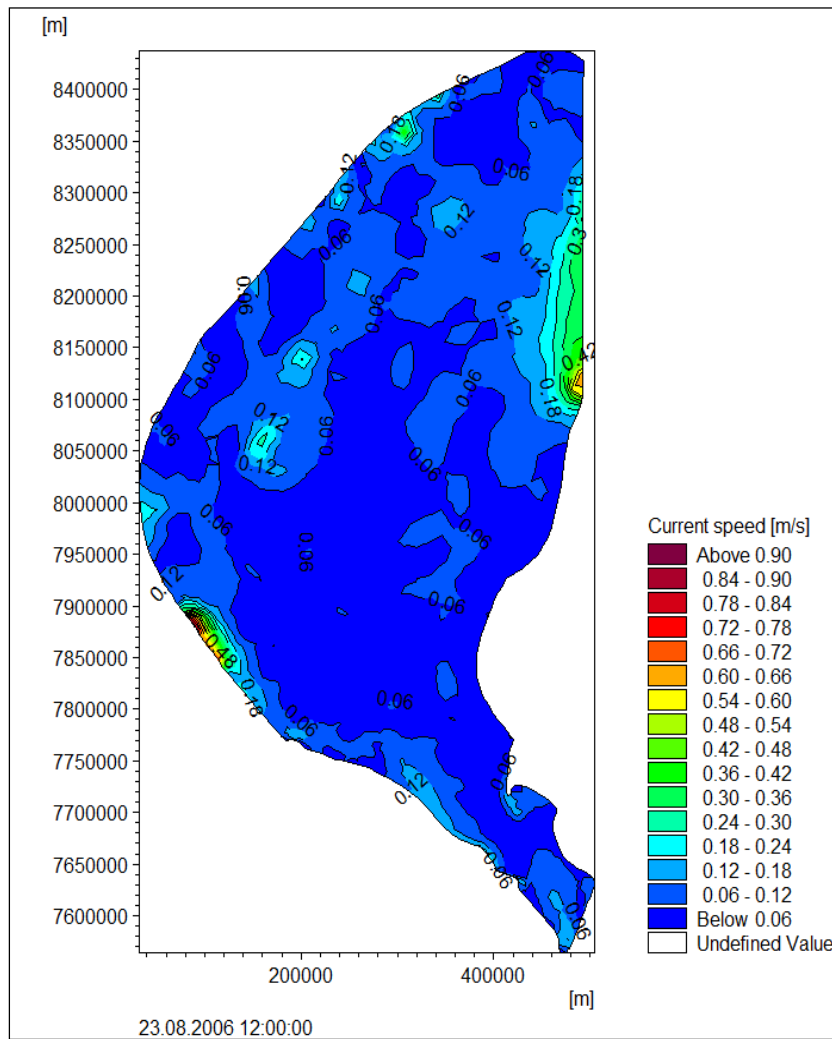
FIGURE 5.11 MODEL EXTRACTED CURRENT VARIATION - KARA SEA
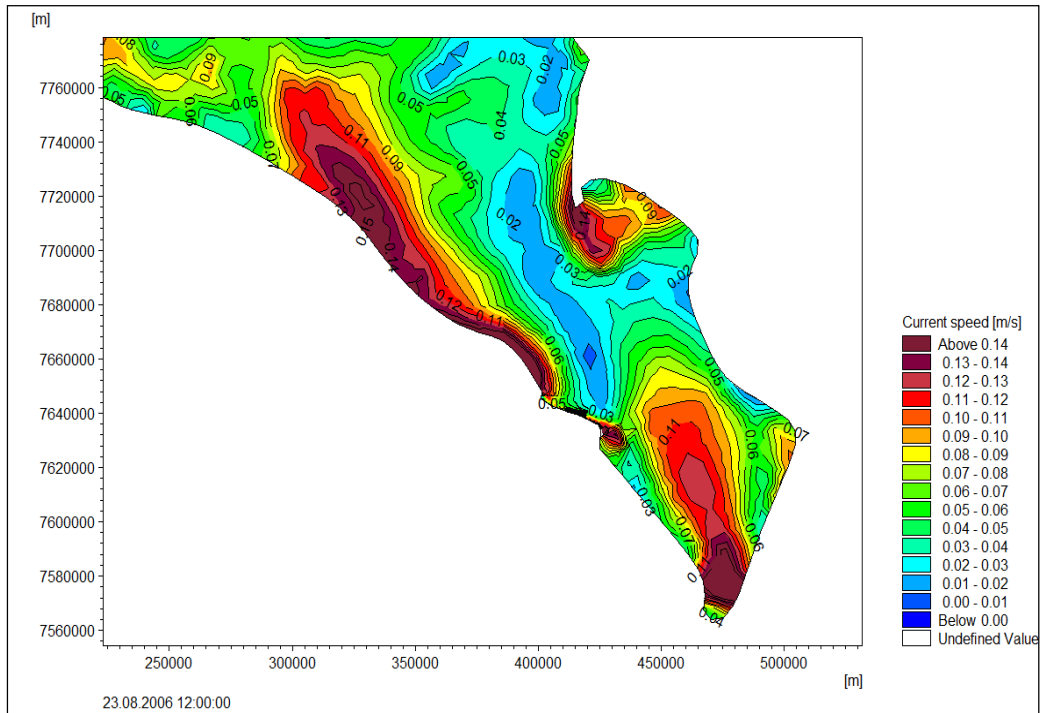
FIGURE 5.12 MODEL EXTRACTED CURRENT VARIATION - BAYDARA BAY

5.1.2 Site of interest – Ural coast

The model is run for attempting a calibration against the data available from Dr. S. Ogorodov (Senior researcher, Moscow State University). The area considered is on the Ural coast covering a distance of approximately 7 km. The simulation period considered is from 01 August 2006 to 31 August 2006.

5.1.2.1 Model setup

A separate mesh was created for running the coupled FM simulation near the area of interest. A domain of 5 km x 7 km was used near the site with increasing resolution (Figure 5.13) towards the coast. The mesh resolution increases towards the point of interest (68°51'11''N, 66°53'48''E) from 150 m to 50 m.

TABLE 5-3 SIMULATION PERIOD AND TIME STEP - SITE OF INTEREST (URAL COAST) – CALIBRATION RUNS

Sl. No.	Period	Duration	Time step (seconds)		Remarks
			SW	HD	
1	1st August 2006 to 31st August 2006	30 days	300	300	For calibration runs

The current and sediment transport will be studied near this area. A default CFL number of 0.8 was adapted for stability for the mesh as well. A time step of 300 seconds was used for the refined mesh.
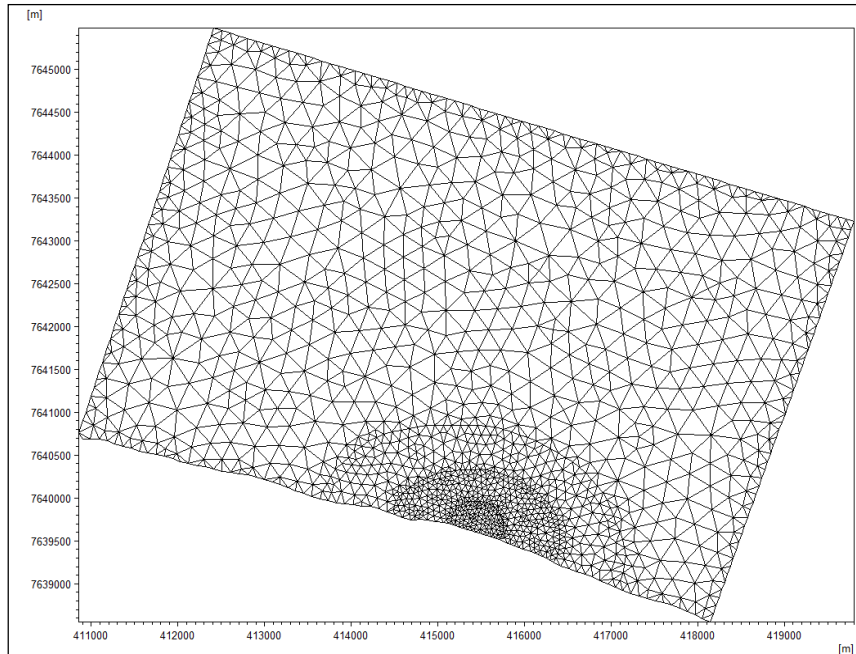
FIGURE 5.13 NESTED MESH FOR URAL COAST

Figure 5.14 show the interpolated bathymetry near the site of interest. The fine resolution ensures that the depth contours are depicted as smooth as possible near the area that has been surveyed by SAMCoT and the location where data is available. The area considered is 5 km in the offshore direction which covers a depth of up to 11.2 m.
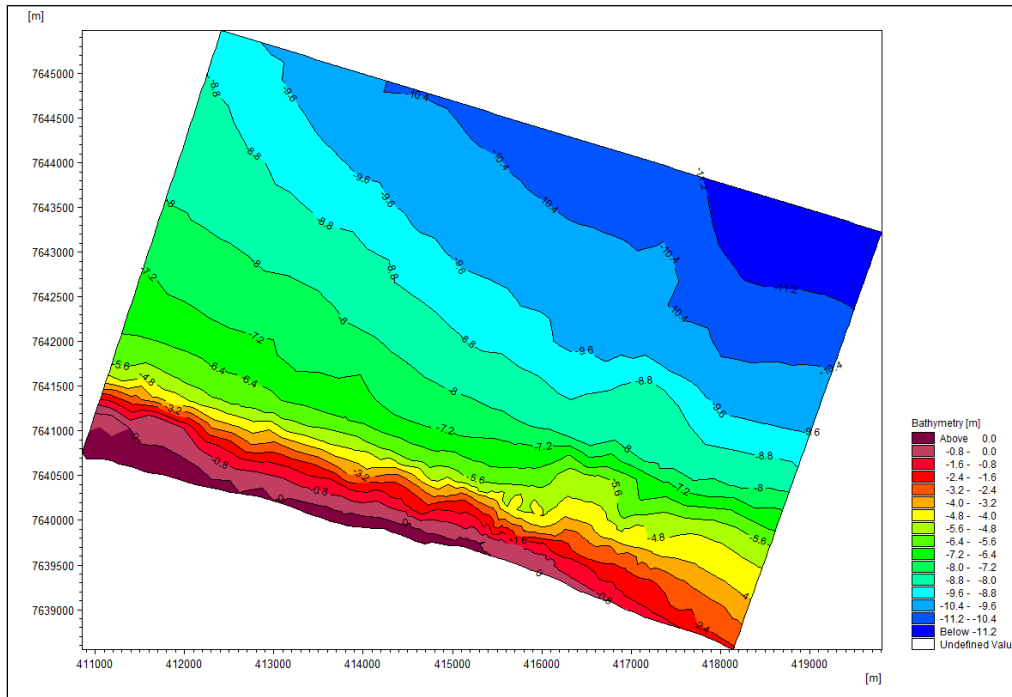
FIGURE 5.14 BATHYMETRY - AREA OF INTEREST (SOURCE: MIKE C-MAP)

The results extracted from the Kara Sea runs were applied as input conditions along the boundaries shown in Figure 5.15.
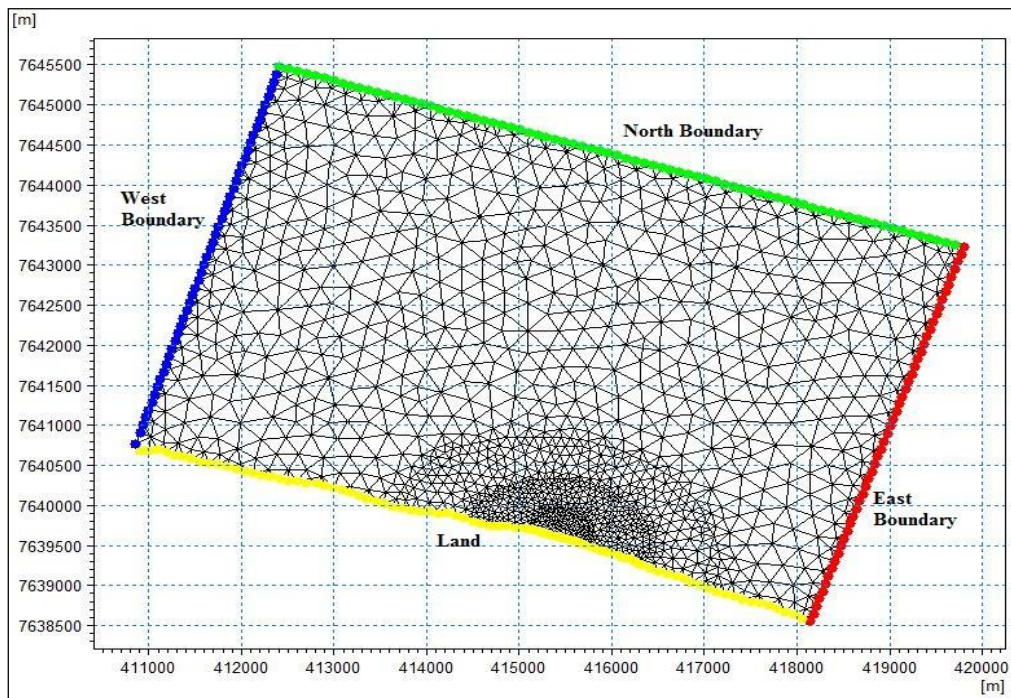
FIGURE 5.15 URAL COAST - DOMAIN BOUNDARIES

MIKE21/3 Coupled FM was used for calibration runs. The Hydrodynamic (HD) and Spectral Wave (SW) module were applied together dynamically. A higher order time and space discretization was applied with a CFL number of 0.8 kept at default. Coriolis and tidal components were neglected for these simulation runs. Eddy viscosity was applied using Smagorinsky formulation with the default constant coefficient of 0.28. An initial surface level of 0.41 was applied over the entire domain. Wave radiation was applied as varying in time and across the domain as a dynamic input from SW simulation. Wind forcing was applied from the ECMWF data for the selected area.

Considering the small area, to avoid blow-up, horizontal and vertical water particle velocities extracted from the Kara Sea calibration runs were applied as varying in time and along the east and west boundaries. Mean water surface level varying in time and along the profile was applied at the northern boundary.

The calibration factor was chosen as Manning's coefficient and wind forcing and was tested for different values. The different configurations used are summarised in Table 5-4.

TABLE 5-4 MODEL SIMULATION CONFIGURATIONS

Sl. No.	Parameter	
	Manning number [m$^{1/3}$/s]	**Wind Friction Factor**
1	32	Constant = 0.001255
2	32	Constant = 0.0025
3	28	Constant = 0.001255
4	50	Constant = 0.001255
5	50	Linearly varying with wind speed: 7 m/s = 0.001255 25 m/s = 0.002425 (Default values)
6	50	Linearly varying with speed: 7 m/s = 0.015 25 m/s = 0.05

In the SW simulation a fully spectral and quasi stationary formulation was applied considering the small area in consideration as recommended in the MIKE21/3 manual. The water level and current variation across the domain are updated dynamically with the HD module. The wind was applied as velocity components in both x & y direction across the domain extracted from the ECMWF data for the area. Ice coverage and diffraction were neglected. Considering the shallow area,

energy transfer was applied using triad-wave interactions (Holthuijsen, 2007) with the default transfer coefficient of 0.25. Bottom friction was applied as a function of sediment diameter (d_{50}) kept as constant valued of 0.375 mm. Wave breaking and white capping parameters were kept as constant during the calibration runs.

The results were analysed and the calibrated input settings were used for simulations in the main runs.

5.1.2.2 Results

The MIKE21/3 Coupled FM module was run for the configurations outlined in the previous section. The data used for calibration was made available by Dr. S. Ogorodov (Senior researcher, Moscow State University). It was collected for a study of suspended particles in the bay. A 2DACM (acoustic current meter) was used at the location to study the vector currents. The observed data from the current meter are mentioned in Table 5-5. The location of readings is shown in Figure 5.16.

TABLE 5-5 CURRENT DATA AT URAL COAST (12.00, 23.08.2006) (SOURCE: DR. S. OGORODOV, MOSCOW STATE UNIVERSITY)

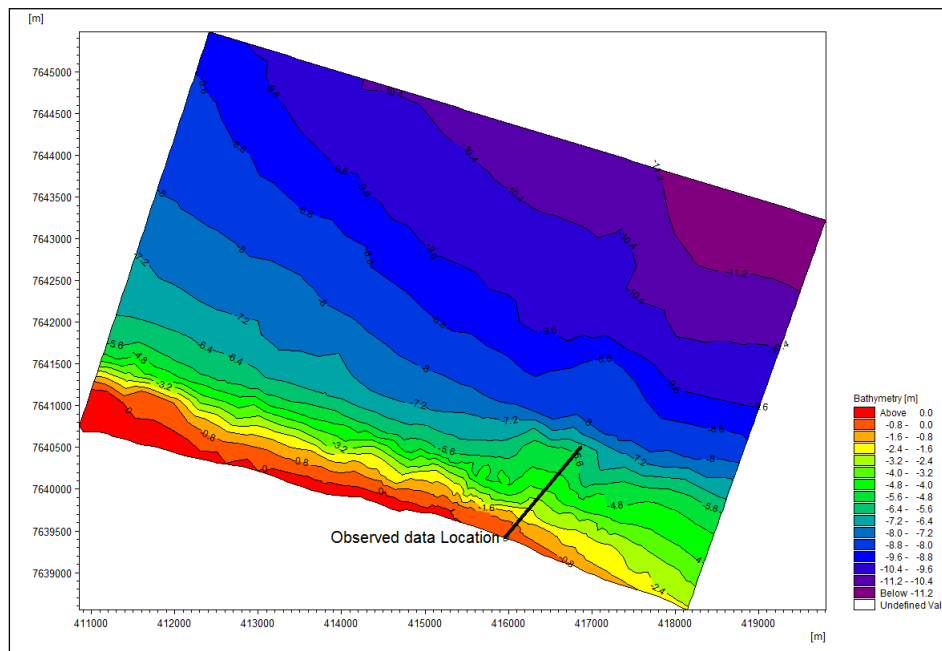| Sl. No.	Depth (m)	Current direction (Degrees)	Current speed (m/s)	Particle diameter (μm)
1	6.1	247	0.270	15.6
2	4.5	249	0.334	18.2
3	3.2	319	0.291	21
4	2.9	330	0.340	19.4
5	2.3	347	0.450	20.1
6	1.5	356	0.396	20
7	2.2	352	0.214	19.9
8	1.6	339	0.294	17
9	1.3	304	0.202	15.1

FIGURE 5.16 EXTRACTION LINE FOR CURRENT DATA

Considering this, a profile series was extracted from the results of the different configurations of the hydrodynamic simulations. Values were extracted at 10 points along the line. The depth of the points was kept similar to the depths of the actual data measurement locations.

It was found that the current speed increases with increase in Manning's number. For a given depth, the current speed was found to also depend on the type of wind forcing applied. As the wind friction factor increases, for a given depth, the current speed also increases. From the different configurations used, it was seen that results with a Manning's number of 50 and a wind friction factor varying linearly with wind speed with default values gave the best match (Figure 5.17).

The data was available for only one time step and a better calibration could have been achieved if a continuous data series was available. The input parameters used for the best fit configuration (Manning number = 50 [$m^{1/3}$/s] and linearly varying wind friction factor) were then used in the main runs.

The high Manning number suggests the presence of highly rough bed which could be due to vegetation or grading of the sediments at the site. Better results were obtained with a linearly varying wind friction factor as it gives more realistic results than using a constant value. It should be noted however, that there is a high uncertainty in these predictions and more detailed data would be required before generalizing these results to the entire bay. However, the configuration can be used as a starting point for understanding the hydrodynamics of the Ural coast.
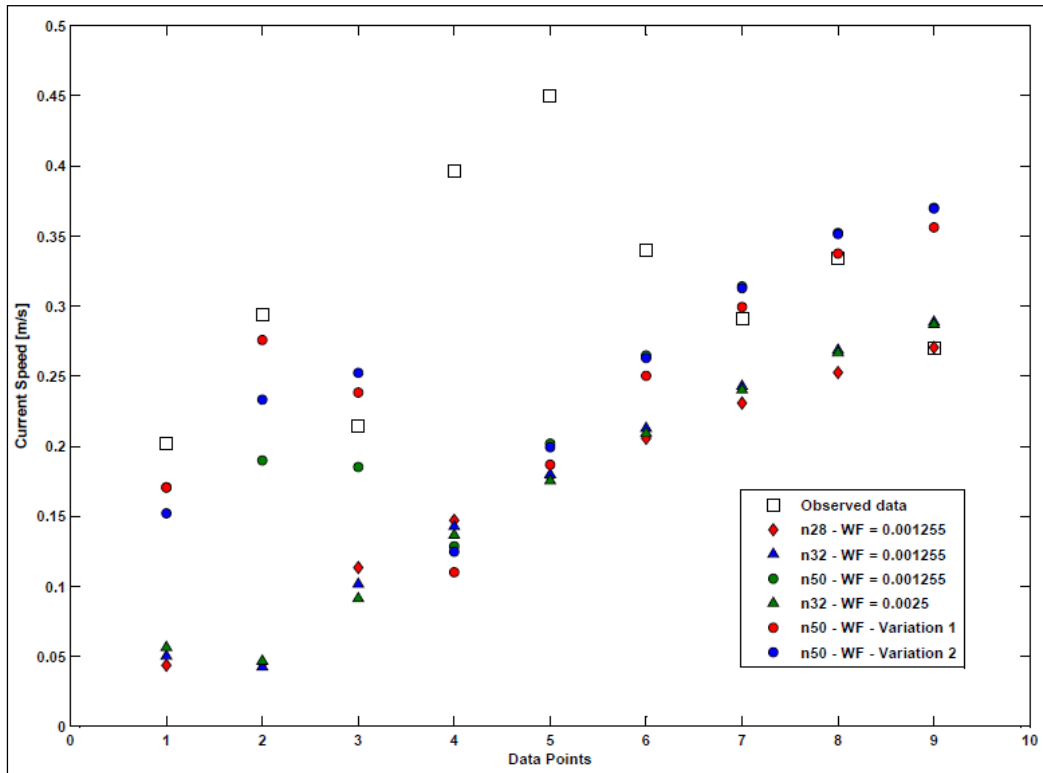
FIGURE 5.17 CALIBRATION OF CURRENT SPEED AT URAL COAST

Figure 5.18 shows the wave height contours at the Ural coast for a time step. The wave heights in the area reach a maximum height (H_s) of 1.2 m with an average of 0.6 m. An average peak period of 4.5 seconds is observed with a maximum of 6 seconds.
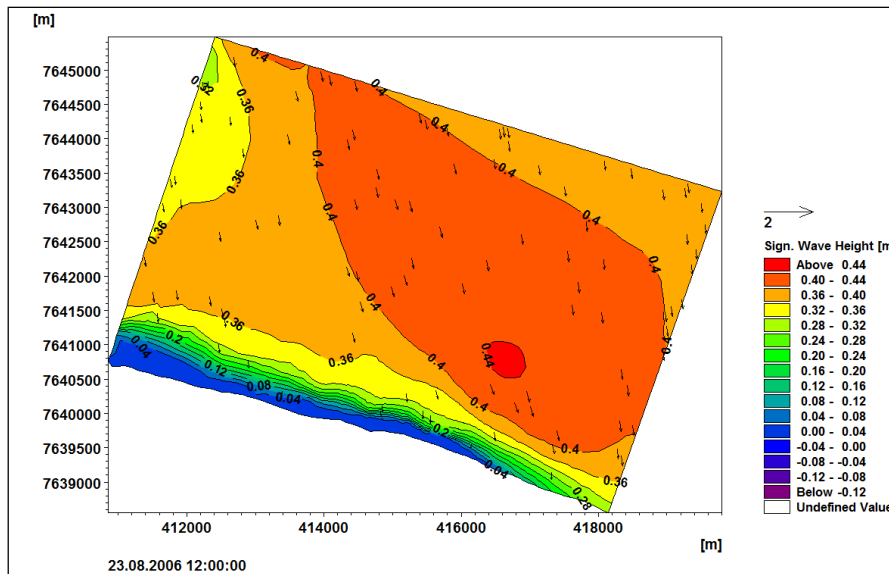
FIGURE 5.18 MODEL EXTRACTED WAVE HEIGHT VARIATION CONTOURS - URAL COAST

The direction of wave approach is fairly constant from the north as seen in Figure 5.19.
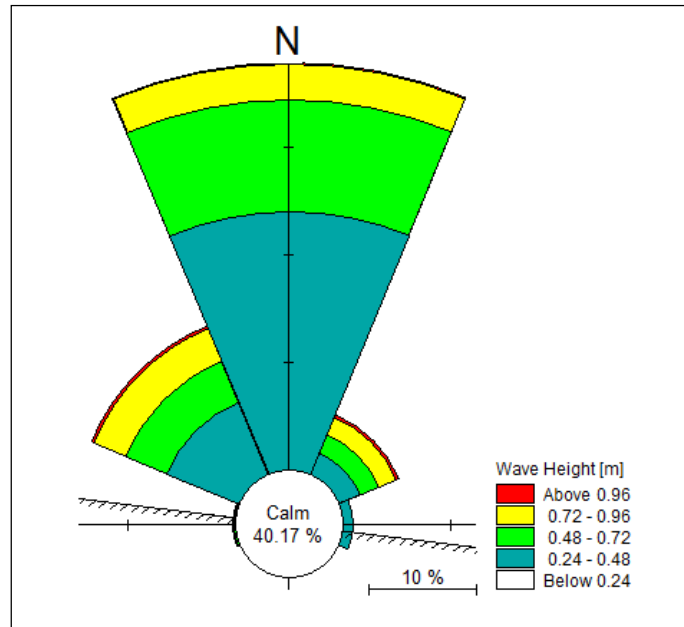
FIGURE 5.19 WAVE ROSE PLOT - URAL COAST

The current speed on the Ural coast reaches maximum values of 0.45 m/s with an average value near 0.15 m/s. shows the current variation near the point of interest for the month of August 2006 (Figure 5.20).
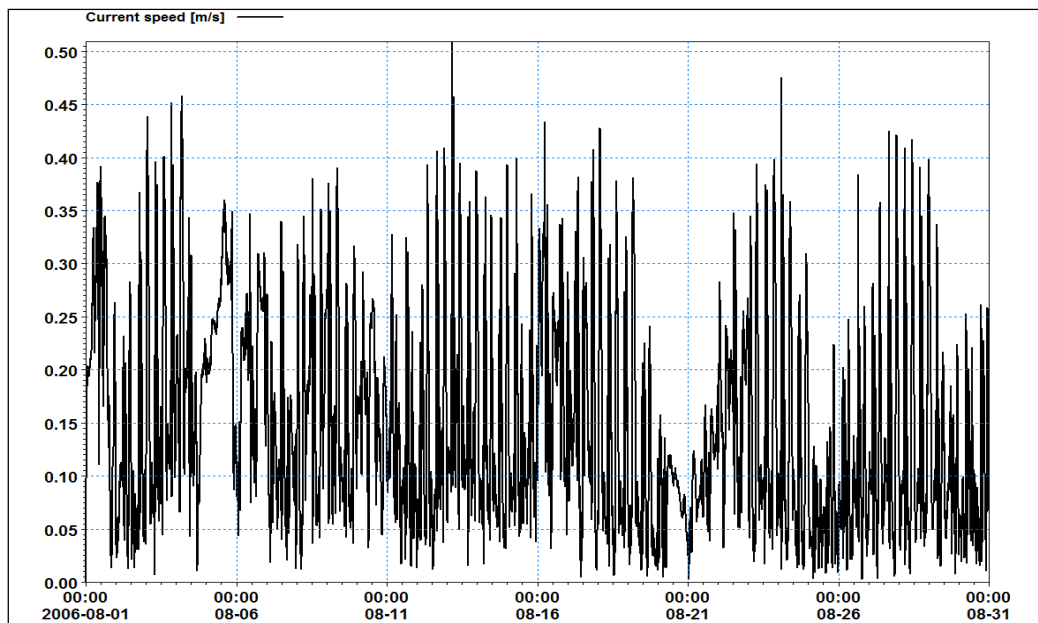
FIGURE 5.20 MODEL EXTRACTED CURRENT SPEED VARIATION AT URAL COAST

5.2 Main runs

The aim of these simulations was to apply the parameters used in the calibration runs for the most recent data available for the Kara Sea and Ural coast to understand the hydrodynamic conditions prevalent in the area. Both the Kara Sea and Ural coast models were run for an entire season (summer and fall) in 2011 – 1 July 2011 to 20 November 2011.

5.2.1 Kara Sea

A similar strategy as the calibration runs was used for the simulations for the summer and fall season in 2011 (July to November). The results from the larger area (Kara Sea) were used to transfer the offshore boundary conditions to the nearshore Ural coast.

5.2.1.1 Model setup

The mesh and bathymetry details were the same as outlined in Section 5.1.1.1. Table 5-6 outlines the simulation period and time steps used in the simulation.

TABLE 5-6 SIMULATION PERIOD AND TIME STEPS - KARA SEA - MAIN RUN

Sl. No.	Period	Duration	Time step (seconds)		Remarks
			SW	HD	
1	1st July 2011 to 20th November 2011	142 days	1800	1800	For obtaining boundary conditions for site of interest (Ural coast)

The boundaries are also the same as shown in Figure 5.6. For the SW runs, a fully spectral and instationary formulation was applied with a logarithmic spectral discretization and separation of wind-sea and swell at a threshold frequency of 8 seconds. An average water level of 0.46 was applied over the entire domain as an initial condition interpolated from the tidal variation at both the boundaries. Wind was applied as components on both x and y axes varying in time and over the entire domain. Waves at the eastern boundary were applied using the data from all the three locations (Figure 4.12) varying in time and along the boundary. The strait at the western boundary was applied with a lateral boundary conditions. All the boundary and domain conditions were applied with a linearly interpolating soft start of 7200 seconds.

Ice coverage was neglected. Diffraction, wave breaking and bottom friction were kept at default values. Energy transfer was included via quadruplet wave-wave

interactions due to the largely varying depths in the domain. Considering the wind dominated wave field, white capping was also included in the calculations with default coefficients as recommended by MIKE21 manual.

The output of wave radiation stresses from the SW simulations was used as input wave radiation stresses in the HD runs. A higher order time and space discretization was applied for the run with a CFL number of 0.8 for stability. An initial level of 0.46 m was used based on the average value of the mean sea level variation at the two boundaries. The mean sea level was applied varying in time and along boundary on the eastern end whereas the mean sea level variation from the closest tidal station was applied over the western boundary. All the boundary and domain conditions were applied with a linearly interpolating soft start of 7200 seconds.

Ice coverage was neglected in the simulations. Coriolis forces and tidal components with default values were applied over the domain. Turbulence was included by applying Smagorinsky formulation with default eddy viscosity coefficient of 0.28. As a result of calibration, the bed resistance was applied using Manning's number of 50 $[m^{1/3}/s]$ and a linearly varying wind friction factor with default values.

The results of the SW and HD run were extracted for the boundary and initial conditions for the smaller area with finer mesh.

5.2.1.2 Results

For the summer of 2011 it was seen that the wave heights arriving at the mouth of the bay have an average value of 1.2 m with a maximum of 3.2 m (Figure 5.21) with an average peak period of 4 .5 seconds.
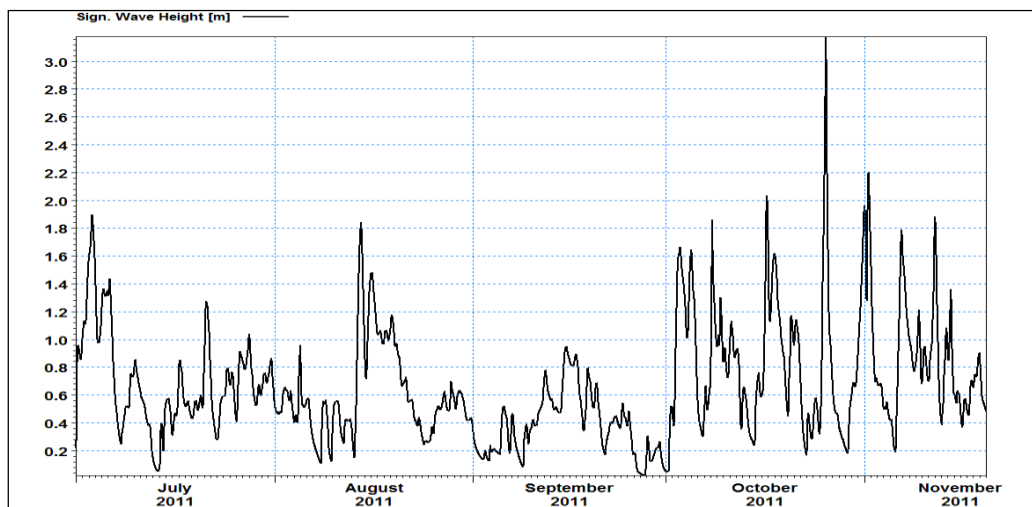
FIGURE 5.21 MODEL EXTRACTED WAVE HEIGHTS AT MOUTH OF BAYDARA BAY

The analysis of the results shows that the waves reaching the bay reduce in height in as they enter the shallower depths of the bay (Figure 5.22). The waves data extracted are representative of two points, one inside the bay and one in the offshore depths.
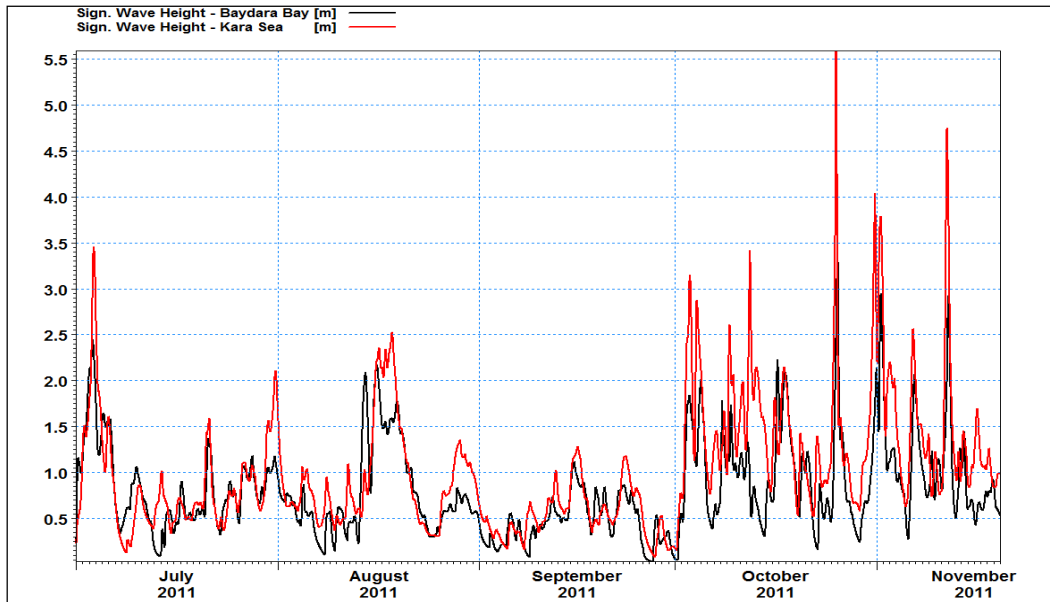
FIGURE 5.22 MODEL EXTRACTED WAVE HEIGHTS INSIDE AND OUTSIDE BAYDARA BAY
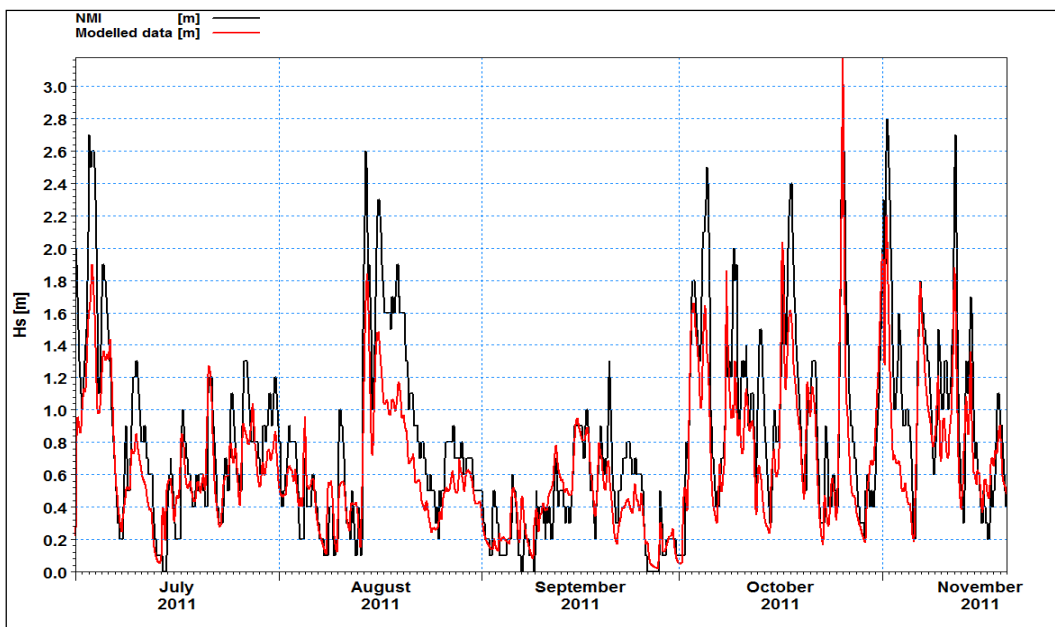
FIGURE 5.23 MODEL EXTRACTED WAVE HEIGHT VERSUS NMI DATA AT LOCATION 3

Figure 5.23 shows the modelled wave heights at Location 3 are in good correlation with the data available from NMI.

Figure 5.24 shows the wave height contours developing across the domain. The current variation across the domain is as shown in Figure 5.25. It can be seen that the currents are stronger near the strait. The currents were found to be congruent to predictions of a tidal dominated system near the mouth of the bay. Current speeds in the order of 5 m/s were calculated near the strait (western boundary).

FIGURE 5.24 MODEL EXTRACTED WAVE HEIGHT CONTOUR - KARA SEA

FIGURE 5.25 MODEL EXTRACTED CURRENT VARIATION - KARA SEA

The currents inside the bay are in general much smaller than near the strait (western boundary) and near the mouth of the bay (Figure 5.26). Currents reach an average value of 0.1 m/s inside the bay with maximum values reaching 1.5 m/s.

FIGURE 5.26 MODEL EXTRACTED CURRENT VARIATION - BAYDARA BAY

5.2.2 Site of interest – Ural coast

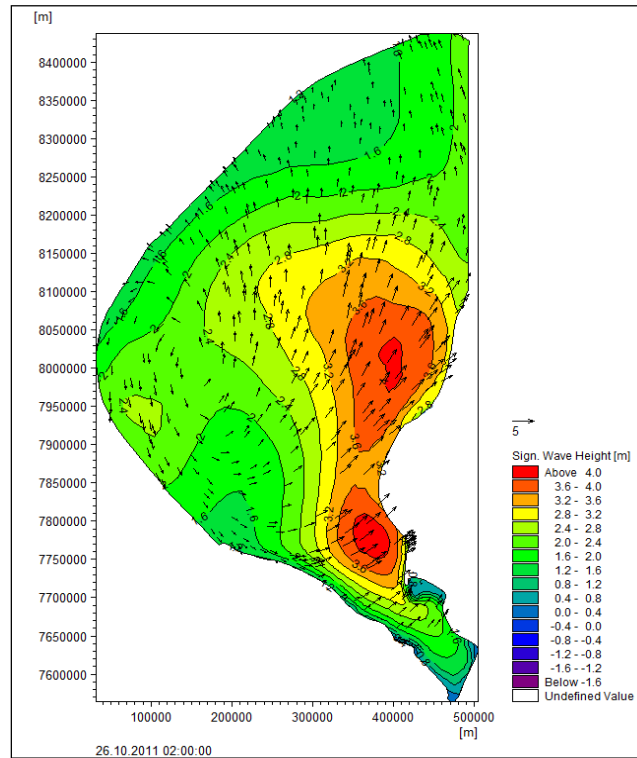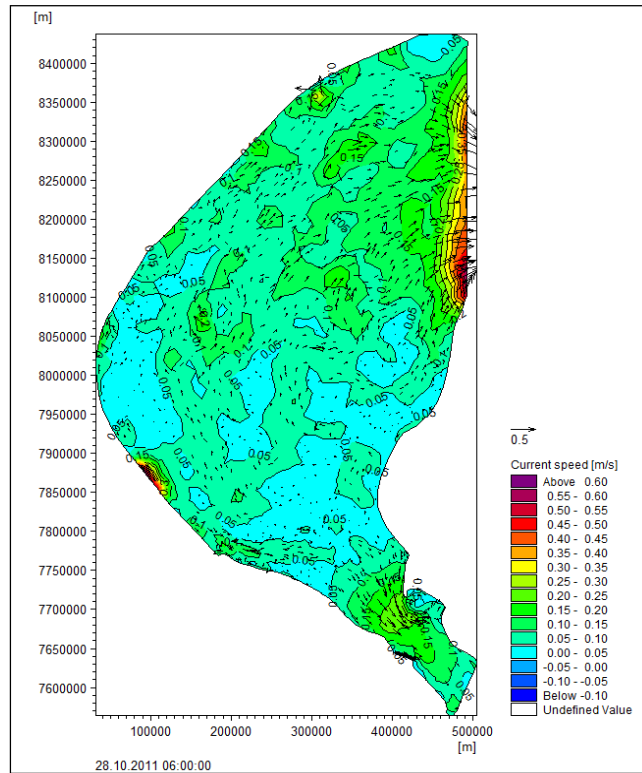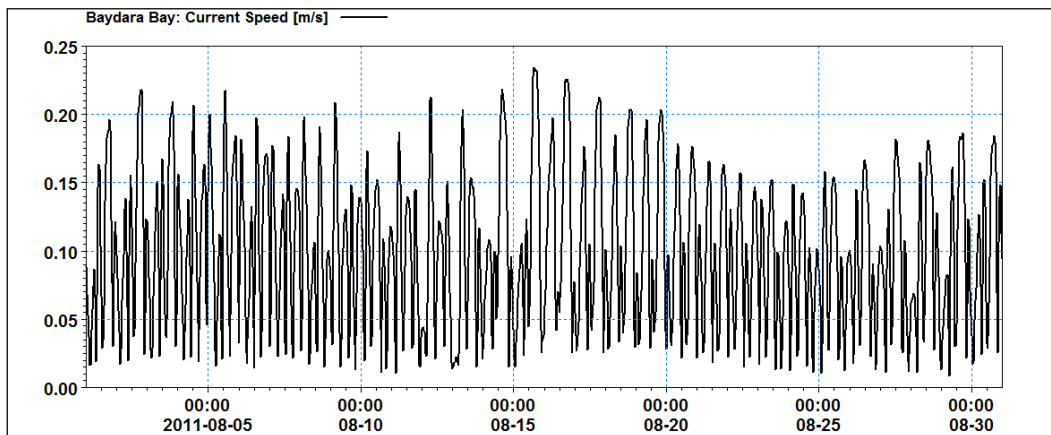The results obtained from the Kara sea run were applied as boundary conditions for the Ural coast simulation. MIKE21 SW module and Flow FM model was used for calculating the hydrodynamic conditions in the area along with the sediment transport patterns. The duration of one season represents the period of the year when wave climate is active in the bay. The results are analysed to understand the factors contributing to the hydrodynamic conditions present on the Ural coast.

5.2.2.1 Model setup

The mesh and bathymetry used have been kept the same as the ones for calibration runs. The time step is reduced to 300 seconds for finer resolution (Table 5-7).

TABLE 5-7 SIMULATION PERIOD AND TIME STEP - URAL COAST - MAIN RUN

Sl. No.	Period	Duration	Time step (seconds)		Remarks
			SW	HD	
1	1st July 2011 to 20th November 2011	142 days	300	300	-

For the spectral wave module, a fully spectral and quasi stationary formulation was used. Logarithmic frequency discretization was used to cover the entire spectrum of wave periods. Surface level and current variation was applied using the results extracted from the Kara Sea runs discussed in Section 5.2.1. Wind forcing was applied using the data extracted for the considered domain from the ECMWF database. Ice coverage and wave diffraction were not included in the calculations. Wave breaking and white capping was included with default coefficient values. Bottom friction was applied as the average sand grain diameter (d50) value of 0.375 mm. Energy transfer between waves is included using triad wave-wave interactions. JONSWAP spectrum with default parameters was used to simulate wave spectrum. Wave profiles were applied as varying in time and space at the boundaries from results extracted from the Kara Sea runs.

For calculating the hydrodynamics at Ural coast, MIKE21 Flow Module FM was used in which the MIKE21 Hydrodynamics was applied in combination with the MIKE21 Sediment Transport Module to simulate conditions where the sediment morphology includes feedback on the calculation of hydrodynamic and subsequent sediment transport conditions. As there is no data available for calibrating the sediment transport at the location, a sensitivity analysis was carried out to study the effects of the various input conditions on the sediment transport characteristics.

The input conditions for Hydrodynamic calculations were kept constant. Although, the effect of feedback from the ST module changes the conditions throughout the simulation. A higher order space and time discretization was applied in solving the shallow water equations. Bed resistance value was kept as 50 $m^{1/3}$/s as found from the calibration runs. Coriolis forcing, ice coverage and tidal potential were neglected considering the small area of the domain. Wind forcing was applied using the ECMWF data with the calibrated wind friction factor varying linearly with the wind speed.

Boundary conditions applied were similar to the calibration runs for Ural coast, where, horizontal and vertical water particle velocities were applied at the eastern and western boundary and varying surface elevation was applied at the northern boundary. All the boundary conditions were extracted from previous Kara Sea simulations.

The results obtained from the SW and HD simulation are discussed below. It should be noted that the HD results discussed here, were the results of simulating the combined action of waves and currents in the ST module, and also the differences between the different configurations for ST module on the HD results was found to be negligible. These results are discussed further in Section 5.2.3.

5.2.2.2 Results

The wave height variation near the coast was found to be in good conformity with the wind speed data available for the location which suggests that the waves arriving at the coast are wind generated and the swell component is negligible (Figure 5.27). Maximum wave heights of 1.2 m were calculated with an average peak period 6 seconds.
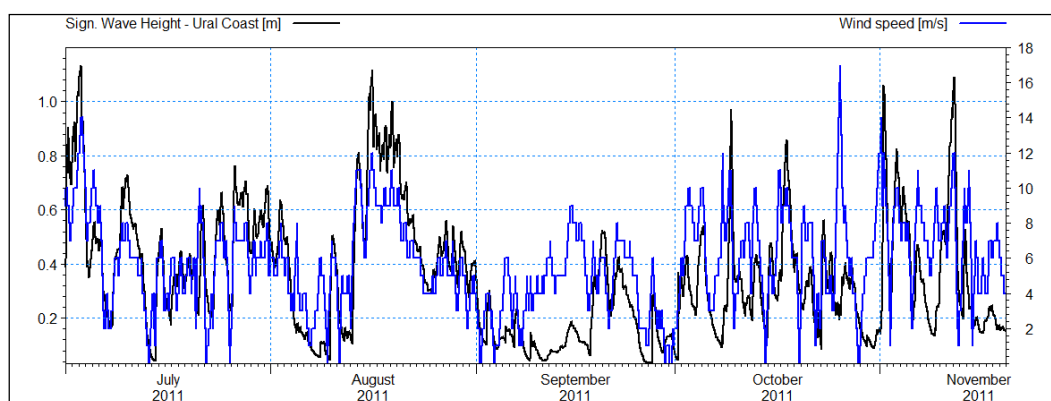
FIGURE 5.27 MODEL EXTRACTED WAVE HEIGHT VERSUS NMI WIND DATA

The waves on the coast are incident mainly from the north direction. Figure 5.28 also shows the orientation of coast relative to wave direction.
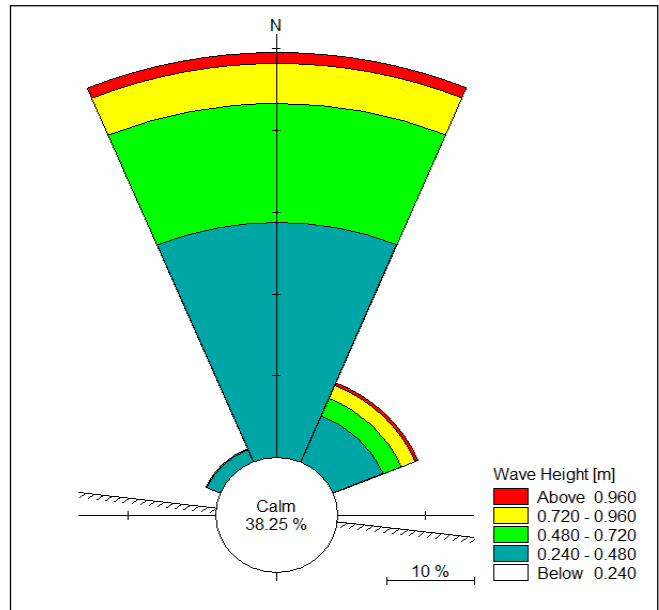
FIGURE 5.28 WAVE ROSE PLOT - URAL COAST - MAIN RUN

Figure 5.29 shows the waves approaching the coast at one time step. The wave heights near the coast have an average value of 0.4 m with a peak period of 4.5 seconds. The waves arriving at the coast are short in nature and mainly wind generated.
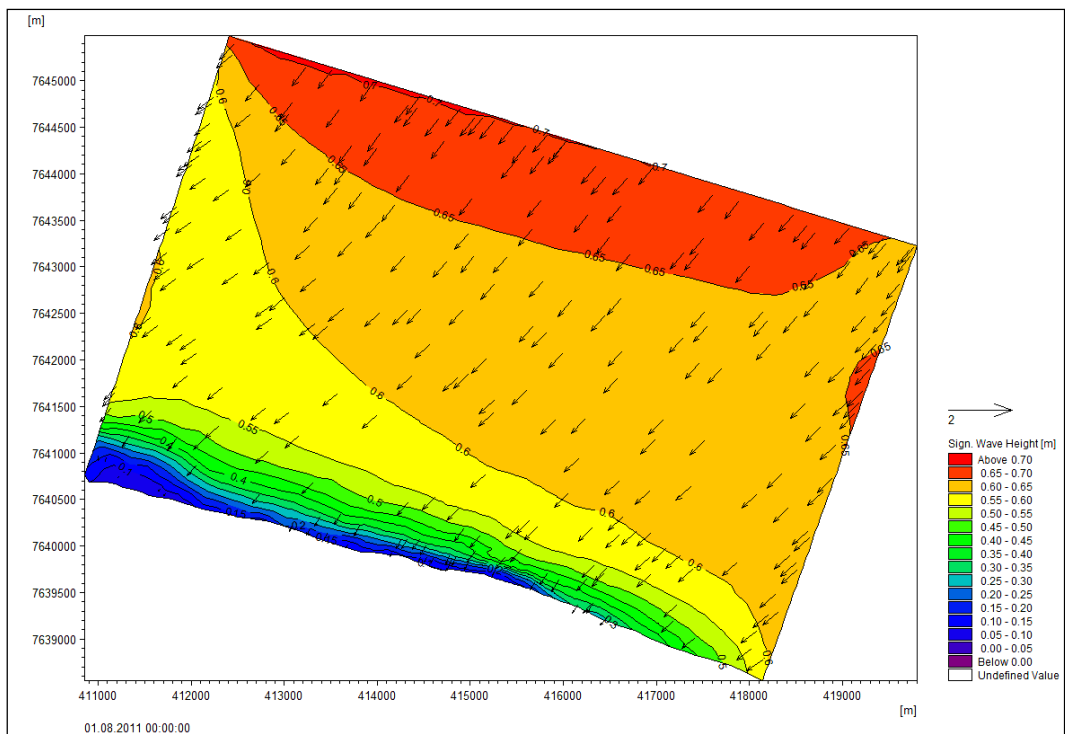
FIGURE 5.29 MODEL EXTRACTED WAVE HEIGHT CONTOURS - URAL COAST - MAIN RUN

Further analysis of the results shows that the radiation stresses near the coast reach a maximum of 0.7 m^3/s^2 along the coast and 0.4 m^3/s^2 perpendicular to the coast (Figure 5.30). Shear radiation stresses are relatively less as the waves approach the coast almost perpendicularly and an average value of S_{xy} was found to be 0.05 m^3/s^2.
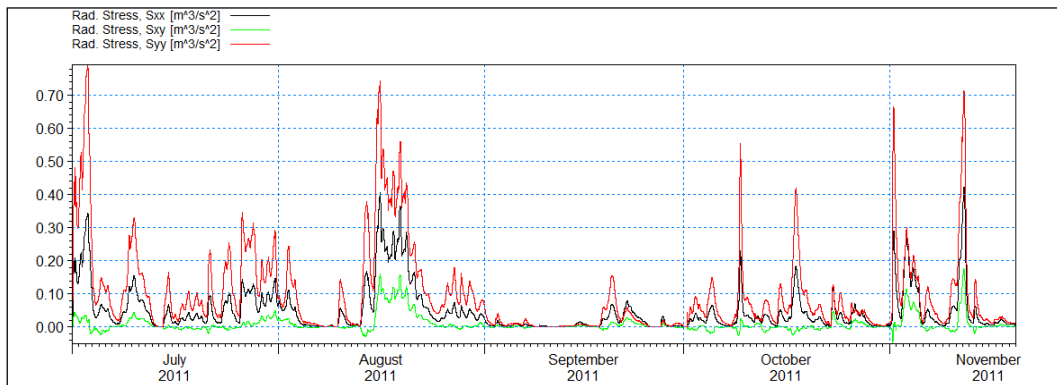
FIGURE 5.30 VARIATION OF RADIATION STRESSES ON THE URAL COAST

The hydrodynamic results discussed here are for a configuration in which the combined action of waves and currents is applied for calculation of sediment transport. Figure 5.31 shows the surface level variation at the Ural coast over the period of a month which shows that the tides arriving at the coast are mixed type with predominantly semi-diurnal characteristics.
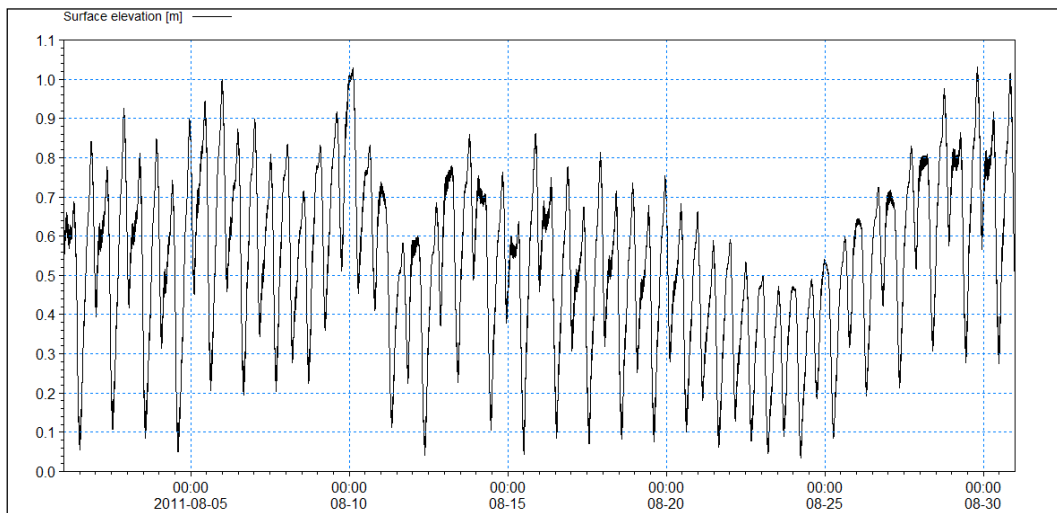
FIGURE 5.31 MODEL EXTRACTED SURFACE ELEVATION OVER ONE MONTH - URAL COAST - MAIN RUN

It is also seen that the Baydara bay is an ebb dominated system as the falling period is much shorter than the rising period (Figure 5.32).
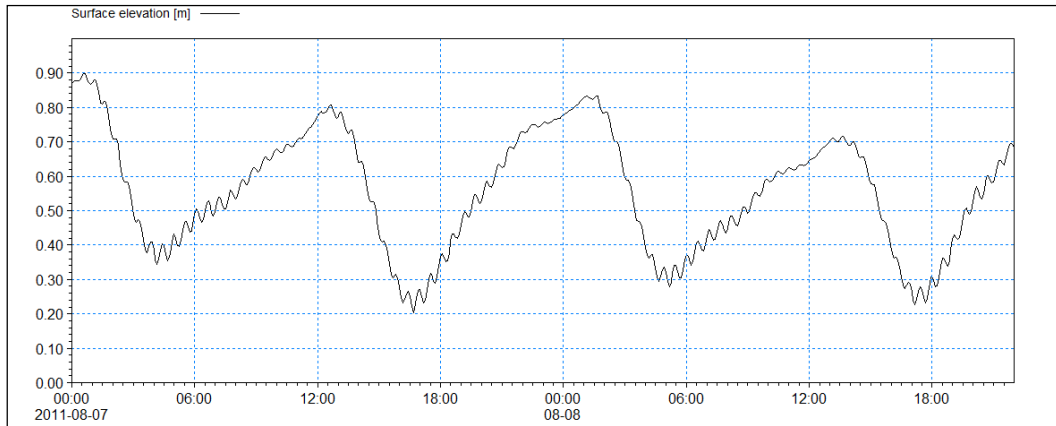
FIGURE 5.32 TIDAL ASYMMETRY INDICATING EBB DOMINANCE

Further analysis of the current flow patterns during the ebb and flow tide are shown in Figure 5.33 and Figure 5.34 for the area of interest on the Ural coast. During the falling period of the tide, the tide driven currents are directed outwards from the bay. Also, the currents during the ebb tide are much stronger than during the flood tide near the coast. In general, the current speed varies in the range of 0.01 to 0.6 m/s but has a low average value of 0.15 m/s. This value was found to be qualitatively similar to the understanding of the system as discussed with Dr. S. Ogorodov where the tidal currents may be of secondary importance in the context of coastal erosion.
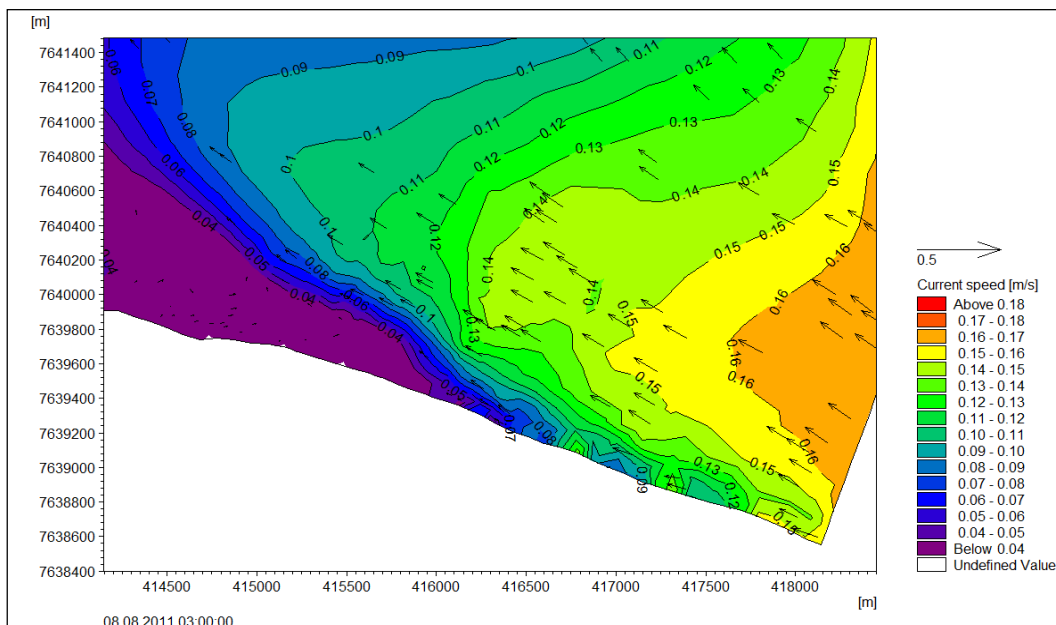
FIGURE 5.33 CURRENT FLOW PATTERN DURING EBB TIDE - URAL COAST - MAIN RUN
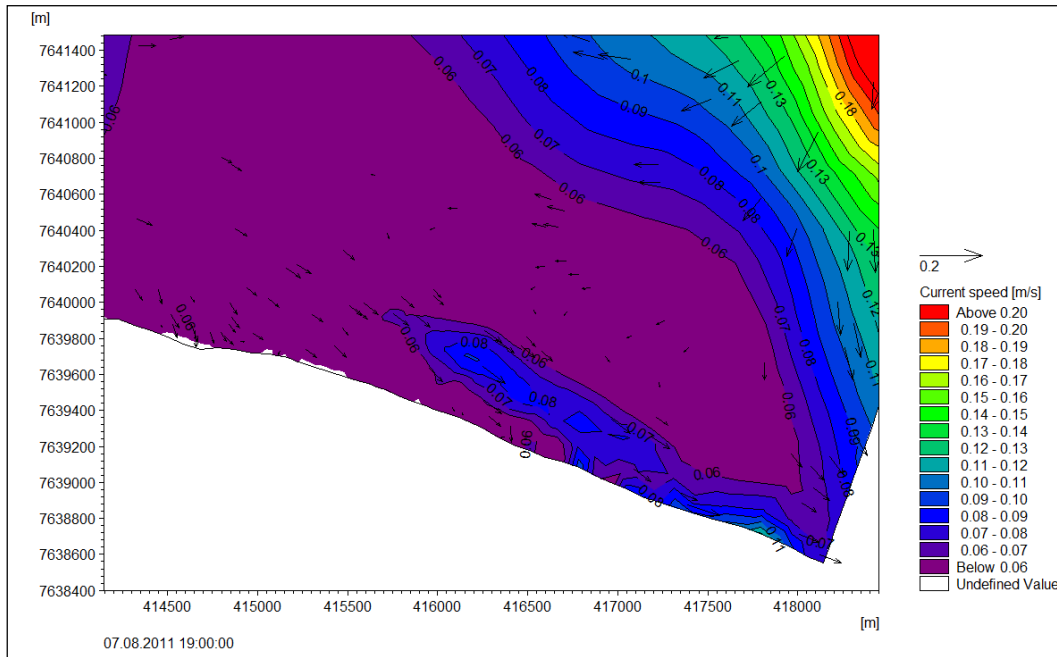
FIGURE 5.34 CURRENT FLOW PATTERN DURING FLOOD TIDE - URAL COAST - MAIN RUN

5.2.3 Sediment Transport – Sensitivity analysis

In combination with the hydrodynamic module, the sediment transport patterns for different configurations were also simulated for the Ural coast. There is very less data available for assessing the validity of a model for the coast. Considering this, the main aim of the simulations is to understand the effect of different parameters on the sediment transport rate in the area. A sensitivity analysis is presented between the configurations possible, and an attempt is made to understand the lithodynamics of the region.

5.2.3.1 Model setup

To understand the effect of the hydrodynamics on the sediment transport in the area directly, MIKE21 HD and ST (Sediment Transport) were run in combination where the feedback from ST is used to recalculate the currents and surface elevations at each time step. Different configurations were simulated for the sediment transport to study their effects on the final result:

- Importance of waves
- Importance of formulation
- Importance of sediment properties

To understand the influence of waves on sediment transport, the two different models available in MIKE21 ST were used – pure current and combined wave and current. As mentioned in Section 3.2, in the pure current model, four different formulations can be used. For the present case study, the formulations proposed by Engelund and Fredsøe and van Rijn were compared.

The known data for sediment properties shows a varying range for sediment diameter between 0.2 mm to 0.5 mm (Figure 4.21). The variation in sediment transport rate for varying sediment grain size was also simulated for the given hydrodynamic conditions. The simulations run for the sensitivity analysis are summarised in Table 5-8.

TABLE 5-8 SEDIMENT TRANSPORT SENSITIVITY ANALYSIS CONFIGURATIONS

Sl. No.	Configuration
1	Combined waves and currents (CW) – d50 = 0.375 mm
2	Pure current – Engelund and Fredsøe formulation (EF)
3	Pure current – van Rijn formulation (vR)
4	Pure current – Engelund and Hansen formulation (EH)
5	Combined waves and currents (CW) – d50 = 0.2 mm
6	Combined waves and currents (CW) – d50 = 0.5 mm

For all the configurations of sediment transport, the initial and boundary conditions for HD model were kept constant. The pure current model was run with two formulations which calculate the sediment and bed load separately – Engelund and Fredsøe (EF) and van Rijn (vR) and a total load calculating model – Engelund and Hansen (EH). For both the models, the sediment grain size was kept at 0.375 mm with a porosity of 0.4 and relative density of 2.64. The Ural coast was assumed to be in equilibrium and the boundary conditions were applied accordingly.

The time step applied was the same as for HD module – 300 seconds, so the sediment transport rates and morphology was recorded and updated every 5 minutes. For the morphological model, a condition of zero sediment flux gradient for outflowing sediment and zero bed level change for inflowing sediment was applied at all the boundaries. A higher order scheme was used for space and time discretization in all cases. Bed resistance was kept at the calibrated value of 50 $m^{1/3}$/s. The morphological model was updated every 5 minutes as well.

For the model with combined wave and current action, the model uses pre-calculated sediment transport rates for a set of specified parameters. For the simulation a sediment transport table was generated beforehand using MIKE21 Toolbox – Q3D Sediment transport table generator. The parameters used in the generation are specified in Table 5-9.

TABLE 5-9 PARAMETER VALUES FOR GENERATING SEDIMENT TRANSPORT TABLE

Sl. No.	Parameter	Value
1	Relative density of sediments	2.64
2	Critical Shield's parameter	0.05
3	Effects Included: Ripples, Bed slope, Streaming Effects excluded: Centrifugal acceleration, Density currents	-
4	Bed concentration formulation: Deterministic – Engelund and Fredsøe (1976) Empirical – Zyserman and Fredsøe (1994)	Deterministic (Engelund and Fredsøe, 1976)
5	Wave theory	Doering and Bowen (1987) semi-empirical theory
6	Breaking wave parameters	$\gamma 1 = 1$ $\gamma 2 = 0.8$

The sediment transport table was then generated to cover the wave, current, sediment and bed slope parameters obtained from the hydrodynamic results and bathymetry. The combine waves and current model was then run using the wave field generated from SW run for Ural coast. A condition of zero sediment flux gradient was applied at the boundaries. The sediment porosity and grading was considered as 0.4 and 1.1 respectively. The effect of variation of sediment grain size was studied on the sediment transport rate and pattern for the combined effect of waves and currents.

5.2.3.2 Results

The sensitivity of current speed was also tested to different formulations and examples are shown in Figure 5.35 and Figure 5.36. It can be seen that the effect of different models on current speed can safely be neglected. Inclusion of combined effect of waves and currents was found to increase the currents speed marginally.
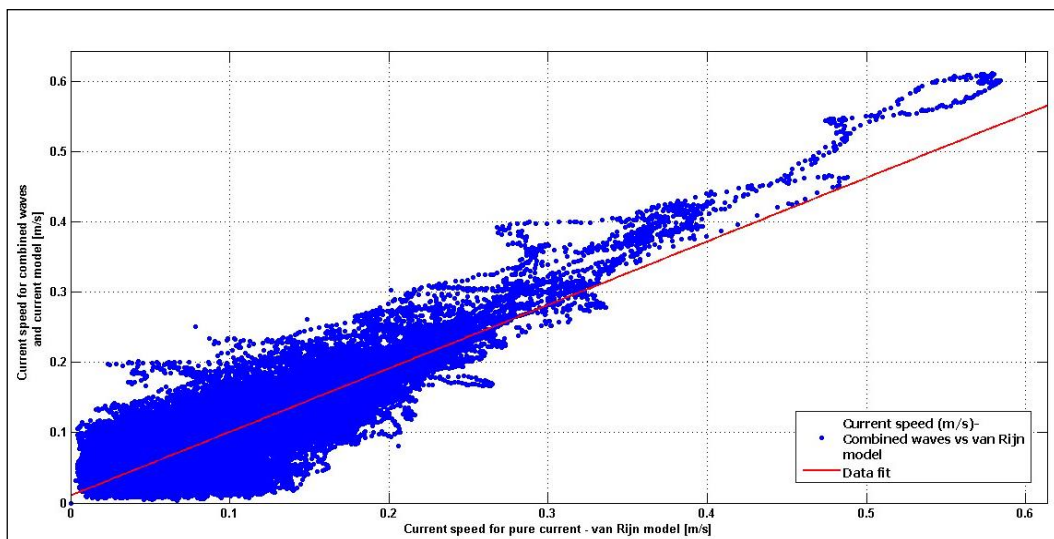
FIGURE 5.35 SCATTER PLOT OF CURRENT SPEED - COMBINED WAVES AND CURRENTS VERSUS VAN RIJN MODEL
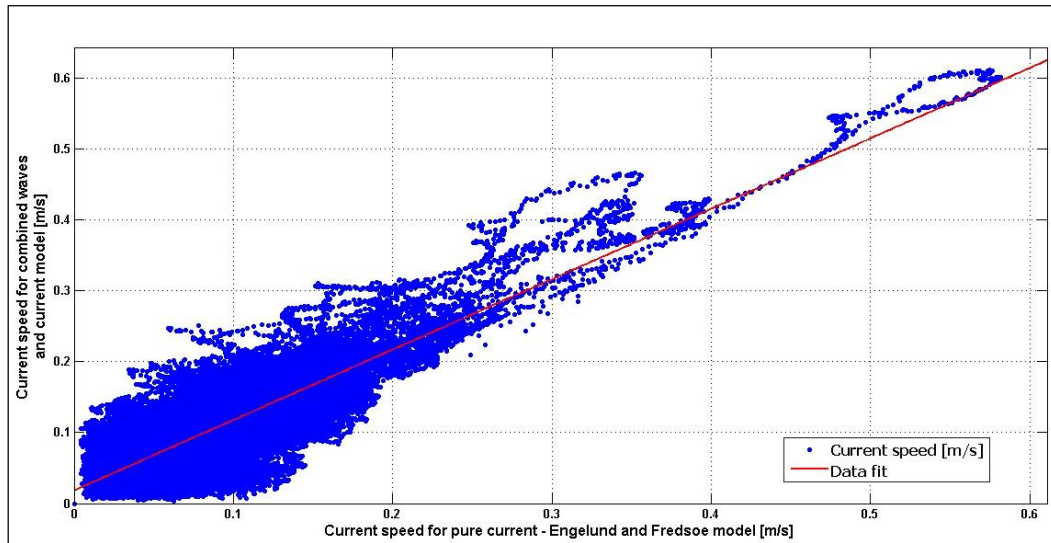
FIGURE 5.36 SCATTER PLOT OF CURRENT SPEED - COMBINED WAVES AND CURRENTS VERSUS ENGELUND AND FREDSØE MODEL

Considering the constant current speed for all the models, the sensitivity of sediment transport was then checked for the different pure current formulations available. Figure 5.37 shows the variation of bed level change for the period of summer 2011 (July – November). The initial bed level spike for all the formulations is due to the time steps required for the model to stabilise and reach equilibrium. In the presence of only currents, the sediment transport occurring is extremely less, suggesting that the tidal currents have very less effect on the sediment transport rates on the Ural coast.
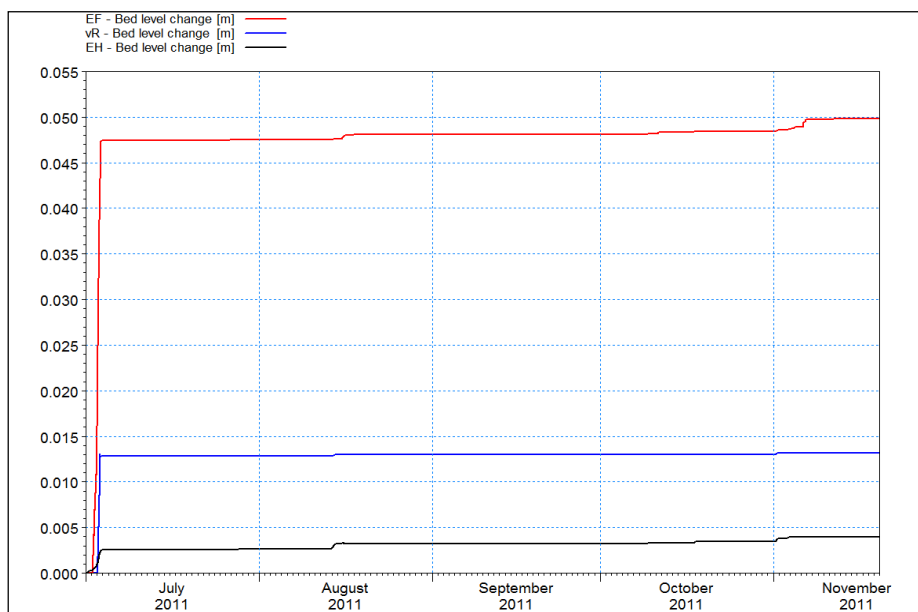
FIGURE 5.37 MODEL EXTRACTED - BED LEVEL CHANGE FOR PURE CURRENT MODELS

Comparison of the different formulations for the pure current models show a value of 0.03 m^3/s/m of total accumulated sediment load for Engelund and Fredsøe (Figure 5.38). The total accumulated load as predicted by Engelund and Hansen & van Rijn lie in the range of 0.0025 to 0.004 m^3/s/m. All the formulations however, reach an equilibrium as stated before and the effect of currents is almost negligible on the sediment transport.
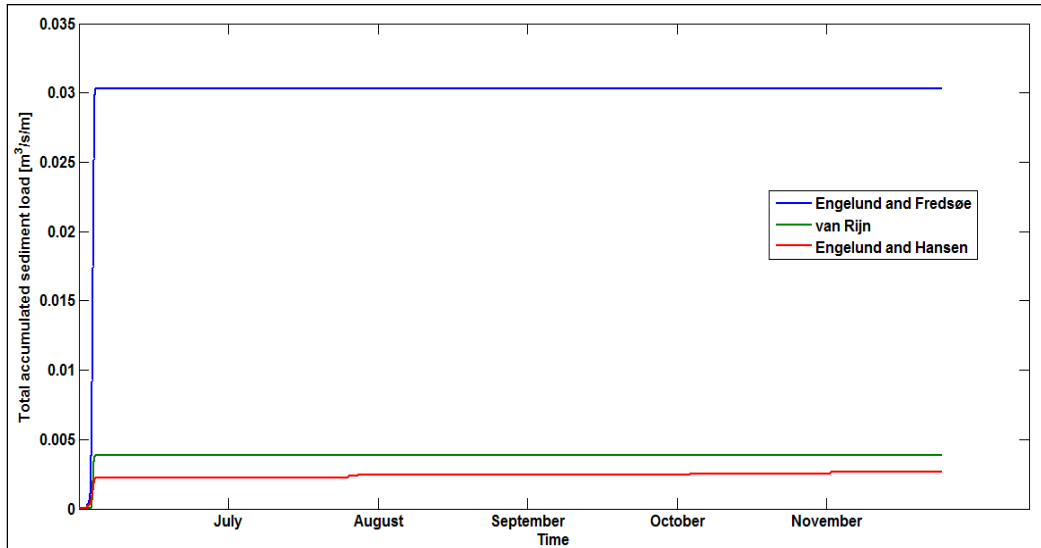
FIGURE 5.38 TOTAL ACCUMULATIVE SEDIMENT LOAD COMPARISON FOR PURE CURRENT FORMULATIONS

The combined wave and current model however predicts a bed level change to the order of 0.2 m (Figure 5.39). The wave field input used to calculate the sediment transport rates was extracted from the results for SW for Ural coast.
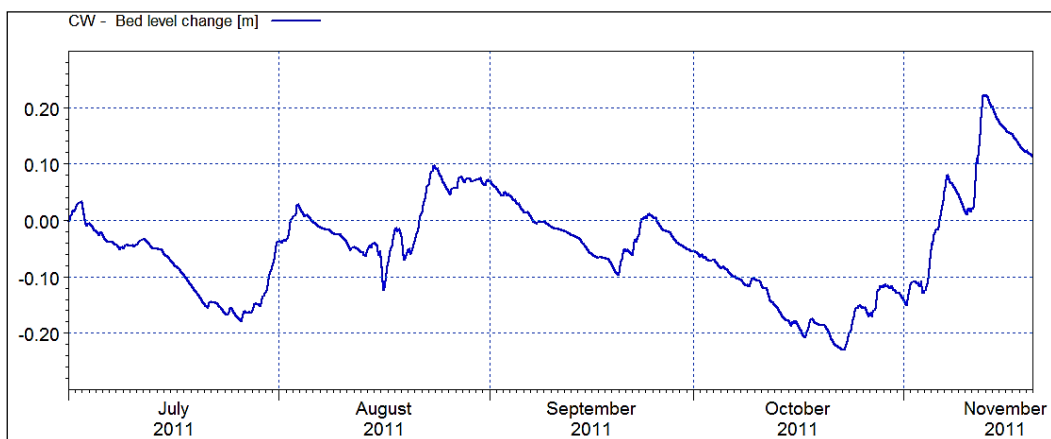
FIGURE 5.39 BED LEVEL CHANGE FOR COMBINED WAVE AND CURRENT MODEL

It can be seen that the wave driven currents are of importance on the coast as the total sediment load transported closely follows the currents (Figure 5.40).
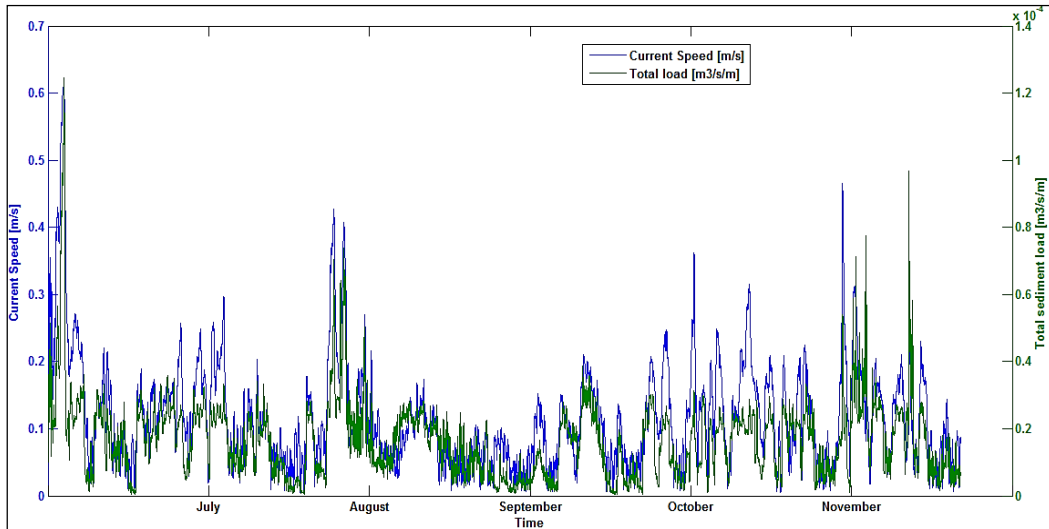
FIGURE 5.40 COMPARISON BETWEEN CURRENT SPEED AND TOTAL SEDIMENT LOAD

The sediment data available for the site was not exact and a range of 0.2 mm to 0.5 mm was determined from the graph provided by Dr. Ogorodov (Figure 4.21). To check the sensitivity of sediment transport at Ural coast due to change in sediment grain size, different configurations were tested with a value of 0.2, 0.375 and 0.5 mm. All the simulations were carried out for the effect of combined waves and currents.

It can be seen from that sediment transport increases as the sediment becomes finer. For the sediment grain size of 0.2 mm, the total accumulated sediment transport rate reaches around 1 m^3/s/m.
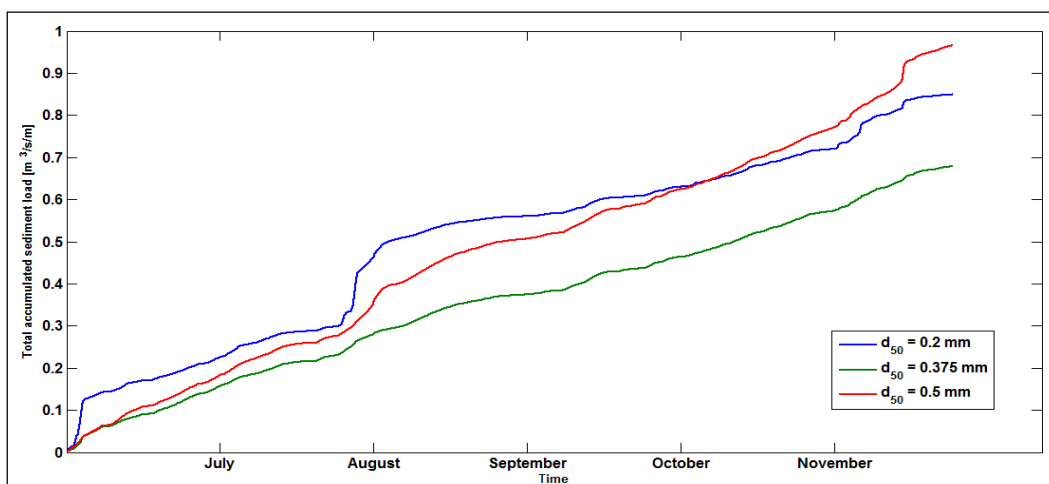
FIGURE 5.41 COMPARISON OF TOTAL ACCUMULATED LOAD FOR DIFFERENT SEDIMENT GRAIN SIZE

It should be noted that the relation between sediment grain size and sediment transport rate is not linearly proportional and is interdependent on other factors such as the wave conditions and bed slope. A more detailed field data would enable a better co-relation between the factors.

The rate of bed level change predicted for the different grain size diameters is shown in Figure 5.42. It can be seen that the variation in bed level for a smaller diameter is much less than that for coarser sediments.
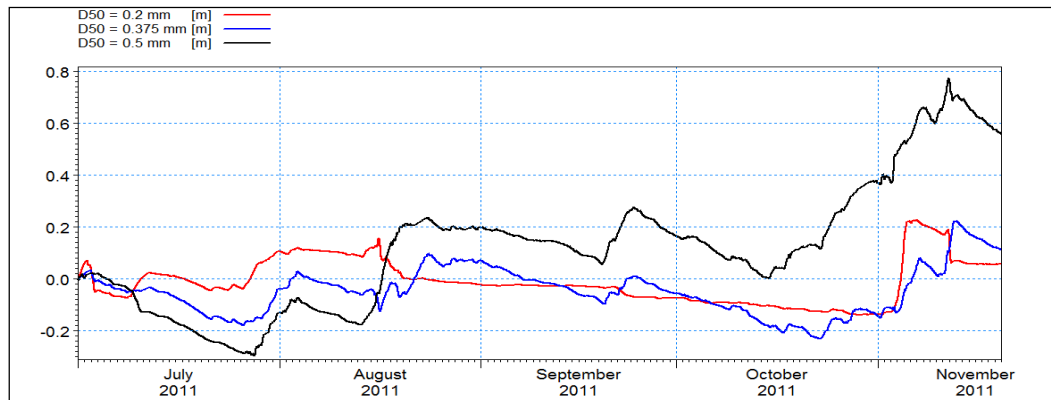
FIGURE 5.42 COMPARISON OF RATE OF BED LEVEL CHANGE FOR DIFFERENT SEDIMENT GRAIN SIZE

6   Conclusion

An attempt to understand the hydrodynamic conditions prevalent in the Baydara bay, Russia was successfully done in the present research. A 2D model with flexible mesh was created using MIKE21 which was calibrated with the current data available for the location. The model showed good correlation with the wave data received from Norwegian meteorological institute at the mouth of the bay. The discrepancies in the correlation between the data are attributed to the presence of ice in the bay for intermediate periods of time which was not modelled in MIKE21. The model is considered to simulate the hydrodynamic behaviour to a good extent inside the Baydara bay. The important findings can be summarized as follows:

- Even though the Ural coast is open to the long fetch length across the Kara Sea, the shallow bathymetry reduces the waves reaching onshore
- The system is microtidal with almost negligible effects of the tides on the current variation near the coast. However the bay in its entirety may be tidally dominated and the effects felt at the coast cannot be extended for the region as a whole.
- Current data provided by Dr. S. Ogorodov for the period of August 2006 was used for calibrating the model. The model showed a good correlation with the data for a high value of Manning's number (50 $m^{1/3}$/s) which suggests a high bed resistance. It can be concluded that the presence of vegetation in the nearshore region and possible ice content in the sediment layer can result in the increased bed resistance.
- No recent current data was available for validation of the model and hence, an attempt was made to identify the main factors contributing to the coastal erosion occurring at the site. Waves and wave driven currents are found to be the driving forces in sediment transport at the coast.
- Hydrodynamic simulations indicate an average current speed of 0.1 m/s inside the Bay and 0.15 m/s near the site of interest. The bay is found to be ebb dominated with a short falling period and a longer rising period. The currents during ebb tide are found to be stronger than during the flood tide.
- It can be concluded that the system is dominated by wind wave action and the sediment transport occurring at the site can be explained by the wave induced transport during the summer period. This is in accordance with the general idea of the bay as proposed by SAMCoT research, where the sediment is thought to be eroded due to thermo-mechanical processes during winter and available for transport for waves when they are active during the summer.
- The sediment transport sensitivity analysis presented, confirms the hypothesis that the tidal currents are secondary in importance, compared to the wave action. It was found that the pure current formulations reach equilibrium and

the effect of currents is negligible after a period suggesting, that the sediment transport is mainly dependent on wave action.

- It is seen that the combined wave and current model gave realistic results and the bed level changes near the site of interest were found to be in the order of 1 m.

- The relation between sediment grain size and sediment transport is not linear and is interdependent on many other factors such as, wave climate, bed slope and bed resistance. Although, the transport and bed level change increases for increasing sediment grain size.

7   Recommendations for further research

There is definite scope of further improvement of the model for the region. The following points should be considered for any further research to be carried out for the location:

- A much better calibration could be achieved with detailed field surveys containing data regarding the surface elevation at the site, wave and wind parameters, and current speed vectors at the location of interest. A time series for a minimum of a year would improve the quality of the model predictions.
- A survey showing the sediment grain size distribution at the coast will also help in realising a realistic bed resistance value and bottom friction parameter. Both the parameters were kept at a constant value in the model and the variations from the measured value can be attributed to this assumption.
- Periodic bed level surveys to a certain prescribed depth showing the evolution of bed profile of the near shore region over a long time period can help in calibrating the sediment transport patterns along the coast.
- The confidence in the results can be further improved by obtaining field data containing detailed sediment gradation and sediment diameter (d_{50}) variation along the coast.

The recommendations for data collection and future research are in line with the expected surveys to be conducted at the site by SAMCoT. MIKE21 can be utilised effectively to model the current and sediment transport occurring at the site. Further research may also include development or improvement of any existing model (CoSMOS, Southgate and Nairn, 1993) that can accommodate inclusion of thermo-mechanical erosion in combination with hydrodynamic effects felt on the coast. This would provide a comprehensive modelling tool to understand the coastal processes active in the Arctic region and avoid damaging effects of coastal erosion.

References

Ackers, P., and White, W., 1973. "Sediment Transport: New Approach and Analysis," Journal of the Hydraulics Division, ASCE, Vol. 99, No. HY11.

Bagnold, R. A., 1966. An approach to the sediment transport problem from general physics. *US Geol. Surv. Prof. Paper*, *422*, 231-291.

Battjes, J. A., & Janssen, J. P. F. M., 1978. Energy loss and set-up due to breaking of random waves. *Coastal Engineering Proceedings*, *1*(16).

Bijker, E.W., 1967. Some considerations about scales for coastal models with movable bed. Delft Hydraulics Laboratory, Publication 50, Delft, The Netherlands.

Bosboom J.and Stive M., 2012. *Coastal Dynamics I*. VSSD, Delft,The Netherlands.

Dee, D. P., Uppala, S. M., Simmons, A. J., Berrisford, P., Poli, P., Kobayashi, S., Andrae, U., Balmaseda, M. A., Balsamo, G., Bauer, P., Bechtold, P., Beljaars, A. C. M., van de Berg, L., Bidlot, J., Bormann, N., Delsol, C., Dragani, R., Fuentes, M., Geer, A. J., Haimberger, L., Healy, S. B., Hersbach, H., Hólm, E. V., Isaksen, L., Kållberg, P., Köhler, M., Matricardi, M., McNally, A. P., Monge-Sanz, B. M., Morcrette, J.-J., Park, B.-K., Peubey, C., de Rosnay, P., Tavolato, C., Thépaut, J.-N. and Vitart, F., 2011. The ERA-Interim reanalysis: configuration and performance of the data assimilation system. Q.J.R. Meteorol. Soc., 137: 553–597.

Doering, J. C., & Bowen, A. J., 1987. Skewness in the nearshore zone: A comparison of estimates from Marsh-McBirney current meters and colocated pressure sensors. *Journal of Geophysical Research: Oceans (1978–2012)*, *92*(C12), 13173-13183.

Donelan, M. A., Hamilton, J., & Hui, W., 1985. Directional spectra of wind-generated waves. *Philosophical Transactions of the Royal Society of London. Series A, Mathematical and Physical Sciences*, *315*(1534), 509-562.

Einstein, H. A., & Krone, R. B., 1962. Experiments to determine modes of cohesive sediment transport in salt water. *Journal of Geophysical Research*, *67*(4), 1451-1461.

Eldeberky, Y., & Battjes, J. A., 1994. Nonlinear coupling in waves propagating over a bar. *Coastal Engineering Proceedings*, *1*(24).

Engelund, F. and Fredsøe, J., 1976. *A sediment transport model for straight alluvial channels.* Nordic Hydrology, 7, pp. 296-306.

Engelund, F. and Hansen, E., 1976. *A Monograph on Sediment Transport in Alluvial Channels.* Nordic Hydrology 7, pp. 293-306.

Frijlink, H.C., 1952. Discussion des formules de debit solide de Kalinske, Einstein et Meyer – Peter et Mueller compte tenue des mesures recentes de transport dans les rivieres Neerlandaises. 2me Journal Hydraulique Societe Hydraulique de France, Grenoble, 98 – 103.

Hasselmann, K., 1962. On the non-linear energy transfer in a gravity-wave spectrum. *J. Fluid Mech*, *12*(481-500), 15.

Hasselmann, S., Hasselmann, K., Allender, J. H., & Barnett, T. P., 1985. Computations and Parameterizations of the Nonlinear Energy Transfer in a Gravity-Wave Specturm. Part II: Parameterizations of the nonlinear energy Transfer for Application in wave models. *Journal of Physical Oceanography*, *15*(11), 1378-1391.

Holthuijsen, L. H., 2007. *Waves in oceanic and coastal waters*. Cambridge University Press.

Holthuijsen, L.H, Booij, N. and Herbers, T.H.C., (1989) A Prediction Model for Stationary, Short-crested Waves in Shallow Water with Ambient Currents, *Coastal Engineering*, 13, 23-54.

Janssen, P. A. E. M., Lionello, P., & Zambresky, L., 1989. On the interaction of wind and waves. *Philosophical Transactions of the Royal Society of London. Series A, Mathematical and Physical Sciences*, *329*(1604), 289-301.

Janssen, P. A., 1991. Quasi-linear theory of wind-wave generation applied to wave forecasting. *Journal of Physical Oceanography*, *21*(11), 1631-1642.

Kalinske, A. A., 1947. Movement of sediment as bed load in rivers. *Transactions, American Geophysical Union*, *28*, 615-620.

Komen, G. J., Cavaleri, L., Donelan, M., Hasselmann, K., Hasselmann, S., & Janssen, P. A. E. M., 1996. *Dynamics and modelling of ocean waves*. Cambridge University Press.

Launder, B. E., & Spalding, D. B., 1974. The numerical computation of turbulent flows. *Computer methods in applied mechanics and engineering*, *3*(2), 269-289.

Leont'yev, I. O., 2003. "Modeling Erosion of Sedimentary Coasts in the Western Russian Arctic," Coastal Eng. 47, 413–429.

Lilly, D. K., 1989, February. The length scale for sub-grid-scale parameterization with anisotropic resolution. In *Annual Research Briefs, 1988* (Vol. 1, pp. 3-9).

Lomonosov Moscow University, Geology faculty, NTNU, Geocryology department, NTNU, 2013. Report on Baydara Bay studies on Arctic coastal erosion, Sfi-SAMCoT Report.

Longuet-Higgins, M. S., & Stewart, R. W., 1964, August. Radiation stresses in water waves; a physical discussion, with applications. In *Deep Sea Research and Oceanographic Abstracts* (Vol. 11, No. 4, pp. 529-562). Elsevier.

Meyer-Peter, E., & Müller, R., 1948, June. Formulas for bed-load transport. In *Proceedings of the 2nd Meeting of the International Association for Hydraulic Structures Research* (pp. 39-64). Delft: International Association of Hydraulic Research.

Miche, M., 1944. Mouvements Ondulatories de la Mer en Profondeur Constante ou Décroissante, Ann. Ponts Chauss., 25-28,131-164,270-292 and 369-406.

MIKE21 and MIKE3 Flow Model – Flexible mesh, Scientific documentation, 2012, DHI.

MIKE21 Hydrodynamic module, Scientific documentation, 2012, DHI.

MIKE21 Sand Transport module, Scientific documentation, 2012, DHI.

MIKE21 Sand Transport module, User manual, 2012, DHI.

MIKE21 Spectral Wave, Scientific documentation, 2012, DHI.

MIKE21 Spectral Wave, User manual, 2012, DHI.

MIKE21/3 Coupled Flow module – Flexible mesh, User manual, 2012, DHI.

Nairn, R. B., Roelvink, J. D., & Southgate, H. N., 1990. Transition zone width and implications for modeling surfzone hydrodynamics. *Coastal Engineering Proceedings*, *1*(22).

Nielsen, P., 1979. Some basic concepts of wave sediment transport, *Series paper 20* Institute of Hydrodynamic and Hydraulic Engineering, Technical University of Denmark, 160 pp.

Odisharia, G. E., Tsvetsinsky, A. S., Mikhailov, N. N., & Dubikov, G. I., 1997. Specialized information system on environment of Yamal Peninsula and Baydaratskaya Bay. *Proceedings of Inrernational Offshore and Polar Engineering Conferense (ISOPE-97)*, 574-581.

Phillips, O. M., 1981. Dispersion of short wavelets in the presence of a dominant long wave. *Journal of Fluid Mechanics*, *107*, 465-85.

Ris, R. C., Holthuijsen, L. H., & Booij, N., 1994. A spectral model for waves in the near shore zone. *Coastal Engineering Proceedings*, *1*(24).

Roelvink, J. A., & Stive, M. J. F., 1989. Bar-generating cross-shore flow mechanisms on a beach. *Journal of Geophysical Research: Oceans (1978–2012)*, *94*(C4), 4785-4800.

Rottner, J., 1959. ''A formula for bed-load transportation.'' Houille Blanche, 14 (3), 285–307.

Ruessink, B. G., Walstra, D. J. R., & Southgate, H. N., 2003. Calibration and verification of a parametric wave model on barred beaches. *Coastal Engineering*, *48*(3), 139-149.

Shields, A., 1936. *Application of Similarity Principles and Turbulence Research to Bedload Movement,* California Institute of Technology, Pasadena (translated from German).

Smagorinsky, J., 1963. General circulation experiments with the primitive equations: i. The basic experiment*. *Monthly weather review*, *91*(3), 99-164.

Southgate, H. N., & Nairn, R. B., 1993. Deterministic profile modelling of nearshore processes. Part 1. Waves and currents. *Coastal Engineering*, *19*(1), 27-56.

Swart D.H., (1976), Predictive equations regarding coastal transports. *Proc 15th Conf Coastal Engng,* 2, pp. 1113–1132.

Tolman, H. L., 1994. Wind waves and moveable-bed bottom friction. *Journal of physical oceanography*, *24*(5), 994-1009.

Van Rijn, L. C., 1984. Sediment transport, part I: bed load transport. *Journal of hydraulic engineering*, *110*(10), 1431-1456.

Van Rijn, L. C., 1987. *Mathematical modelling of morphological processes in the case of suspended sediment transport* (Doctoral dissertation, Waterloopkundig Lab., Delft Hydraulics Comm-382).

Van Rijn, L. C., 1993. *Principles of sediment transport in rivers, estuaries and coastal seas* (Vol. 1006). Amsterdam: Aqua publications.

Weber, N., 1991. Bottom friction for wind sea and swell in extreme depth-limited situations. *Journal of physical oceanography*, *21*(1), 149-172.

Wilcox, D. C., 1994. Simulation of transition with a two-equation turbulence model. *AIAA journal*, *32*(2), 247-255.

Young, I. R., & Van Vledder, G. P., 1993. A review of the central role of nonlinear interactions in wind-wave evolution. *Philosophical Transactions of the Royal Society of London. Series A: Physical and Engineering Sciences*, *342*(1666), 505-524.

Young, I. R., 1999. *Wind generated ocean waves* (Vol. 2). Elsevier Science.

Zyserman, J.A. and Fredsøe, J. *Inclusion of the Effect of Graded Sediment in a Deterministic Sediment Transport Model*. MAST G6M-Coastal Morphodynamics Final Workshop, Abstracts-in-depth. Pisa, Italy, May 1992.